We thank the reviewer for the comments and feel they will improve the manuscript. In response to these comments, we have made substantial changes to the manuscript. Below, we respond to the reviewers comments in detail and indicate changes we have made to the manuscript. Referee comments are in black, plain text. Our response to referees is in black, *italic* text. Changes to the text are listed in blue text.

Referee #1

Referee comments on "Aircraft Observations of Aerosol in the Manaus Urban Plume

and Surrounding Tropical Forest during GoAmazon 2014/15" by Shilling et al., 2018.

MS No.: acp-2018-193.

The authors have done large number of research flights over the Amazon basin. The measurements are done with state-of-the-art instrumentation (HR-AMS, PTR-MS etc). However, currently the data analysis and representation is unfortunately lacking. The authors are giving a very narrow overview of the general situation and are focusing to only one flight in more detail. I believe this dataset is important and worth publishing but that first the data presentation needs to be significantly improved.

Major comments: 1) The title of article is very broad. I recommend clarifying the article title to be more inline with content. Also, check that the aim of this article (defined at the end of introduction) is inline with the title and results.

We have updated the title. We have also revised the last portion of the introduction.

Aircraft Observations of the Chemical Composition and Aging of Aerosol in the Manaus Urban Plume during GoAmazon 2014/5

In this manuscript we report on measurements from instruments deployed on the G-1 focusing primarily on measurements of aerosol species and trace gases that impact the aerosol lifecycle. In the first part of the manuscript, we provide an overview of aerosol and VOC measurements and compare and contrast the wet and dry season data. In the second portion of the manuscript, we examine, in detail, the first 4 – 6.5 hours of photochemical aging of the Manaus plume as it is transported into the surrounding tropical forest and interacts with biogenic emissions.

2) Improve the chapter 3.1, especially figure 2 and table 1. Clarify the figure 2 to be clear and easy to understand. Maybe remove unnecessary panels. Table 1: Please add general meteorological information (like conditions, T, RH, wind during flights), also probably would be more useful to show averages over the flight legs (1-5) or average values for different heights (500m,1000m) separately, instead of whole flight average PM composition. Also, please include the PTR-MS results to this overview (fig2, table1).

In regard to Figure 1, please see our response to a similar comment below.

We have added an additional table (Table 1) summarizing the flight conditions the reviewer suggest. We have added text pointing to Table 1 in the text.

Table 1 lists takeoff and landing times, the altitude of level flight legs, and meteorological parameters measured by the G-1 instrumentation shortly after takeoff on each flight. Flights generally departed in the late morning or early afternoon and lasted between 3 and 3.5 hours (Table 1).

Flight Date[a]	Takeoff [b]	Landing [b]	Altitude(s) of Level Flight Legs (m)[c]	T (°C)[d]	RH (% water)[d]	Wind Speed (m/s)[d]	Wind Heading[d]
Wet Season							
2/22/2014	10:37:11	13:25:28	600, 1600	25	80	5	ENE
2/25/2014	12:30:31	14:43:04	600, 1300	26	80	8	ENE
3/1/2014 a	9:33:09	11:31:31	600	25	80	6	NE
3/1/2014 b	13:13:59	14:49:34	1100, 4500, 6400	24	80	4	NE
3/3/2014	13:46:34	15:11:57	600	26	90	N/A	N/A
3/7/2014	9:08:11	11:39:18	600, 1300, 1900, 3200, 3800, 4500, 5800	26	65	10	NNE
3/11/2014	10:39:59	13:51:10	600, 1500	25	85	7	ENE
3/12/2014	13:20:25	15:29:44	600	22	80	16	NE
3/13/2014	10:14:14	13:21:29	500, 1100	25	80	7	ENE
3/14/2014	10:17:07	12:48:25	500, 1200, 2200, 3200	25	80	8	E
3/16/2014	10:38:18	13:30:33	500, 1000, 1200, 1600	25	80	5	E
3/17/2014	12:23:11	15:26:38	600, 1200, 1500	26	75	10	ENE
3/19/2014	10:25:33	13:21:48	600, 1600, 3200, 4800, 6500, 7100	22	95	7	ENE
3/21/2014	12:32:34	15:00:22	600, 800, 1300	23	90	6	ENE
3/23/2014	10:56:47	13:46:34	600	23	90	5	NNE
Dry Season							
9/6/2014	11:16:07	13:39:03	500, 1700	29	N/A	4	ESE
9/9/2014	11:01:14	14:11:01	500, 1600, 1900, 5800	25	80	4	NE
9/11/2014	10:32:40	13:37:38	500	27	70	7	ENE
9/12/2014	10:41:26	13:08:04	600, 1600	25	65	6	E
9/13/2014	10:50:05	13:43:21	500, 800, 1600, 2100, 2600	27	70	5	ENE
9/15/2014	10:59:06	14:01:47	500, 1800, 1900, 2600	28	60	5	E
9/16/2014	11:40:15	14:27:54	500, 1900	28	65	3	NE
9/18/2014	10:35:59	13:26:01	500, 1900, 4900	27	70	2	E
9/19/2014	10:30:23	13:46:44	500, 1600	28	70	2	NE
9/21/2014	11:17:32	14:20:51	500, 1300, 1600, 1900, 2500, 4800	26	70	5	ENE

9/22/2014	10:23:40	13:37:40	500, 1800	28	60	3	NE
9/23/2014	11:46:45	14:43:13	500, 1900	28	60	2	E
9/25/2014	13:09:24	15:53:59	500, 1600, 1800	28	70	4	E
9/27/2014	14:29:21	16:21:40	600, 2300	29	55	5	ENE
9/28/2014	11:09:12	14:07:27	600, 1800, 2100	28	65	5	ENE
9/30/2014	10:55:10	13:10:19	500, 2000, 3200	29	55	3	E
10/1/2014	10:39:01	13:09:54	600, 1000, 1300, 1600, 2100, 2500	26	65	6	E
10/3/2014	10:50:51	13:54:57	800, 1000, 1200, 1600, 1900, 2600, 3300, 3900	26	75	4	ESE
10/4/2014	12:24:46	13:52:31	600	27	55	N/A	N/A

[a]The flight on March 10, 2014 is omitted from this table due to an AMS failure.

[b]local time

[c]altitude above mean sea level from GPS data, only level flight legs on which AMS data were collected listed

[d]immediately after takeoff, altitude < 1000 m, wind speed and heading from Aventech Research AIMMS-20 probe

T from Rosemount 102E probe, RH calculated from T and dewpoint measured by General Eastern 1011-B probe

Table 1. Flight times, altitude of level legs, and meteorological parameters measured by instrumentation onboard the G-1 research aircraft for research flights described in this manuscript. Temperature, RH, wind speed, and wind heading correspond to values measured shortly after takeoff at altitudes less than 1000 m. Note that meteorological parameters are not homogeneous in space or time.

Table 2 (formerly Table 1) compares the average and median aerosol mass loading of the low altitude legs to the same quantities averaged over all altitudes. We wish to focus the discussion on the evolution of the Manaus plume and therefore chose to highlight the lowest altitude data in Table 1. All flights did not follow identical flight patterns, so segregating into flight legs is not possible. A visualization of all the flight patterns is shown in Martin et al., 2016.

We have added a figure and table showing the PTR-MS data at the reviewer's suggestion. We have incorporated a discussion of this data into the text.

GoAmazon 2014/5 Wet Season

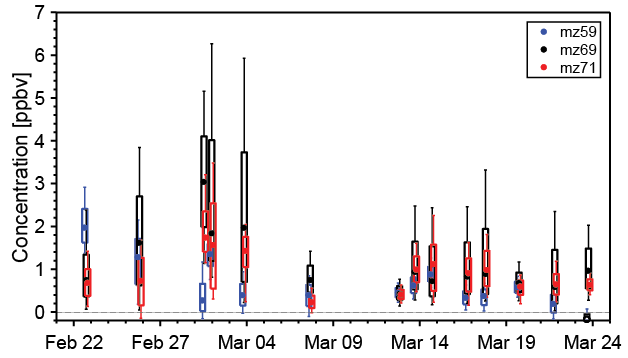

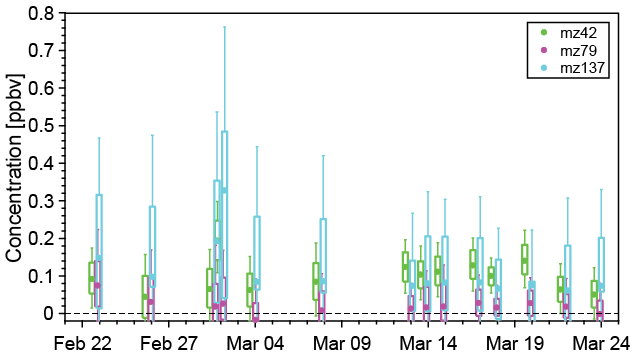

GoAmazon 2014/5 Dry Season

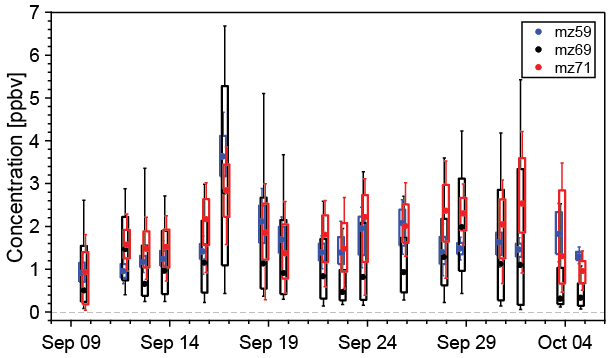

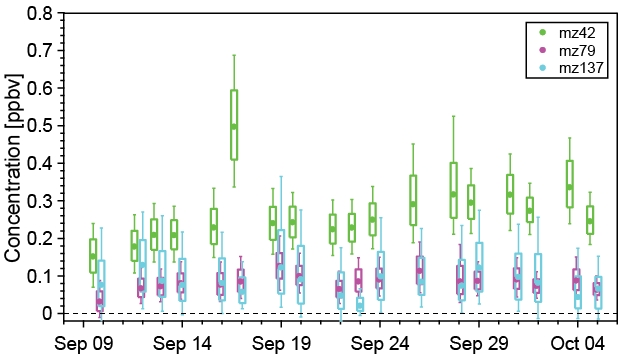

	Wet Season	Dry Season
Median Concentration (all data)		
m/z 42 (acetonitrile)	0.1	0.25
m/z 59 (acetone)	0.47	1.46
m/z 69 (isoprene)	0.43	1.09
m/z 71 (isoprene oxidation products)	0.66	1.84
m/z 79 (benzene)	0.03	0.08
m/z 137 (monoterpenes)	0.1	0.08
Median Concentration (<700 m)		
m/z 42 (acetonitrile)	0.09	0.26
m/z 59 (acetone)	0.43	1.65
m/z 69 (isoprene)	0.52	1.86
m/z 71 (isoprene oxidation products)	0.76	2.16

m/z 79 (benzene)	0.02	0.09
m/z 137 (monoterpenes)	0.12	0.11
Mean Concentration (all data)		
m/z 42 (acetonitrile)	0.12	0.36
m/z 59 (acetone)	0.59	1.91
m/z 69 (isoprene)	0.67	1.82
m/z 71 (isoprene oxidation products)	0.87	1.99
m/z 79 (benzene)	0.04	0.1
m/z 137 (monoterpenes)	0.12	0.11
Mean Concentration (<700 m)		
m/z 42 (acetonitrile)	0.11	0.4
m/z 59 (acetone)	0.7	2.31
m/z 69 (isoprene)	0.82	2.37
m/z 71 (isoprene oxidation products)	1.07	2.4
m/z 79 (benzene)	0.04	0.11
m/z 137 (monoterpenes)	0.15	0.14

Table 3. Measurements of VOC species made by the PTR-MS onboard the G-1. Units are ppbv. The statistics for altitudes less than 700 m capture the lowest altitude data during the campaign (Table 1).

While this manuscript will focus on the particulate data, measurements of the volatile organic compounds provide insights into the precursors that are oxidized to form OA and help to identify the source of an air parcel. Figure 3 and Table 3 summarize the concentrations of several relevant VOCs measured on board the G-1 with the PTR-MS. Similar to the trends seen in the aerosol mass loading data, concentrations of most VOCs measured by the PTR-MS are significantly higher in the dry season than in the wet season. Concentrations of isoprene and its oxidation products, biogenic precursors of OA, are a factor of 2-3 times higher in the dry season than the wet season. The average daily high temperatures in Manaus are 33.5°C in September (dry season) and 30.9°C in March (wet season) and isoprene emissions have been shown to scale with temperature, among other variables (Guenther et al., 2012). Measurements of benzene, which is primarily anthropogenic in origin, were also significantly higher in the dry season. While benzene itself is unlikely to significantly contribute to SOA formation over the timescales we observe on the G-1 flights (4-6.5 hours) due to its ~5 day atmospheric lifetime (Atkinson and Arey, 2003), other unmeasured anthropogenic VOC concentrations which would contribute to more immediate OA formation may have been higher as well. The higher VOC concentrations may contribute to the higher OA concentrations measured in the dry season. However,

the PTR-MS data, in addition to satellite and remote sensing measurements (Martin et al., 2016), also show that biomass burning significantly impacted the region. Measurements of acetonitrile, whose major source is biomass burning (Yokelson et al., 2009;Yokelson et al., 2007), are 2-3 times higher in the dry season than the wet season, indicating a significant biomass burning impact in the region. Biomass burning is a known source of OA (Jolleys et al., 2012;Bond et al., 2004;Yokelson et al., 2009;Ferek et al., 1998) and would also contribute to the higher aerosol concentrations observed in the dry season.

3) Why unit mass data is used in fig 2? I strongly suggest replacing all the UMR data with HR data as authors have it and it is considered to be more accurate. Assumable all other data in figures and text is HR data? Also, PMF is assumable run on HR-data? I strongly suggest using only HR data as it is available and tools are developed for the data analysis.

We have replaced the use of UMR data with HR data in Figure 2 and Table 1. In the original manuscript PMF was run using HR data. All data presented in the paper now use HR data analysis.

All AMS data in the manuscript have been processed using the high-resolution data analysis routine.

4) Why PMF was run only to wet season data? Why not dry season? The authors speculate that during dry season biomass burning was a major source. PMF should certainly show this. PMF for dry season would give important information on differences in PM sources between seasons also. I recommend running PMF on data from both seasons. Improved chapter 3.1 and PMF run for both seasons would help to provide a better comparison between seasons. I recommend running PMF for both seasons to do proper source analysis.

PMF analysis is in progress for the dry season. A full description of the PMF analysis results will be the subject of a future publication. For this reason, we have also refrained from describing the PMF results for the entire wet season dataset and only present the PMF analysis on the March 13 flight. Our goal in section 3.1 is not to do a full and comprehensive source analysis, but to present a high-level overview of the observations in the wet and dry season. We have added references for the impact of biomass burning on the aerosol concentrations throughout the manuscript.

5) The aim of flights was to study evolution of Manaus plume during aging. Is it not possible to find another flight for comparison for this "golden" one? It would be interesting to see if $\Delta org/\Delta CO$ would be as low and constant also in other flights.

At the reviewer's suggestion, we have screened the data and analyzed additional flights during the wet season. We selected flights on which there was: a clear contrast between the plume and background data, data collected in the boundary layer, a complete dataset from key instrument (AMS, CO detector), minimal interference from biomass burning emissions and cloud processing, and a flight plan extending a similar downwind distance. We were able to identify two additional flights that can be presented, March 11 and March 16. Additional flights Both show similar trends in the data with $\Delta org/\Delta CO$ *values averaging* $34 \mu g/m^3$ $ppmv^{-1}$ *and showing little trend with aging. We have added a figure to the manuscript showing this additional data and have added a discussion of this data to the manuscript. In addition, as we cite in the manuscript, and analysis of data at the T2 and T3 ground sites by Cirino et al., 2018 shows no*

change in Δorg/ΔCO from T2 to T3. The data thus suggest the behavior is representative for the wet season. Of course, repeated measurements over several years would be valuable to assess whether 2014 was a typical or atypical wet season.

Thus far, we have focused on a detailed analysis of the March 13, 2014 plume because there is a clear contrast between the background and plume data through the portion of the flight in the boundary layer, there is little interference from biomass burning and cloud processing, the flight pattern was extended far enough downwind to investigate a significant aging time, and the data from all key instruments are available and complete. In an effort to understand whether the Δorg/ΔCO observations on March 13 are representative of plume aging in the wet season, we have screened the rest of the wet season flight data and, based on the criteria mentioned above, we have identified two additional flights, March 11 and March 16, 2014, for analysis. The Δorg/ΔCO values for these data as a function of distance from Manaus are shown in Figure 8. On March 11, Δorg/ΔCO values average 29.9 $\mu g/m^3$ $ppmv^{-1}$, show little change with distance from Manaus, and show similar variability as the March 13 flight data. The mean wind speed for the analyzed portion of the flight was 5.3 m/s translating to an approximate maximum plume age of 5-5.5 hours. On March 16, Δorg/ΔCO values average 42.0 $\mu g/m^3$ $ppmv^{-1}$, show little significant increase with distance from Manaus, and exhibit a larger range of values than the other two datasets. The mean wind speed for the analyzed portion of the March 16 flight was 4.6 m/s translating to an approximate maximum plume age of 6-6.5 hours. We estimate that the error in the Δorg/ΔCO measurement is approximately 10 $\mu g/m^3$ $ppmv^{-1}$, thus the difference in average Δorg/ΔCO values between the March 16 and the March 11 and 13 datasets are at the edge of what we would consider significant. The average Δorg/ΔCO is 34.3 $\mu g/m^3$ $ppmv^{-1}$ for all flights and collectively represent the first 4 – 6.5 hours of aging. In addition to the aircraft data, Cirino et al. (2018) report that the median Δorg/ΔCO values for the plume as measured at the T2 and T3 sites are nearly identical to one another in the wet season and similar to measurements from the G-1(Cirino et al.). Thus, the data from both G-1 and the ground sites suggests that Δorg/ΔCO values of 30-40 $\mu g/m^3$ $ppmv^{-1}$ that change little in the first 4-6.5 hours of plume aging are representative of the Manaus plume behaviour in the wet season.

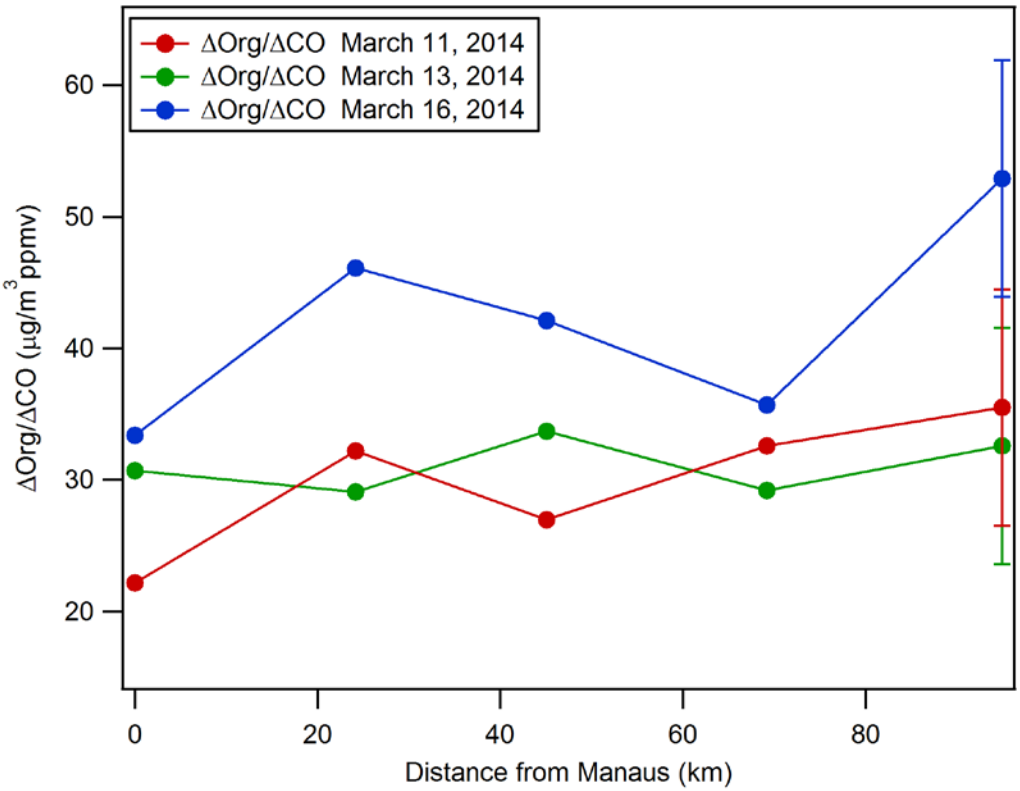

Also, would it be possible to identify any "golden" day from the dry season? The comparison in SOA aging between dry and wet season would be very interesting. Currently, as you show that the Δorg/ΔCO is quite low and does not change, it is not sure if it was only one time occurrence or the normal situation.

The dry season data are complicated by the presence of a regional (and sometimes local) biomass burning background. Understanding and separating the evolution of the Manaus urban plume from evolution of the biomass burning is a complex task and will be the focus of a future publication. In the current manuscript, we want to focus on the evolution of the plume in the wet season since this represents, clean background conditions. We show in the manuscript that these observation are unique relative to that is typically observed in other parts of the world. Adding detailed information on the evolution of biomass burning plumes is a separate topic and would warrant a separate publication.

Also, please provide some statistics how often the manaus plume was observed during the flights for wet and dry season.

In the wet season, we encounter the Manaus plume between 15 – 25% of the total flight time. In the dry season, we encounter the Manaus plume between 15 – 35% of the total flight time. These statistics are much more uncertain for the dry season. In the dry season, we frequently encounter biomass burning plumes, and it is at times difficult to differentiate a biomass burning plume from the Manaus urban plume, particularly when they mix.

6) I assume that there are a large number of publications from this campaign already published. Please provide a short summary about those and how this differs from those previously published.

The goals of GoAmazon were very broad. Summarizing all publications form GoAmazon would be beyond the scope of this work and would introduce information that is not directly relevant to this manuscript. We believe we have adequately referenced both past work in the Amazon region and the GoAmazon 2014/5 publications that are relevant to this study, particularly those investigating the impact of the Manaus plume on SOA, in the text. In total, we cite and discuss 14 GoAmazon manuscripts. We feel it is better to discuss these manuscripts by subject as we have done, rather than as a separate section on GoAmazon 2014/5 as the reviewer suggests. Currently, there are no other publications in the literature describing the G-1 AMS measurements from GoAmazon 2014/5 or the evolution and aging of the Manaus plume, so this manuscript is unique.

7) Please check that all abbreviations (PTR-MS, HR-ToF-AMS, G-1 etc.) are explained when first mentioned.

We have checked these abbreviations and spelled them out the first time they are mentioned.

As part of this campaign, the DOE Gulfstream-1 (G-1) research aircraft

An Aerodyne High-Resolution Time of Flight Aerosol Mass Spectrometer (abbreviated as AMS hereafter) was deployed on

An Ionicon quadrupole high-sensitivity Proton Transfer Reaction Mass Spectrometer (PTR-MS) was used to measure selected

Detailed comments:

Page 1, Line 31. Please define “golden”

“Golden day” is colloquialism used in discussing field studies to indicate an exemplar day. We have replace golden with exemplar.

In the second portion of the manuscript, we discuss the evolution of the Manaus plume on March 13, 2014, one of the exemplar days in the wet season.

Page 2, Line 24. Define Lagrangian.

Lagrangian evolution here refers to measuring the properties of the same air parcel as it evolves. We have added a brief discussion of Lagrangian sampling in the text. Additional information can be found in: (Seinfeld, 1998;Jacob, 1999).

For several years, there has been an interest in studying the Lagrangian (i.e., within the same air parcel) evolution of organic aerosol from the emissions of urban centers.

Most studies of this type are best described as pseudo-Lagrangian as repeatedly sampling the same air parcel is difficult with mobile platforms and impossible with fixed sites. Dilution and mixing of the air parcel with background air also alter the plume composition.

Page 4, line 25. The aim of this study could be better defined. Especially the scientific aim.

We have revised lines 24-25.

In this manuscript we report on measurements from instruments deployed on the G-1 focusing primarily on measurements of aerosol species and trace gases that impact the aerosol lifecycle. In the first part of the manuscript, we provide an overview of aerosol and VOC measurements and compare and contrast the wet and dry season data. In the second portion of the manuscript, we examine, in detail, the first 4 – 6.5 hours of photochemical aging of the Manaus plume as it is transported into the surrounding tropical forest and interacts with biogenic emissions.

Page 5, line 15. Explain why 13 seconds time interval was chosen? AMS can be used with much better time resolution (Hz), especially when ptof is not used.

The sampling time was chosen as a compromise between adequate time resolution and achieving adequate signal, particularly for the wet season where aerosol loadings were low. The need for higher S/N outweighed the need for higher time resolution, which we deemed adequate. See also our response to a similar question from Reviewer 2.

Page 5, line 25. Define the software models used for the data analysis (igor version+ Squirrel and PIKA versions+ PMF software). Also, please add details about PMF analysis (number of factors tested, how nr of factors was decided, were factors constrained, ME2 etc.).The main parameters should be in the manuscript also, since not many people does not read the supplement.

We have added the software versions used in the analysis to the manuscript.

…using the PMF Evaluation Tool (v 2.06) and the PFM2 algorithm (v 4.2)…

Data was analyzed in Igor Pro (v6.37) using the high-resolution analysis package (Squirrel v1.55H, PIKA v1.44H) and techniques described in the literature (Canagaratna et al., 2015;Kroll et al., 2011;Aiken et al., 2007;Allan et al., 2003;Jimenez et al., 2003). All AMS data in the manuscript have been processed using the high-resolution data analysis routine. The O:C and H:C values reported here use the updated calibrations described in Canagaratna et al. (2015).

We have added details on the PMF analysis and on choosing the appropriate number of factors. We moved the discussion of PMF to the appendix at the reviewer's suggestion. The changes made to the manuscript are detailed in a response similar comment from Reviewer #2 (below).

Page 5, line 25-26. Please explain why data was normalized to 23C and 1013 hPA?

These are the laboratory conditions under which the flow calibration was performed. We have added this to the manuscript.

All AMS data are normalized to the laboratory calibration conditions of 23 $^{\circ}$C 1013 hPa.

Page 5, line 28. Please provide the model and manufacturer for the PTR-MS and all other instruments.

The text states: "An Ionicon quadrupole high-sensitivity PTR-MS was used to measure selected gas-phase volatile organic carbon (VOC) concentrations (Lindinger et al., 1998)" *The manufacturer is*

Ionicon and they specify the model as a high-sensitivity PTR-MS. Further information on all instruments deployed on the G-1 is available in the supplemental information of Martin et al., 2016. We have added a reference to Martin et al. 2016.

Additional information on the instrumentation deployed on the G-1 can be found in the supplementary information of Martin *et al.*, 2016.

Page 6. Chapter 3.1. Please add a description of local conditions (temp, RH, wind etc) during the wet and dry periods. Also, provide info about the flight altitudes, times etc. It is hard to compare the results when it is not known if the difference is due to altitude or time of day or due to different source. Are the points in fig 2. top panel average values over the flights (including all altitudes?)?were all flights similar?

At the reviewer's suggestion, we have added a table listing meteorological conditions (Table 1) during each flight and referenced this table in the text. It is important to note that each flight samples a wide range of T, RH, wind speed, wind direction values. The listed values are for the lowest flight legs near the start of the flight. We have also added a brief overview of the meteorology in the wet and dry seasons.

The top panel of Figure 2 is a box and whisker plot showing the 10, 25, 50, 75, and 90th percentile values for each flight. Each box and whisker summarizes all the data for a particular flight, including all altitudes.

The timing of these flight missions was chosen to provide a contrast between the wet and dry seasons (Martin et al., 2016). In the wet season, back trajectory analysis indicated that the Manaus region was typically under the influence of air originating from the North Atlantic Ocean (Martin et al., 2016). Regular, organized mesoscale convective systems triggered by sea breeze circulation brought widespread, moderate rate precipitation to the region (Giangrande et al., 2017;Machado et al., 2018;Burleyson et al., 2016). The high level of rainfall and moisture in the wet season inhibited biomass burning and a low number of fires were observed (Martin et al., 2016;Machado et al., 2018). Under these conditions, the Amazon basin is one of the cleanest continental regions on Earth onto which the Manaus plume represents a significant perturbation (Martin et al., 2010;Artaxo et al., 2013). In the dry season, back trajectory analysis indicate air masses originate from the Southern Hemisphere and travel up the Amazon River transporting pollution from the northern coastal cities (Martin et al., 2016). In addition, recirculation events transported air from the southern Amazon basin into the Manaus region (Martin et al., 2016). Intense biomass burning fires in the central and southern portion of the Amazon basin and in central Africa were observed in the dry season and a portion of these emissions were transported to the Manaus region (Martin et al., 2016;Artaxo et al., 2013;Martin et al., 2010). In the dry season, more intense but less frequent convection produced approximately one quarter of the total rainfall observed in the wet season. As a result of the combination of transport and precipitation frequency, the Manaus region is significantly more polluted in the dry season.

Page 6, line 20-30/table 1. Are all these concentrations above the AMS detection limit? Especially the ammonium tends to have higher detection limits in aerosol mass spectrometers.

Based methodology described in DeCarlo et al., 2006, we calculate the detection limits of the AMS at the 13s averaging interval as 0.12, 0.01, 0.014, and 0.005 for organics, sulfate, nitrate,

and ammonium. We have added these detection limits to the manuscript. The values reported in Table 1 are above the detection limits.

Based on the standard deviation of these blank measurements (3σ) as described in the literature (DeCarlo et al., 2006), the detection limit of the AMS at the 13s sampling interval were 0.12, 0.01, 0.014, and 0.005 μg/m^3 for organics, sulfate, nitrate, and ammonium respectively.

Page 7. Line 15-16. Is there any proof for this? High CO2, CO, BC or levoglucosan values? Or tracers of levoglucosan (HR ions at m/z 63,70) at mass spectra?

We have added references in multiple locations in the text for the presence of biomass burning in the dry season. PTR-MS measurements of acetonitrile show an influence of biomass burning, as do measurements of CO. The changes to the manuscript are provided in our response to a similar comment from Reviewer #2 (below).

Page 8. The title of chapter 3.2 (Case Study, March 13, 2014 Flight) is not very descriptive. Consider changing it to something that describes content.

We have changed the heading to be more descriptive.

3.2 Evolution of Organic Aerosol in the Manaus Plume

Page 11. Line 30. How the age of plume was estimated to be 4-5 hours?

The text states: "Based on the mean wind speeds observed along the flight track (7.3 m s^{-1}) and the transport distance (up to 100 km), we estimate that the plume was 4-5 hours old at the farthest leg and freshly emitted over the city " . *The age of the plume was estimated from the transport distance and the measured mean wind speed along the flight track. The plume age was calculated using the equation: distance=wind speed*time.*

Page 11. Please define "photochemical clock"

A photochemical clock is a method of estimating the photochemical age of an air parcel based on measuring the ratios of two chemicals which are photochemically removed from the atmosphere at different and known rates. More details can be found in the following references, which have been added to the manuscript (de Gouw et al., 2005;Kleinman et al., 2003;Parrish et al., 1992).

Unfortunately, photochemical clocks could not be used to more precisely calculate the photochemical age of the plume (de Gouw et al., 2005;Kleinman et al., 2003;Parrish et al., 1992).

Page 13. Chapter 3.3. I am confused. This is not based on the case study, but on all flights where manaus plume was observed?

We have specified in the text when we are specifically discussing the March 13 flight and when we are discussing the data in general.

Page 13, row 11, 25. Please replace " SO4 " to sulphate.

We have made the suggested change.

Figures

Fig 1. Are these T1-T3 ground stations used in this article?

Only data from the aircraft are directly analyzed in this manuscript. Data collected at the T2 and T3 sites are referenced in the article. The aircraft data are compared to the ground site data in the manuscript, particularly those collected at the T3 site.

Fig 2. All the panels are showing same thing. Maybe consider how this figure could be condensed to a smaller figure? Also, the connecting lines between the average values are misleading. Maybe mark the median values with different colors. Also in top plot, some of the points (e.g.point between feb 27 and Mar 04) seems to maybe overlap? Fix these please.

We have fixed the slight overlap of the points.

We disagree with the reviewer's statement that all the panels show the same thing. The top panel shows box and whisker plots of the absolute mass loadings for each flight. The middle panel shows the relative non-refractory PM composition averaged on a per-flight basis. The bottom panel shows the average non-refractory PM composition of all flights in each season. Thus, one panel shows absolute mass while the other two show different versions of relative mass. The most similar panels are the lower two and we feel there is value in showing the average non-refractory PM composition both on a per-flight basis and as season-averages. These types of figures are common in the literature and we prefer to keep them.

The figure caption states that the lines are shown to guide the eye. We disagree that the lines connecting the median values are misleading and the reviewer isn't clear on why they think so. Nevertheless, we have changed them from solid lines to dotted lines to assuage some of the reviewer's concern. We feel the lines are useful, particularly for the inorganic species which are present in much lower concentrations and thus harder to see.

Fig 5.Legends from bottom panel are missing

We have added a legend to the bottom panel.

Referee #2

This manuscript reports observations from an aircraft study over Manaus, Brazil. The discussions mainly focus on the chemical evolution of aerosol particles in the Manaus plume sampled on March 13, 2014 as it was transported to the surrounding and nearby Amazon tropical rainforest. A particularly interesting observation is that $\Delta org/\Delta CO$ ratio stayed nearly constant in the Manaus urban plume although OA oxidation increased continuously during aging. The G1 measurement data from the GoAmazon campaign are very rich and this manuscript provides new and timely information on aerosol particles from an important, but poorly studied, environment. The finding of no net SOA formation in fresh urban emissions that is different from most published results on urban outflows is unique and may motivate future studies. Overall, this

manuscript is worthy of publication and ACP is a suitable journal for it. Following are some detailed comments.

The overview of the G-1 aerosol data is a bit cursory. The discussions could be expanded a bit more and other measurement results are incorporated to give a more in depth view about the atmospheric characteristics and seasonal differences. For example, the authors could consider adding other measurement data on Fig 2 and discuss them in connection with the AMS aerosol data. In addition, in section 3.1, more background information on the dry and wet seasons may be necessary to establish the purpose and the significance of the comparison.

We have added Figure 3 and Table 3 showing the PTR-MS data and text discussing this data in reponse to this comment and a similar comment from Reviewer #1. See also our response to a similar comment from Reviewer #1.

While this manuscript will focus on the particulate data, measurements of the volatile organic compounds provide insights into the precursors that are oxidized to form OA and help to identify the source of an air parcel. Figure 3 and Table 3 summarize the concentrations of several relevant VOCs measured onboard the G-1 with the PTR-MS. Similar to the trends seen in the aerosol mass loading data, concentrations of most VOCs measured by the PTR-MS are significantly higher in the dry season than in the wet season. Concentrations of isoprene and its oxidation products, biogenic precursors of OA, are a factor of 2-3 times higher in the dry season than the wet season. Mean temperatures during the dry season are XX higher and isoprene emissions have been shown to scale with temperature, among other variables [REF Guenther]. Measurements of benzene, which is primarily anthropogenic in origin, were also significantly higher in the dry season. While benzene itself is unlikely to significantly contribute to SOA formation over the timescales we observe on the G-1 flights (4-5 hours) due to its ~5 day atmospheric lifetime, other unmeasured anthropogenic VOC concentrations which would contribute to more immediate OA formation may have been higher as well. The higher measured VOC concentrations may contribute to the higher OA concentrations measured in the dry season. However, the PTR-MS data, in addition to satellite and remote sensing measurements (Martin et al., 2016), also show that biomass burning significantly impacted the region. Measurements of acetonitrile, whose major source is biomass burning (Yokelson et al., 2009;Yokelson et al., 2007), are 2-3 times higher in the dry season than the wet season, indicating a significant biomass burning impact in the region. Biomass burning is a known source of OA (Jolleys et al., 2012;Bond et al., 2004;Yokelson et al., 2009;Ferek et al., 1998) and would also contribute to the higher aerosol concentrations observed in the dry season.

We have also added additional background information on the wet and dry seasons.

The timing of these flight missions was chosen to provide a contrast between the wet and dry seasons (Martin et al., 2016). In the wet season, back trajectory analysis indicated that the Manaus region was typically under the influence of air originating from the North Atlantic Ocean (Martin et al., 2016). Regular, organized mesoscale convective systems triggered by sea breeze circulation brought widespread, moderate rate precipitation to the region (Giangrande et al., 2017;Machado et al., 2018;Burleyson et al., 2016). The high level of rainfall and moisture in the wet season inhibited biomass burning and low number fires were observed (Martin et al., 2016;Machado et al., 2018). Under these conditions, the Amazon basin is one of the cleanest continental regions on Earth onto which the Manaus plume represents a significant perturbation (Martin et al., 2010;Artaxo et al., 2013). In the dry season,

back trajectory analysis indicate airmasses originate from the Southern Hemisphere and travel up the Amazon River transporting pollution from the northern coastal cities (Martin et al., 2016). In addition, recirculation events transported air from the southern Amazon basin into the Manaus region (Martin et al., 2016). Intense biomass burning fires in the central and southern portion of the Amazon basin and in central Africa were observed in the dry season and a portion of the emissions were transported to the Manaus region (Martin et al., 2016;Artaxo et al., 2013;Martin et al., 2010). In the dry season, more intense but less frequent convection produced approximately one quarter of the total rainfall observed in the wet season. As a result of the combination of transport and precipitation, the Manaus region is significantly more polluted in the dry season.

More detailed diagnostic information should be presented to confirm the PMF results.

We have included 4 new figures to the supplementary material and 1 new table in the appendix showing PMF diagnostics. We have also moved our discussion on the PMF factor choices into the appendix and expanded that text.

Positive Matrix Factorization (PMF) analysis was performed on the high-resolution organic aerosol mass spectra and error matrix that were measured using the HR-ToF-AMS on the G-1. The organic aerosol mass spectra ($m/z < 122$) and error matrix were initially prepared using the high resolution AMS analysis package (Squirrel v1.55H, PIKA v1.44H) as described in the literature (Jimenez et al., 2003;Allan et al., 2004;DeCarlo et al., 2006;Aiken et al., 2007;Aiken et al., 2008). As described in the main text, the AMS organic mass loading data were normalized to the laboratory calibration conditions of 23 °C 1013 hPa. Error was estimated from the ion counting statistics (Allan et al., 2003) and a minimum amount of error was assigned to each signal (Ulbrich et al., 2009). Ion with signal below 0 (due to noise) were removed from the matrix. In addition, ions with an average signal to noise (S/N) less than 0.75 were removed from the analysis and ions with average S/N between 0.75 and 2 were downweighted by a factor of two (Ulbrich et al., 2009). Ions whose signals are fixed based on the measured CO_2 signal in the ratios described by Aiken et al., 2008 (CO^+, H_2O^+, HO^+, O^+) are also downweighted by a factor of two (Ulbrich et al., 2009). The PFM2 algorithm version 4.2 (Paatero, 1997;Paatero and Tapper, 1994) was used to analyze the matrix and results were visualized and evaluated using the PMF Evaluation Tool (v 2.06) described by Ulbrich et al. 2009. PMF analysis of this data set was challenging, due the combination of low concentrations of organic aerosol, fast sampling required for aircraft operations, and the often small changes in aerosol concentrations across the flight domain. PMF analysis on a data from a single flight often (though not always) resulted in a failure to resolve factors that are described in the literature (e.g., HOA, IEPOX SOA); instead, we often observes split factors that are largely dominated by a single high S/N ion (CHO^+, CO_2^+, $C_2H_3O^+$). For example, the IEPOX SOA factor was not resolved when the March 13 flight was analyzed on its own, largely due to the small mass loading of this factor (Figure 5 of main text). Therefore, data from all flights during the wet season was combined into a single matrix and analyzed together, which also forces a common solution for the entire dataset.

We chose a five factor solution to the combined matrix based on number of criteria, including; the residuals and fit quality, the correlation of chosen factors with independently measured species (e.g., CO, ozone), by examining the factor mass spectra for realism (are the spectra representative of a physical compound), and by comparing the factor spectra to literature data. Table A1 summarizes the residuals as a function of the number of factors and a short summary of the results. First, as seen in Table A1, the residuals continue to significantly decrease in moving from a 2 to 3 to 4 factor solution. For

example, Q/Q_{exp} decreases from 0.31 to 0.24 and the fraction of the residual aerosol mass decreases from 5% to 0.1% in moving from the one to the five factor solution. Figure S2 shows the residuals and scaled residuals for each time point in the matrix for the 5 factor solution, indicating that all the data are well fit. Solutions with 3 or fewer factors failed to separate the HOA and the IEPOX SOA factors, which are well described in the literature and were reasonably expected to be present in the data. One of the OOA-like spectra in the three factor solution also appeared to have signs of both the HOA and IEPOX SOA factor in the spectra, as evidenced by significant signal of the key marker ions $C_4H_9^+$ (m/z 57) for HOA and $C_5H_6O^+$ (m/z 82) for IEPOX SOA. In the four factor solution, an HOA factor was resolved along with three OOA-like spectra, though the OOA spectra show evidence of factor splitting (discussed below). The five factor solution was able to resolve an HOA, IEPOX-SOA and three OOA-like factors.

Figure S3 and S4 show the mass spectra and time series for the five factor solution. Examination of the mass spectra (Figure S3) suggests that the OOA factor has split. For example, the mass spectrum of Factor 3 is dominated by the CHO^+ ion with little signal through the rest of the spectra. The spectrum of Factor 1 is dominate by CO_2^+ and other ions that are based on the CO_2^+ signal (CO^+, H_2O^+, HO^+, O^+) in prescribed ratios (Aiken et al., 2008). These factors are unlikely to represent some real aerosol component, as no known OA produces such simple spectra. In addition, the time series of Factors 1 and 2 are highly correlated in time (see Figure S5). In summary, two factors are highly correlated in time (Factors 1 and 2) and a third factor is dominated by a single ion. Thus, we recombine Factors 1, 2, and 3 into a single factor, which we label OOA. The spectra of the resultant three factors (after re-combining) are shown in Figure S6 and the recombined factor is presented in the main text. The mathematical reason for the factor splitting is clear; aerosol loading is low, the AMS is sampling at a relatively fast rate (13 s averaging time), and the AMS spectra are dominated by a relatively small number of high S/N ions. In separate experiments, we downweighted the CHO^+, $C_2H_3O^+$, and CO_2^+ ion signals by factors of 2-10 in an attempt to minimize the splitting of the OOA factor, but were unsuccessful.

Comparison of the factor mass spectra to literature PMF spectra and correlation of the factor time profiles with independent measurements provides further support for the 5-factor solution. The combined OOA factor compares well with the spectra presented in the literature for OOA (e.g., (Zhang et al., 2007;Zhang et al., 2011;Zhang et al., 2005;Ng et al., 2010). As shown in Figure 6 in the main text, the OOA factor correlates well with ozone, a known secondary species that also forms through photochemical reactions. Similarly, the spectrum of Factor 4 compares well with the mass spectrum of HOA widely reported in the literature (e.g., (Zhang et al., 2007;Zhang et al., 2011;Zhang et al., 2005;Ng et al., 2010). As discussed in the text and shown in Figure 6, the HOA factor correlates well with CO, a known tracer of anthropogenic combustion processes. We label Factor 5 as the IEPOX SOA factor that is widely reported in the literature and believed to represent SOA formed from the heterogeneous uptake of isoprene epoxydiols onto pre-existing aerosol (Hu et al., 2015;Robinson et al., 2011;Lin et al., 2012). Our assignment is based on comparison with the factor mass spectral profile with those in the literature e.g., (Hu et al., 2015).

Number of Factors	Q/Q_{exp}	Notes
2	0.28	4% of mass unresolved, OOA-like factors resolved but look mixed

3	0.26	2% of mass still unresolved, OOA factors looks split and unrealistic, no HOA or IEPOX SOA factor
4	0.25	Most of mass resolved (0.1 % residual) , HOA factor now resolved, OOA factor split, unrealistic
5	0.24	IEPOX factor resolved, split OOA factor split, unrealistic

Table A1. Summary of scaled residuals and reasoning used in the choice of a 5 factor solution in the PMF analysis of the wet season HR-AMS data.

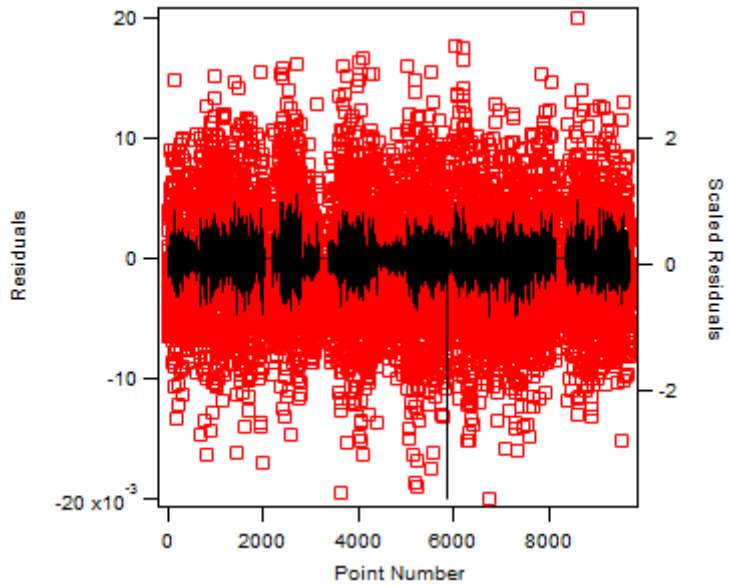

Figure S2. Absolute and scaled residuals for the wet season data matrix.

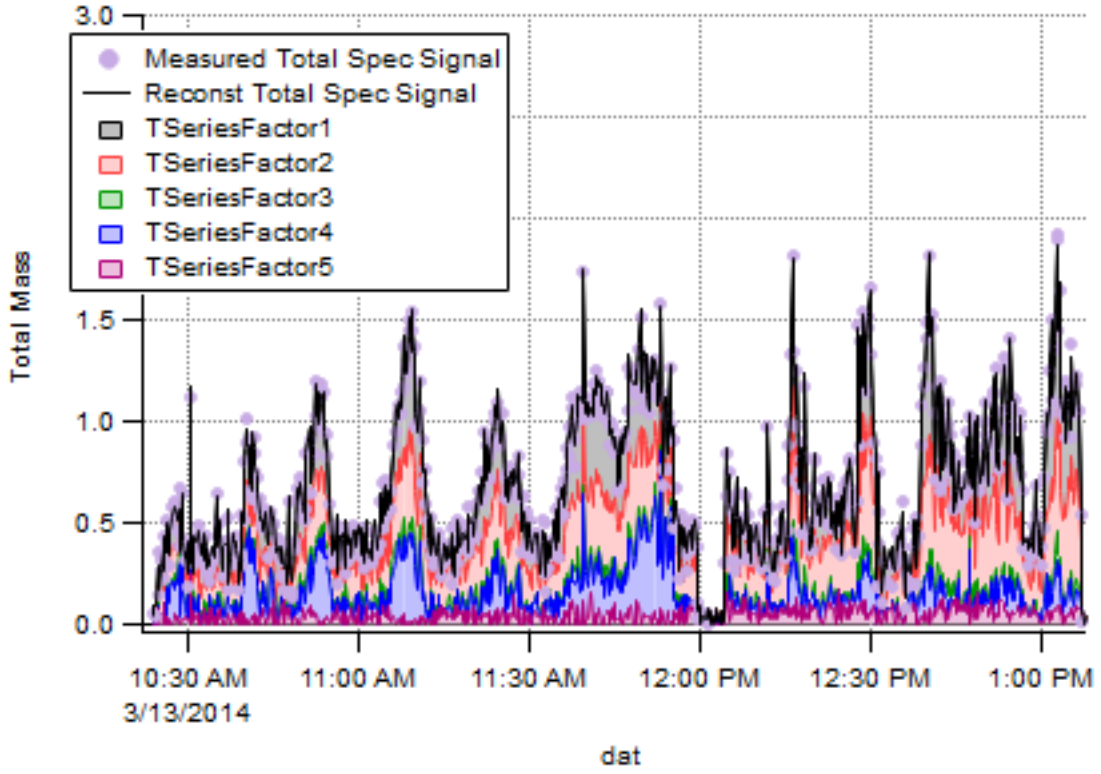

Figure S3. Reconstruction of the mass of the 5 Factor solution chosen for the wet season data set. The total measure mass is shown in the purple dots and the reconstructed mass is shown as a black line. Individual factors are color coded. To make the information legible, we have chosen to highlight the data for the March 13 flight presented in the main text. Factors 1, 2, and 3 were combined into a single OOA factor when reported in the main text as discussed in the SI above.

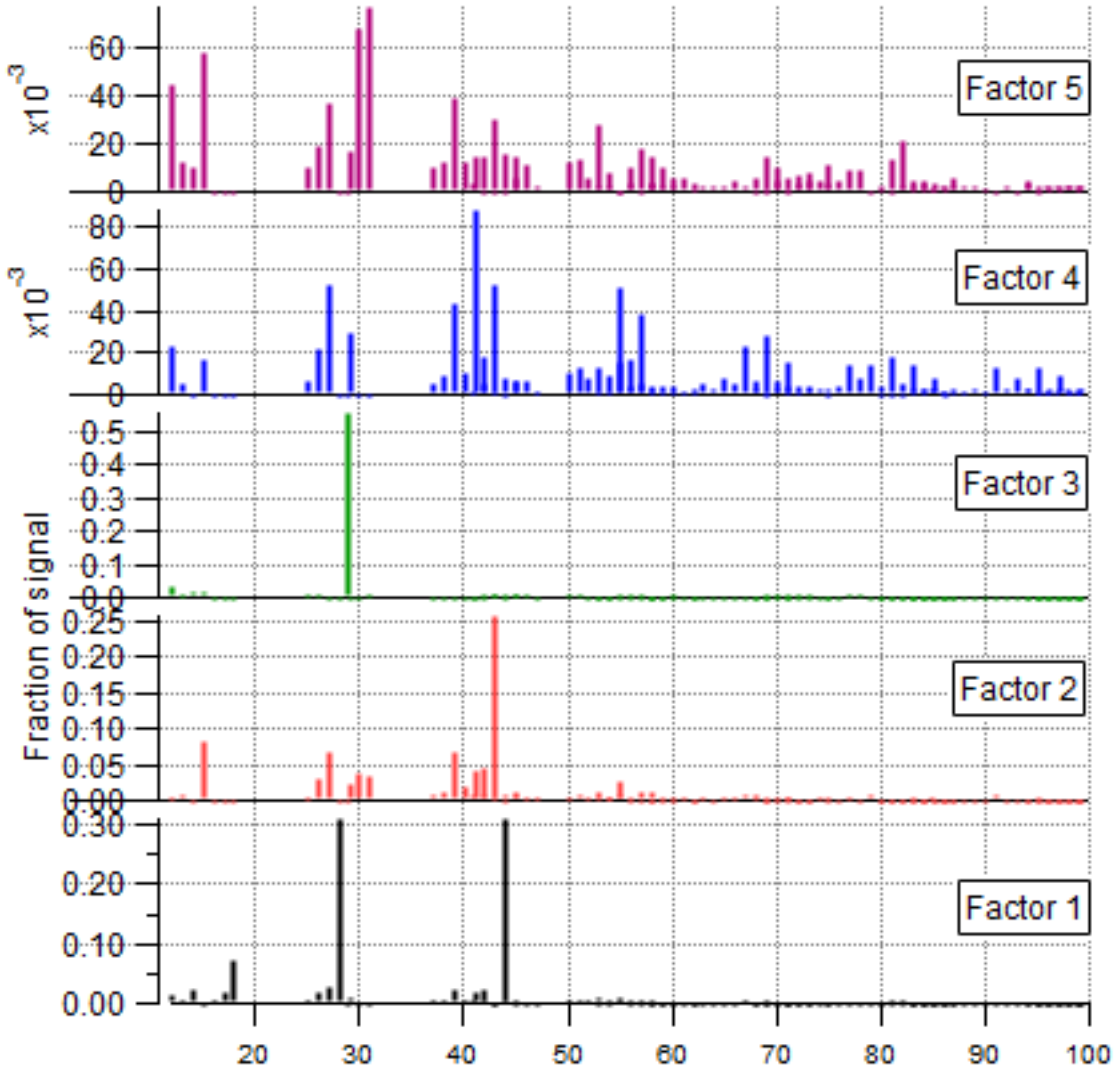

Figure S4. Mass spectral profiles of the 5 factor solution chosen for the wet season data. Factors 1, 2, and 3 were combined when reported in the main text as discussed in the SI.

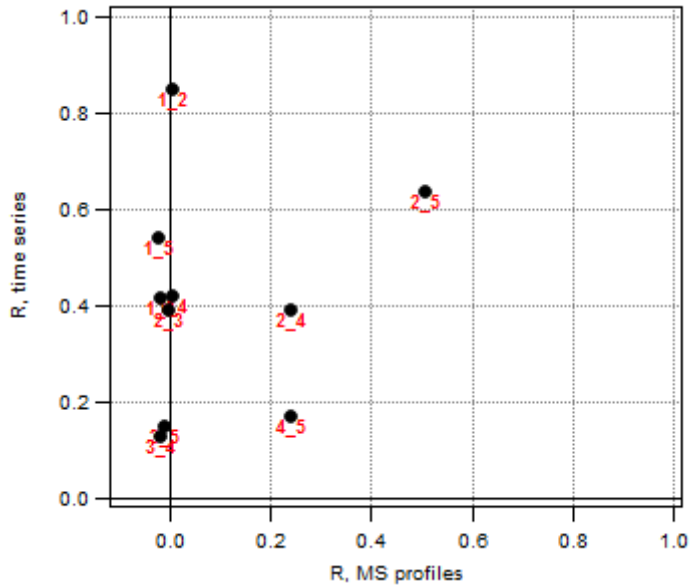

Figure S5. Plot of the correlation coefficients between the time series and mass spectra of the 5 factor solution.

For the finding of constant Δorg/ΔCO and increasing aerosol oxidation in an aging urban plumes, one question is the behaviors of VOCs according to PTR-MS measurements?

Concentrations of isoprene display a non-monotonic dependence on the distance of the plume from Manaus. The average isoprene concentrations are 1.49, 1.36, 0.88, 1.12, and 1.11 ppbv for plume transport distances of 0, 25, 45, 69, and 95 km, respectively. We note that fresh isoprene will continuously mix into the plume as it is transported over the forest. The concentration of m/z 71 (isoprene oxidation products) monotonically increase from 0.96 ppbv directly over the city to 1.27 at 95 km distance. The average tolene:benzene ratio also monotonically decreased with plume age, though conversion of this ratio to a plume age resulted in unrealistic values. We have added this information to the text.

Concentrations of isoprene are lower in the plume than the background values observed outside of it. Concentrations of isoprene inside the plume do not show a monotonic dependence on plume age, The concentration of isoprene oxidation products measured in the plume by the PTR-MS at m/z 71 monotonically increases with plume aging, from 0.96 ppbv directly over the city to 1.27 ppbv at the farthest leg. The average toluene:benzene ratio in the plume also monotonically decreases with plume aging as would be expected, though attempts to convert these ratios into a photochemical age resulted in unrealistically high estimates of the plume age, likely due to noise in the data as mentioned above (de Gouw et al., 2005).

Was the March 13 flight an isolated case or is the phenomenon more general for the Manaus emissions? What are the Δorg vs ΔCO values for other flights? How do they compare? Are there seasonal differences?

We have analyzed additional data and discussed this question in more detail in the revised manuscript and added Figure 7 to address it. Please see our response to Reviewer #1 (above)

which details the changes made to the manuscript. In short, the Δorg vs ΔCO values for two additional flights are similar to the March 13 data.

1. Page 5, line 15, what does the "13s data sampling interval" correspond to? Was the AMS operated under the standard MS mode (equal chopper-open and closed positions) or the fast sampling mode typically used for aircraft sampling?

The AMS was operated in the standard MS mode, with equal chopper open and closed periods. See also our response to a similar comment from Reviewer #1.

The AMS operated only in the standard "V"- MS mode (the particle sizing mode was not used) with a 13s data sampling interval and equal chopper open and closed periods of 3 seconds.

2. Page 5, line 28, what's the m/z range for the PTR-MS measurement?

The PTR-MS was run in an ion monitoring mode in which a limited number of pre-selected masses were monitored, rather than a scanning mode where the entire mass spectrum is recorded. In this study, the highest m/z value monitored was 137, corresponding to monoterpenes. We have updated the text to make this more clear. The spectrometer is capable of scanning up to m/z 500.

The PTR-MS was run in the ion monitoring mode in which the signals of a limited number of pre-selected of m/z values are sequentially measured with one measurement cycle taking 3.5 s.

3. Page 6, line 1, define E/N.

We have defined E/N in the manuscript.

Drift tube temperature, pressure and voltage were held at 60 °C, 2.22 hPa, and 600 V, respectively resulting in an electric field to gas density (E/N) ratio of 134 Td (1 Td $=1\times10^{-17}$ $cm^2V^{-1}s^{-1}$).

4. Page 6, what's SAMBBA?

We have defined SAMBBA in the text.

…the South American Biomass Burning Analysis (SAMBBA) campaign…

5. Page 6, line 31, mention the year and month for the Chen et al. study.

The year and month for the Chen study have been added.

Chen et al. reported AMS-measured wet-season (February 7 to March 13, 2008) campaign average organic and sulfate loadings

6. Page 7, Line 13, are there diurnal mixed layer height data to justify the usage of 700 m?

As seen in Table 1, the lowest flight legs were flow at 500 m or 600 m altitude above sea level and averaging data below 700 m captures these legs. The 700 m altitude was chosen so that any small altitude corrections due to underlying terrain or any small error in the altitude reading did not exclude data on the lowest altitude legs. Radiosonde balloons were launched from the T3 site

5 times a day every day during the campaign. The average diurnal mixed layer heights for both the wet and dry season GoAmazon 2014/15 periods based on these radiosondes are shown in Figure 3 of Giagrande et al. (2017) (Giangrande et al., 2017) They report average mixed layer heights of greater than 1000m above ground level by 10:00 local time in both the wet and dry seasons. The Manaus elevation is ~100 m, so yes, on average we were sampling the boundary layer at 700 m altitude during the flights. We have added a this information to the manuscript.

Giagrande et al. (2017) analyzed radiosonde data from the T3 site and report average mixed layer heights of greater than 1000 m above ground level at 10:00 local time in both the wet and dry seasons. Thus, the G-1 was typically sampling in the boundary layer on the lowest flight legs and the 700 m data should represent boundary layer conditions.

Page 7, line 18, what does 'sources' mean in this context?

We are referring to the influence of biomass burning in the dry season. We have revised this sentence to be more clear.

The fractional contribution of each species to the total loading is nearly identical when comparing seasons, despite the large differences in aerosol absolute mass concentrations and the larger influence of biomass burning in the dry season (Martin, 2016).

8. Page 7, line 22, what does "aircraft product distribution' mean?

Aircraft product distribution means averaged fractional composition of the aerosol measured from the aircraft. We have revised this sentence to be more clear.

The fractional contributions of each chemical species described herein are nearly identical to the previous reports from Chen et al. (2009, 2015).

9. Page 7 line 24, "suggests"

Corrected.

10. Page 7, line 30 - 31, was biomass burning influence detected during this study? What are the evidences? The citations were clearly not from Go-Amazon 2014/15.

Yes, biomass burning influence was detected through remote sensing, both by satellite and ground-based instruments as described in Martin 2016. We have added that reference to lines 30-31 and throughout the manuscript. In addition, the PTR-MS measurements of acetonitrile suggest a significant biomass burning influence. We have added this information to the text. Finally, the biomass burning background was often readily observed by the naked eye both from the aircraft and from the ground. The haze observed visually in the dry season was in stark contrast the clear conditions observed in the wet season.

In the dry season, back trajectory analysis indicate air masses originate from the Southern Hemisphere and travel up the Amazon River transporting pollution from the northern coastal cities (Martin et al., 2016). In addition, recirculation events transported air from the southern Amazon basin into the Manaus region (Martin et al., 2016). Intense biomass burning fires in the central and southern portion of the Amazon basin and in central Africa were observed in the dry season and a portion of these emissions

were transported to the Manaus region (Martin et al., 2016;Artaxo et al., 2013;Martin et al., 2010). In the dry season, more intense but less frequent convection produced approximately one quarter of the total rainfall observed in the wet season. As a result of the combination of transport and precipitation frequency, the Manaus region is significantly more polluted in the dry season.

However, the PTR-MS data, in addition to satellite and remote sensing measurements (Martin et al., 2016), also show that biomass burning significantly impacted the region. Measurements of acetonitrile, whose major source is biomass burning (Yokelson et al., 2009;Yokelson et al., 2007), are 2-3 times higher in the dry season than the wet season, indicating a significant biomass burning impact in the region. Biomass burning is a known source of OA (Jolleys et al., 2012;Bond et al., 2004;Yokelson et al., 2009;Ferek et al., 1998) and would also contribute to the higher aerosol concentrations observed in the dry season.

11. Page 7, line 32, spell out MSA.

We have spelled out MSA.

12. Page 8, line 1-2, give citation.

We were discussing our own observations, but have decided to delete this sentence as it was not illustrated in the figures and thus confusing.

13. How well is the correlation between IEPOX-SOA and m/z 82?

The correlation between the IEPOX SOA factor and the C_5H_6O ion has a Pearson correlation coefficient of r=0.80 for the entire wet season dataset.

14. Page 10, line 5, "this date"

We have fixed this error.

15. Page 10, line 15 – 16, might be useful to report the correlation coefficients.

We have added the correlation coefficients. As discussed in detail in the manuscript, the slope of these correlations changes with plume age. As a result, the correlations are degraded by the changing slope and correlation coefficients for individual legs are larger.

The HOA factor correlates strongly with CO (r=0.79 for all data at 500 m) while the OOA factor correlates strongly with ozone (r=0.81 for all data at 500 m), though we will show below that the slope of the correlation changes with plume age. The changing slope has the effect of degrading the HOA/CO and OOA/ozone correlations which are larger for individual plume legs.

16. Page 10, line 18, clarify the meaning of "transformation of HOA to SOA/OOA", e.g., through what mechanisms. Is oxidized POA counted as SOA?

As discussed later in the text (e.g., page 12 lines, 20-26) we are unsure of the chemical mechanism. The previous literature observations have generally attributed this conversion to evaporation of HOA, oxidation of the volatilized HOA in the gas phase, and re-condensation of the oxidized HOA as SOA (Robinson et al., 2007;Sage et al., 2008). In this mechanism, oxidized POA would be counted as SOA. Alternative possibilities leading to loss of HOA include dry

deposition and evaporation of HOA without oxidation and re-deposition of SOA. In this case, SOA deposition could come from either anthropogenic VOCs emitted in the Manaus plume or from oxidation of biogenic VOCs in the plume. We are unable to differentiate these mechanism sufficiently and we therefore tried to write the indicated text so as not to rule out any of these possibilities.

17. Page 10, line 23 - 24, this sentence is vague. What chemical mechanism?

We refer to heterogeneous uptake of gas-phase IEPOX on pre-existing aerosol surfaces to form IEPOX-derived SOA. We have revised the sentence to be more clear.

The IEPOX SOA factor does not appear to change with passage through the plume and does not correlate with sulfate aerosol on this day as may be expected based on the chemical mechanism, which requires heterogeneous uptake of gas-phase IEPOX onto inorganic aerosol to generate IEPOX SOA…

18. Page 10, line 26, limit of detection for IEPOX SOA was mentioned. What's the value and how was it determined?

The limit of detection for organics in this study, based on analysis of filter measurements as described in DeCarlo et al. (2006), is approximately 0.12 ug/m3, for the 13s averaging time we utilized. We have added this information to the manuscript (see also our response to a question on detection limits by reviewer #1). In addition, Ulbrich et al. (2009) report that factors that are less than 5% of the total mass are not accurately retrieved by the PMF routine. On the 500 m flight leg for the March 13 flight, neither criteria are met. We note that on other flights, IEPOX-SOA is above these detection limits.

Based on the standard deviation of these blank measurements (3σ) as described in the literature (DeCarlo et al., 2006), the detection limit of the AMS at the 13s sampling interval were 0.12, 0.01, 0.014, and 0.005 μg/m^3 for organics, sulfate, nitrate, and ammonium respectively.

19. Page 11, line 5 -9, how was Δorg/ΔCO determined, through background subtraction or linear fit? Either way, please provide details, e.g., the choice of background values or quality of linear fit etc. Consider to move some information in the supplementary to main body of the manuscript.

We use method 1 (linear fit with no background subtraction) for data shown in the main manuscript. However, it is important to note that, as we show in the supplementary material, results are insensitive to the chosen method and to reasonable choices of background CO and org values. We have moved some information on the Δorg/ΔCO calculate from the SI to the main text.

The Δorg/ΔCO values shown in Figure 7 were calculated as the slope of a linear regression line between the AMS-measured organic mass loadings and CO concentrations. All data for each flight leg perpendicular to the wind direction were included. Background values of OA and CO were not subtracted from the data and the regression was not forced through the origin. We acknowledge that calculation of Δorg/ΔCO values can be sensitive to the calculation method and choice of background values for both OA and CO; therefore, we performed calculations using different methods and assuming

different background concentrations for both OA and CO and find general agreement between these methods (see SI for more details).

20. Page 12, line 14 – 15, change “occurring” to “is occurring”.

We have corrected this error.

21. Page 13, line 18, speaking of sulfur emissions and oxidation of compounds such as DMS, it would be necessary to check for the presence of methylate /MSA in particles. BTW, DMS should be defined.

We have defined DMS.

The most recent literature method for identifying MSA in aerosol involve utilizing the $CH_3SO_2,^+$ ion as a signature (Huang et al., 2017). Due to its mass defect, this ion is well separated from other typical aerosol components so it should be easily detectable if present. We do not detect evidence of this ion in our dataset. Thus, we can’t positively identify MSA in the particles. The oxidation of DMS and H_2S was described in other literature studies as significant sources of sulfate in the Amazon Basin, though not the major source (Andreae et al., 1990;Chen et al., 2009). We are unsure if this represents a discrepancy or not. One possible explanation is that H_2S, which was found in approximately 10x the concentration of DMS, is responsible for most of the biogenic sulfate production (Andreae et al., 1990). Our background measurements are roughly consistent with the literature estimate of the natural in-basin contribution to sulfate aerosol.

22. Page 14, line 5, it is not that aerosol composition “did not change” but rather “did not change significantly”.

We have made the suggested edit.

23. Figure 1, consider to mention in the figure caption the duration of the flight.

We have added the flight time to the figure caption. In response to a comment from Reviewer 1, we have also added a table with the flight times for all research flights.

Takeoff time was 10:14 (local time) and landing time was 13:21 for a total flight duration of three hours and nine minutes.

24. Figure 2, how were the average pie charts calculated, straight averages of the fractions or mass weighted averages?

The Figure 2 pie charts were calculated by binning all the mass loading data from a particular season together and calculating the fractions. We have added this clarification to the text.

The bottom panel shows the distribution of the chemical species as a mass weighted average of all data from the respective measurement season.

25. Figure 4, What are the aerosol species concentrations, same as mentioned in Fig. 2 (23C and 1 atm)?

All data presented in the manuscript are normalized to 23 C, 1 atm. We have added a note to all figure captions mentioning the normalization. We have also pointed out in the experimental section that data presented in the manuscript are normalized to 23 C, 1 atm.

26. According to Figure 4, the time series of O3 and CO appear to correlate quite well. Figure 5 shows that HOA and OOA go up and down together as well. It would be interesting to know the cross correlations between OOA, HOA, CO and O3.

A cross correlation table listing the Pearson correlation coefficient (r) for each species is shown below. In general, ozone and CO are correlated but the slope of the correlation changes as ozone is formed with plume aging. This correlation breaks down very close the city, as seen in figure 4 around 11:45 where ozone and CO are briefly anti-correlated. On this portion of the flight, the correlation of HOA and OOA also breaks down.

	OOA	**HOA**	**Ozone**	**CO**
OOA		0.64	0.81	0.77
HOA	0.64		0.58	0.79
Ozone	0.81	0.58		0.71
CO	0.77	0.79	0.71	

27. Figure 5, was NO2 measured? How does Ox time series look like?

NO_2 measurements were attempted, but exposure of the instrument to high NOx concentrations on the airport tarmac lead to artificially high NO_2 measurements, particularly early in the flights. The figure below shows the ozone, Ox and NO_2 trace appended to a simplified version of Figure 5. Also below is a table presenting the mean ozone and Ox measured in the plume as a function of leg number and hence plume aging. The figure shows that Ox is dominated by ozone, though NO2 may be a significant fraction of Ox close to the city (e.g. around 11:45). The table shows that these quantities increase from Legs 1-4 and decrease on Leg 5. Trends in peak ozone/Ox show a similar pattern. Due to the bias in the NO_2 measurement, we prefer not to publish the Ox time series in the final manuscript.

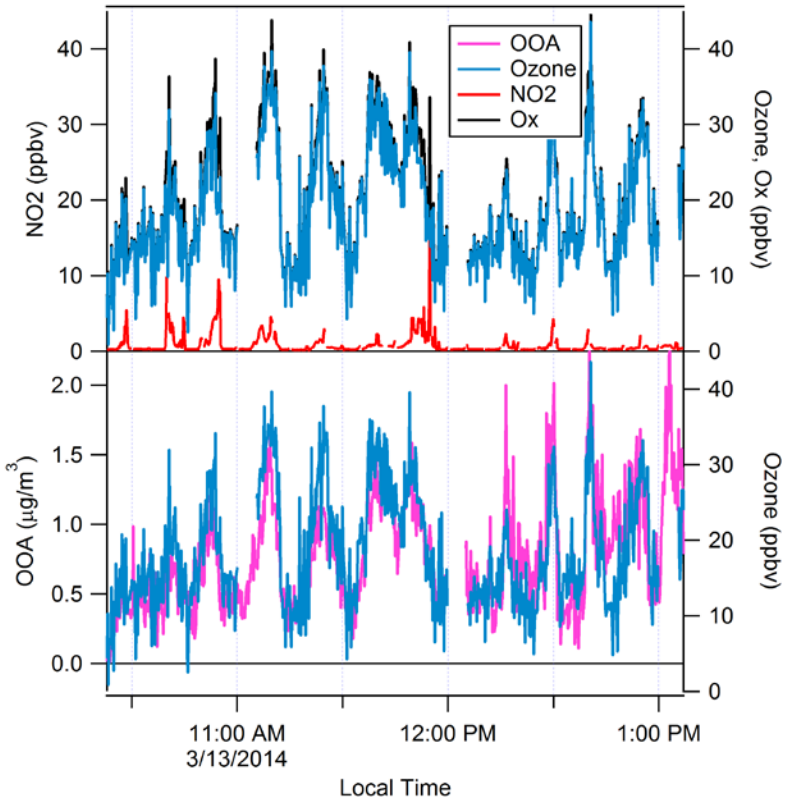

	Distance (km)	mean NO_2 (ppb)	mean O_3 (ppbv)	mean O_x (ppbv)
Leg 1	0	0.77	12.14	12.89
Leg 2	24	1.49	16.27	17.73
Leg 3	45	2.29	20.84	23.07
Leg 4	69	1.31	25.96	27.54
Leg 5	95	0.69	21.95	22.63

28. Figure 6, consider to add error bars for the data.

We have added error bars to the data. The error bars are based on standard addition of errors of the AMS and CO measurements. To keep the graph legible and clear, we added an error bar to only one point in each measurement series.

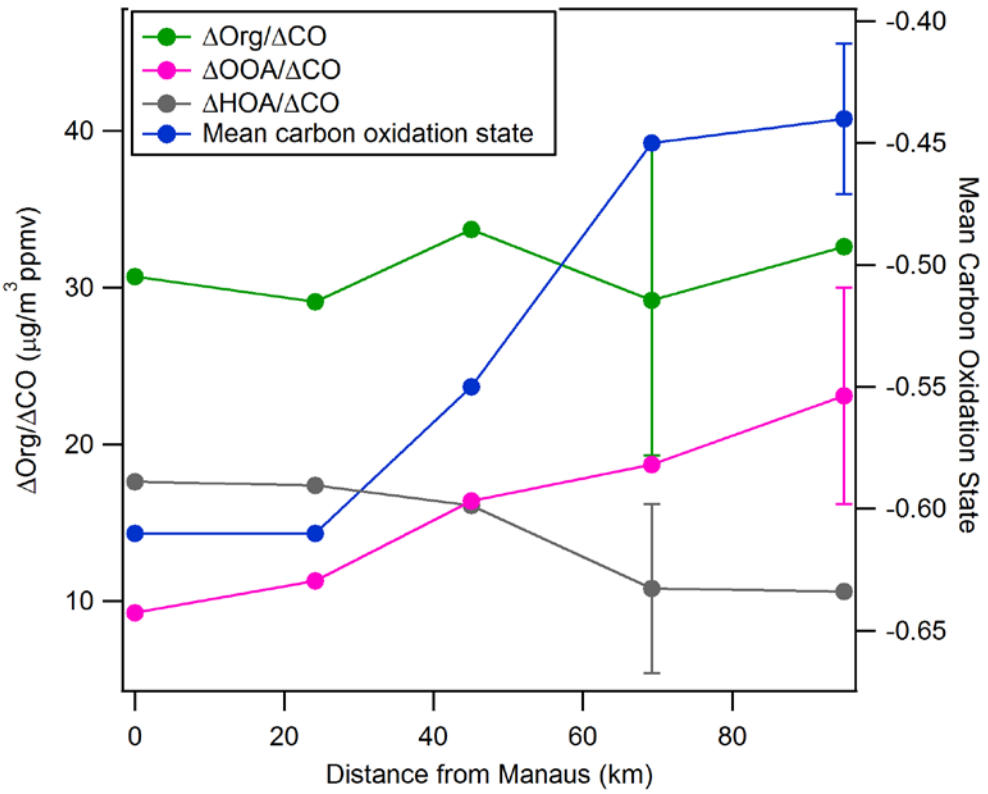

References

Aiken, A. C., DeCarlo, P. F., and Jimenez, J. L.: Elemental analysis of organic species with electron ionization high-resolution mass spectrometry, Anal Chem, 79, 8350-8358, 10.1021/ac071150w, 2007.

Aiken, A. C., DeCarlo, P. F., Kroll, J. H., Worsnop, D. R., Huffman, J. A., Docherty, K., Ulbrich, I. M., Mohr, C., Kimmel, J. R., Sueper, D., Zhang, Q., Sun, Y., Trimborn, A., Northway, M., Ziemann, P. J., Canagaratna, M. R., Alfarra, R., Prevot, A. S. H., Dommen, J., Duplissy, J., Metzger, A., Baltensperger, U., and Jimenez, J. L.: O/C and OM/OC Ratios of Primary, Secondary, and Ambient Organic Aerosols with High Resolution Time-of-Flight Aerosol Mass Spectrometry, Environ. Sci. Technol., 42, 4478-4485, doi:10.1021/es703009q, 2008.

Allan, J. D., Jiminez, J. L., Williams, P. I., Alfarra, M. R., Bower, K. N., Jayne, J. T., Coe, H., and Worsnop, D. R.: Quantitative sampling using an Aerodyne aerosol mass spectrometer - 1. Techniques of data interpretation and error analysis, J. Geophys. Res., 108, 4090, 2003.

Allan, J. D., Delia, A. E., Coe, H., Bower, K. N., Alfarra, M. R., Jimenez, J. L., Middlebrook, A. M., Drewnick, F., Onasch, T. B., Canagaratna, M. R., Jayne, J. T., and Worsnopf, D. R.: A generalised method for the extraction of chemically resolved mass spectra from aerodyne aerosol mass spectrometer data, Journal of Aerosol Science, 35, 909-922, 2004.

Andreae, M. O., Berresheim, H., Bingemer, H., Jacob, D. J., Lewis, B. L., Li, S. M., and Talbot, R. W.: The Atmospheric Sulfur Cycle over the Amazon Basin .2. Wet Season, Journal of Geophysical Research-Atmospheres, 95, 16813-16824, DOI 10.1029/JD095iD10p16813, 1990.

Artaxo, P., Rizzo, L. V., Brito, J. F., Barbosa, H. M. J., Arana, A., Sena, E. T., Cirino, G. G., Bastos, W., Martin, S. T., and Andreae, M. O.: Atmospheric aerosols in Amazonia and land use change: from natural biogenic to biomass burning conditions, Faraday Discussions, 165, 203-235, 10.1039/C3FD00052D, 2013.

Atkinson, R., and Arey, J.: Atmospheric Degradation of Volatile Organic Compounds, Chemical Reviews, 103, 4605-4638, 10.1021/cr0206420, 2003.

Bond, T. C., Streets, D. G., Yarber, K. F., Nelson, S. M., Woo, J. H., and Klimont, Z.: A technology-based global inventory of black and organic carbon emissions from combustion, Journal of Geophysical Research-Atmospheres, 109, n/a-n/a, Artn D14203

10.1029/2003jd003697, 2004.

Burleyson, C. D., Feng, Z., Hagos, S. M., Fast, J., Machado, L. A. T., and Martin, S. T.: Spatial Variability of the Background Diurnal Cycle of Deep Convection around the GoAmazon2014/5 Field Campaign Sites, Journal of Applied Meteorology and Climatology, 55, 1579-1598, 10.1175/jamc-d-15-0229.1, 2016.

Canagaratna, M. R., Jimenez, J. L., Kroll, J. H., Chen, Q., Kessler, S. H., Massoli, P., Hildebrandt Ruiz, L., Fortner, E., Williams, L. R., Wilson, K. R., Surratt, J. D., Donahue, N. M., Jayne, J. T., and Worsnop, D. R.: Elemental ratio measurements of organic compounds using aerosol mass spectrometry: characterization, improved calibration, and implications, Atmos. Chem. Phys., 15, 253-272, 10.5194/acp-15-253-2015, 2015.

Chen, Q., Farmer, D. K., Schneider, J., Zorn, S. R., Heald, C. L., Karl, T. G., Guenther, A., Allan, J. D., Robinson, N., Coe, H., Kimmel, J. R., Pauliquevis, T., Borrmann, S., Poschl, U., Andreae, M. O., Artaxo, P., Jimenez, J. L., and Martin, S. T.: Mass spectral characterization of submicron biogenic organic particles in the Amazon Basin, Geophys. Res. Lett., 36, 5, Artn L20806

10.1029/2009gl039880, 2009.

Cirino, G. G., Brito, J., Barbosa, H. J. M., Rizzo, L. V., Carbone, S., de Sa, S. S., Tunved, P., Jimenez, J. L., Palm, B., Souza, R. A. F., Lavric, J., Tota, J., Oliveira, M., Wolff, S., Martin, S. T., and Artaxo, P.: Ground site observations of Manaus city plume evolution in GoAmazon2014/5, In preparation for Atmsopheric Chemistry and Physics, 2018.

de Gouw, J. A., Middlebrook, A. M., Warneke, C., Goldan, P. D., Kuster, W. C., Roberts, J. M., Fehsenfeld, F. C., Worsnop, D. R., Canagaratna, M. R., Pszenny, A. A. P., Keene, W. C., Marchewka, M., Bertman, S. B., and Bates, T. S.: Budget of organic carbon in a polluted atmosphere: Results from the New England Air Quality Study in 2002, J. Geophys. Res.-Atmos., 110, 10.1029/2004JD005623, 2005.

DeCarlo, P. F., Kimmel, J. R., Trimborn, A., Northway, M. J., Jayne, J. T., Aiken, A. C., Gonin, M., Fuhrer, K., Horvath, T., Docherty, K. S., Worsnop, D. R., and Jimenez, J. L.: Field-deployable, high-resolution, time-of-flight aerosol mass spectrometer, Anal Chem, 78, 8281-8289, 10.1021/ac061249n, 2006.

Ferek, R. J., Reid, J. S., Hobbs, P. V., Blake, D. R., and Liousse, C.: Emission factors of hydrocarbons, halocarbons, trace gases and particles from biomass burning in Brazil, Journal of Geophysical Research-Atmospheres, 103, 32107-32118, Doi 10.1029/98jd00692, 1998.

Giangrande, S. E., Feng, Z., Jensen, M. P., Comstock, J. M., Johnson, K. L., Toto, T., Wang, M., Burleyson, C., Bharadwaj, N., Mei, F., Machado, L. A. T., Manzi, A. O., Xie, S., Tang, S., Silva Dias, M. A. F., de Souza, R. A. F., Schumacher, C., and Martin, S. T.: Cloud characteristics, thermodynamic controls and radiative impacts during the Observations and Modeling of the Green Ocean Amazon (GoAmazon2014/5) experiment, Atmos. Chem. Phys., 17, 14519-14541, 10.5194/acp-17-14519-2017, 2017.

Guenther, A. B., Jiang, X., Heald, C. L., Sakulyanontvittaya, T., Duhl, T., Emmons, L. K., and Wang, X.: The Model of Emissions of Gases and Aerosols from Nature version 2.1 (MEGAN2.1): an extended and updated framework for modeling biogenic emissions, Geosci. Model Dev., 5, 1471-1492, 10.5194/gmd-5-1471-2012, 2012.

Hu, W. W., Campuzano-Jost, P., Palm, B. B., Day, D. A., Ortega, A. M., Hayes, P. L., Krechmer, J. E., Chen, Q., Kuwata, M., Liu, Y. J., de Sa, S. S., McKinney, K., Martin, S. T., Hu, M., Budisulistiorini, S. H., Riva, M., Surratt, J. D., St Clair, J. M., Isaacman-Van Wertz, G., Yee, L. D., Goldstein, A. H., Carbone, S., Brito, J., Artaxo, P., de Gouw, J. A., Koss, A., Wisthaler, A., Mikoviny, T., Karl, T., Kaser, L., Jud, W., Hansel, A., Docherty, K. S., Alexander, M. L., Robinson, N. H., Coe, H., Allan, J. D., Canagaratna, M. R., Paulot, F., and Jimenez, J. L.: Characterization of a real-time tracer for isoprene epoxydiols-derived secondary organic aerosol (IEPOX-SOA) from aerosol mass spectrometer measurements, Atmos. Chem. Phys., 15, 11807-11833, 10.5194/acp-15-11807-2015, 2015.

Huang, S., Poulain, L., van Pinxteren, D., van Pinxteren, M., Wu, Z., Herrmann, H., and Wiedensohler, A.: Latitudinal and Seasonal Distribution of Particulate MSA over the Atlantic using a Validated Quantification Method with HR-ToF-AMS, Environ. Sci. Technol., 51, 418-426, 10.1021/acs.est.6b03186, 2017.

Jacob, D. J.: Introduction to Atmospheric Chemistry, Princeton University Press, 1999.

Jimenez, J. L., Jayne, J. T., Shi, Q., Kolb, C. E., Worsnop, D. R., Yourshaw, I., Seinfeld, J. H., Flagan, R. C., Zhang, X. F., Smith, K. A., Morris, J. W., and Davidovits, P.: Ambient aerosol sampling using the Aerodyne Aerosol Mass Spectrometer, Journal of Geophysical Research-Atmospheres, 108, 8425, Artn 8425

10.1029/2001jd001213, 2003.

Jolleys, M. D., Coe, H., McFiggans, G., Capes, G., Allan, J. D., Crosier, J., Williams, P. I., Allen, G., Bower, K. N., Jimenez, J. L., Russell, L. M., Grutter, M., and Baumgardner, D.: Characterizing the aging of biomass burning organic aerosol by use of mixing ratios: a meta-analysis of four regions, Environ Sci Technol, 46, 13093-13102, 10.1021/es302386v, 2012.

Kleinman, L. I., Daum, P. H., Lee, Y. N., Nunnermacker, L. J., Springston, S. R., Weinstein-Lloyd, J., Hyde, P., Doskey, P., Rudolph, J., Fast, J., and Berkowitz, C.: Photochemical age determinations in the Phoenix metropolitan area, Journal of Geophysical Research-Atmospheres, 108, 14, 10.1029/2002jd002621, 2003.

Kroll, J. H., Donahue, N. M., Jimenez, J. L., Kessler, S. H., Canagaratna, M. R., Wilson, K. R., Altieri, K. E., Mazzoleni, L. R., Wozniak, A. S., Bluhm, H., Mysak, E. R., Smith, J. D., Kolb, C. E., and Worsnop, D. R.: Carbon oxidation state as a metric for describing the chemistry of atmospheric organic aerosol, Nat Chem, 3, 133-139, 10.1038/nchem.948, 2011.

Lin, Y. H., Zhang, Z., Docherty, K. S., Zhang, H., Budisulistiorini, S. H., Rubitschun, C. L., Shaw, S. L., Knipping, E. M., Edgerton, E. S., Kleindienst, T. E., Gold, A., and Surratt, J. D.: Isoprene epoxydiols as precursors to secondary organic aerosol formation: acid-catalyzed reactive uptake studies with authentic compounds, Environ Sci Technol, 46, 250-258, 10.1021/es202554c, 2012.

Lindinger, W., Hansel, A., and Jordan, A.: On-line monitoring of volatile organic compounds at pptv levels by means of proton-transfer-reaction mass spectrometry (PTR-MS) - Medical applications, food control and environmental research, Int. J. Mass Spectrom., 173, 191-241, Doi 10.1016/S0168-1176(97)00281-4, 1998.

Machado, L. A. T., Calheiros, A. J. P., Biscaro, T., Giangrande, S., Silva Dias, M. A. F., Cecchini, M. A., Albrecht, R., Andreae, M. O., Araujo, W. F., Artaxo, P., Borrmann, S., Braga, R., Burleyson, C., Eichholz, C. W., Fan, J., Feng, Z., Fisch, G. F., Jensen, M. P., Martin, S. T., Pöschl, U., Pöhlker, C., Pöhlker, M. L., Ribaud, J. F., Rosenfeld, D., Saraiva, J. M. B., Schumacher, C., Thalman, R., Walter, D., and Wendisch, M.: Overview: Precipitation characteristics and sensitivities to environmental conditions during GoAmazon2014/5 and ACRIDICON-CHUVA, Atmos. Chem. Phys., 18, 6461-6482, 10.5194/acp-18-6461-2018, 2018.

Martin, S. T., Andreae, M. O., Artaxo, P., Baumgardner, D., Chen, Q., Goldstein, A. H., Guenther, A., Heald, C. L., Mayol-Bracero, O. L., McMurry, P. H., Pauliquevis, T., Poschl, U., Prather, K. A., Roberts, G. C., Saleska, S. R., Dias, M. A. S., Spracklen, D. V., Swietlicki, E., and Trebs, I.: Sources and Properties of Amazonian Aerosol Particles, Reviews of Geophysics, 48, n/a-n/a, Artn Rg2002

10.1029/2008rg000280, 2010.

Martin, S. T., Artaxo, P., Machado, L. A. T., Manzi, A. O., Souza, R. A. F., Schumacher, C., Wang, J., Andreae, M. O., Barbosa, H. M. J., Fan, J., Fisch, G., Goldstein, A. H., Guenther, A., Jimenez, J. L., Poschl, U., Dias, M. A. S., Smith, J. N., and Wendisch, M.: Introduction: Observations and Modeling of the Green

Ocean Amazon (GoAmazon2014/5), Atmos. Chem. Phys., 16, 4785-4797, 10.5194/acp-16-4785-2016, 2016.

Ng, N. L., Canagaratna, M. R., Zhang, Q., Jimenez, J. L., Tian, J., Ulbrich, I. M., Kroll, J. H., Docherty, K. S., Chhabra, P. S., Bahreini, R., Murphy, S. M., Seinfeld, J. H., Hildebrandt, L., Donahue, N. M., DeCarlo, P. F., Lanz, V. A., Prevot, A. S. H., Dinar, E., Rudich, Y., and Worsnop, D. R.: Organic aerosol components observed in Northern Hemispheric datasets from Aerosol Mass Spectrometry, Atmos. Chem. Phys., 10, 4625-4641, 10.5194/acp-10-4625-2010, 2010.

Paatero, P., and Tapper, U.: Positive matrix factorization: A non-negative factor model with optimal utilization of error estimates of data values, Environmetrics, 5, 111-126, 10.1002/env.3170050203, 1994.

Paatero, P.: Least squares formulation of robust non-negative factor analysis, Chemometrics and Intelligent Laboratory Systems, 37, 23-35, Doi 10.1016/S0169-7439(96)00044-5, 1997.

Parrish, D. D., Hahn, C. J., Williams, E. J., Norton, R. B., Fehsenfeld, F. C., Singh, H. B., Shetter, J. D., Gandrud, B. W., and Ridley, B. A.: INDICATIONS OF PHOTOCHEMICAL HISTORIES OF PACIFIC AIR MASSES FROM MEASUREMENTS OF ATMOSPHERIC TRACE SPECIES AT POINT ARENA, CALIFORNIA, Journal of Geophysical Research-Atmospheres, 97, 15883-15901, 10.1029/92jd01242, 1992.

Robinson, A. L., Donahue, N. M., Shrivastava, M. K., Weitkamp, E. A., Sage, A. M., Grieshop, A. P., Lane, T. E., Pierce, J. R., and Pandis, S. N.: Rethinking organic aerosols: semivolatile emissions and photochemical aging, Science, 315, 1259-1262, 10.1126/science.1133061, 2007.

Robinson, N. H., Hamilton, J. F., Allan, J. D., Langford, B., Oram, D. E., Chen, Q., Docherty, K., Farmer, D. K., Jimenez, J. L., Ward, M. W., Hewitt, C. N., Barley, M. H., Jenkin, M. E., Rickard, A. R., Martin, S. T., McFiggans, G., and Coe, H.: Evidence for a significant proportion of Secondary Organic Aerosol from isoprene above a maritime tropical forest, Atmos. Chem. Phys., 11, 1039-1050, 10.5194/acp-11-1039-2011, 2011.

Sage, A. M., Weitkamp, E. A., Robinson, A. L., and Donahue, N. M.: Evolving mass spectra of the oxidized component of organic aerosol: results from aerosol mass spectrometer analyses of aged diesel emissions, Atmos. Chem. Phys., 8, 1139-1152, DOI 10.5194/acp-8-1139-2008, 2008.

Seinfeld, J. H.: Clouds, contrails, and climate., Nature, 391, 837-838, 1998.

Ulbrich, I. M., Canagaratna, M. R., Zhang, Q., Worsnop, D. R., and Jimenez, J. L.: Interpretation of organic components from Positive Matrix Factorization of aerosol mass spectrometric data, Atmos. Chem. Phys., 9, 2891-2918, 10.5194/acp-9-2891-2009, 2009.

Yokelson, R. J., Karl, T., Artaxo, P., Blake, D. R., Christian, T. J., Griffith, D. W. T., Guenther, A., and Hao, W. M.: The Tropical Forest and Fire Emissions Experiment: overview and airborne fire emission factor measurements, Atmos. Chem. Phys., 7, 5175-5196, 10.5194/acp-7-5175-2007, 2007.

Yokelson, R. J., Crounse, J. D., DeCarlo, P. F., Karl, T., Urbanski, S., Atlas, E., Campos, T., Shinozuka, Y., Kapustin, V., Clarke, A. D., Weinheimer, A., Knapp, D. J., Montzka, D. D., Holloway, J., Weibring, P., Flocke, F., Zheng, W., Toohey, D., Wennberg, P. O., Wiedinmyer, C., Mauldin, L., Fried, A., Richter, D., Walega, J., Jimenez, J. L., Adachi, K., Buseck, P. R., Hall, S. R., and Shetter, R.: Emissions from biomass burning in the Yucatan, Atmos. Chem. Phys., 9, 5785-5812, DOI 10.5194/acp-9-5785-2009, 2009.

Zhang, Q., Worsnop, D. R., Canagaratna, M. R., and Jimenez, J. L.: Hydrocarbon-like and oxygenated organic aerosols in Pittsburgh: insights into sources and processes of organic aerosols, Atmos. Chem. Phys., 5, 3289-3311, 2005.

Zhang, Q., Jimenez, J. L., Canagaratna, M. R., Allan, J. D., Coe, H., Ulbrich, I., Alfarra, M. R., Takami, A., Middlebrook, A. M., Sun, Y. L., Dzepina, K., Dunlea, E., Docherty, K., DeCarlo, P. F., Salcedo, D., Onasch, T., Jayne, J. T., Miyoshi, T., Shimono, A., Hatakeyama, S., Takegawa, N., Kondo, Y., Schneider, J., Drewnick, F., Borrmann, S., Weimer, S., Demerjian, K., Williams, P., Bower, K., Bahreini, R., Cottrell, L., Griffin, R. J., Rautiainen, J., Sun, J. Y., Zhang, Y. M., and Worsnop, D. R.: Ubiquity and dominance of oxygenated species in organic aerosols in anthropogenically-influenced Northern Hemisphere midlatitudes, Geophys. Res. Lett., 34, n/a-n/a, 10.1029/2007gl029979, 2007.

Zhang, Q., Jimenez, J. L., Canagaratna, M. R., Ulbrich, I. M., Ng, N. L., Worsnop, D. R., and Sun, Y.: Understanding atmospheric organic aerosols via factor analysis of aerosol mass spectrometry: a review, Anal Bioanal Chem, 401, 3045-3067, 10.1007/s00216-011-5355-y, 2011.

~~Aircraft Observations of Aerosol in the Manaus Urban Plume and Surrounding Tropical Forest during GoAmazon 2014/15~~
Aircraft Observations of the Chemical Composition and Aging of Aerosol in the Manaus Urban Plume during GoAmazon 2014/5

John E. Shilling[1], Mikhail S. Pekour[1], Edward C. Fortner[2], Paulo Artaxo[3], Suzane de Sá[4], John M. Hubbe[1], Karla M. Longo[5], Luiz A.T. Machado[6], Scot T. Martin[4,7], Stephen R. Springston[8], Jason Tomlinson[1], Jian Wang[8]

[1]Atmospheric Sciences and Global Change Division, Pacific Northwest National Laboratory, Richland, Washington, USA
[2]Center for Aerosol and Cloud Chemistry, Aerodyne Research, Billerica, Massachusetts, USA
[3]Institute of Physics, University of Sao Paulo, Sao Paulo, Brazil
[4]John A. Paulson School of Engineering and Applied Sciences and Department of Earth and Planetary Sciences, Harvard University, Cambridge, Massachusetts, USA
[5]University Space Research Association/Goddard Earth Sciences Technology and Research (USRA/GESTAR), National Aeronautics and Space Administration, Goddard Space Flight Center, Columbia, Maryland, USA
[6]Centro de Previsao de Tempo e Estudos Climaticos – Instituto Nacional de Pesquisas Espaciais, Sao Jose dos Campos, Brazil
[7]Department of Earth and Planetary Sciences, Harvard University, Cambridge, Massachusetts, USA
[8]Environmental and Climate Sciences Department, Brookhaven National Laboratory, Upton, New York, USA

Correspondence to: John E. Shilling (john.shilling@pnnl.gov)

Abstract. The Green Ocean Amazon (GoAmazon 2014/5) campaign, conducted from January 2014 – December 2015 in the vicinity of Manaus, Brazil, was designed to study the aerosol lifecycle and aerosol-cloud interactions in both pristine and anthropogenically-influenced conditions. As part of this campaign, the U.S. Department of Energy (DOE) G-1 research aircraft was deployed from February 17 – March 25, 2014 (wet season) and September 6 – October 5, 2014 (dry season) to investigate aerosol and cloud properties aloft. Here, we present results from the G-1 deployments focusing on measurements of the aerosol chemical composition and discussion of aerosol sources and secondary organic aerosol formation and aging.

In the first portion of the manuscript, we provide an overview of the data and compare and contrast the data from the wet and dry season. Organic aerosol (OA) dominates the deployment-averaged chemical composition, comprising ~~78~~80% of the non-refractory PM_1 aerosol mass with sulfate comprising ~~13~~14%, nitrate ~~5~~2%, and ammonium 4%. This product distribution was unchanged between seasons, despite the fact that total aerosol loading was significantly higher in the dry season and that regional and local biomass burning was a significant source of OA mass in the dry, but not wet, season. However, the OA was more oxidized in the dry season, with the median of the mean carbon oxidation state increasing from -0.45 in the wet season to -0.02 in the dry season.

In the second portion of the manuscript, we discuss the evolution of the Manaus plume~~.~~, focusing on March 13, 2014, one of the ~~golden~~ exemplar days in the wet season. On this flight, we observe a clear increase in OA concentrations in the Manaus

plume relative to the background. As the plume is transported downwind and ages, we observe dynamic changes in the OA. The mean carbon oxidation state of the OA increases from -0.6 to -0.45 during the 4-5 hours of photochemical aging. Hydrocarbon-like organic aerosol (HOA) mass is lost with ΔHOA/ΔCO values decreasing from 17.6 μg/m^3 ppmv^{-1} over Manaus to 10.6 μg/m^3 ppmv^{-1} 95 km downwind. Loss of HOA is balanced out by formation of oxygenated organic aerosol (OOA) with ΔOOA/ΔCO increasing from 9.2 to 23.1 μg/m^3 ppmv^{-1}. Because HOA loss is balanced by OOA formation, we observe little change in the net Δorg/ΔCO values; Δorg/ΔCO averages 31 μg/m^3 ppmv^{-1} and does not increase with aging. Analysis of the Manaus plume evolution using data from two additional flights in the wet season showed similar trends in Δorg/ΔCO as the March 13 flight; Δorg/ΔCO values averaged 34 μg/m^3 ppmv^{-1} and showed little change over 4-6.5 hours of aging. Our observation of constant Δorg/ΔCO are in contrast to literature studies of the outflow of several North American cities, which report significant increases in Δorg/ΔCO for the first day of plume aging. These observations suggest that SOA formation in the Manaus plume occurs, at least in part, by a different mechanism than observed in urban outflow plumes in most other literature studies. Constant Δorg/ΔCO with plume aging has been observed in many biomass burning plumes, but we are unaware of reports of fresh urban emissions aging in this manner. These observations show that urban pollution emitted from Manaus in the wet season forms much less particulate downwind than urban pollution emitted from North American cities.

1 Introduction

Aerosol particles have important impacts on visibility, human health, and the Earth's energy balance and water cycle. The impact of aerosol particles on radiation balance, in particular their impact on cloud properties and lifetimes, continues to be a significant source of uncertainty for global climate models (Intergovernmental Panel on Climate, 2014). An extensive series of field studies has shown that a large fraction of the total non-refractory aerosol mass is organic aerosol (OA) and that a large fraction of this OA mass forms in the atmosphere when organic compounds in the gas phase are oxidized and subsequently condense as secondary organic aerosol (SOA) (Zhang et al., 2007;Jimenez et al., 2009). Because SOA is such a large fraction of the aerosol mass, condensation of SOA is critical to growing nucleation-mode particles, which are initially too small to serve as cloud condensation nuclei (CCN), to sizes that are capable of forming cloud droplets (Ehn et al., 2014;Riipinen et al., 2011;Pierce et al., 2012), though a recent study showed that unique conditions in the Amazon allowed particles smaller than 50 nm ~~acted~~ to act as CCN during GoAmazon 2014/5 (Fan et al., 2018). Thus, accurate descriptions of SOA condensation and aerosol growth kinetics are crucial to accurately predicting aerosol size distributions and therefore CCN number concentrations and aerosol optical properties, both of which are required for accurately predicting the impact of aerosols on climate (Scott et al., 2015;Riipinen et al., 2012;Zaveri et al., 2014).

For several years, there has been an interest in studying the Lagrangian (i.e., within the same air parcel) evolution of organic aerosol from the emissions of urban centers. Field studies have investigated the evolution of pollution plumes ~~generally accomplish this~~ by arranging fixed observation sites at different distances downwind of a city along the direction of the

prevailing wind or by tracking the plume with a mobile platform, such as an aircraft. Larger campaigns may employ both strategies. Most studies of this type are best described as pseudo-Lagrangian as repeatedly sampling the same air parcel is difficult with mobile platforms and impossible with fixed sites. Dilution and mixing of the air parcel with background air also alter the plume composition. To account for atmospheric dilution and spatial and temporal variability in emissions, studies often utilize the ratio of excess OA to that of an inert tracer as a metric for evaluating OA formation in a plume (Kleinman et al., 2008;Sullivan and Weber, 2006;Takegawa et al., 2006;de Gouw et al., 2005). CO is a common choice for the inert tracer because it is emitted during combustion and other anthropogenic processes, is significantly enhanced in urban plumes relative to the background, and is routinely and robustly measured. Measurements of Δorg/ΔCO in aged urban outflow have spanned a range from 47 $\mu g/m^3$ $ppmv^{-1}$ in the NE US (de Gouw et al., 2008), to 62-80 $\mu g/m^3$ $ppmv^{-1}$in Mexico City (DeCarlo et al., 2008;Kleinman et al., 2008), to 100 $\mu g/m^3$ $ppmv^{-1}$ in the Po Valley, Italy (Crosier et al., 2007), to 44 – 197 $\mu g/m^3$ $ppmv^{-1}$ in Sacramento, CA (Shilling et al., 2013;Setyan et al., 2012), to 97-133 $\mu g/m^3$ $ppmv^{-1}$ in Paris (Freney et al., 2014). The same studies have found that Δorg/ΔCO increases roughly linearly with ~~airmass~~air mass age for the first 1 day of aging and levels off after approximately 2 days (de Gouw and Jimenez, 2009;DeCarlo et al., 2010;Kleinman et al., 2008;Takegawa et al., 2006;Sullivan et al., 2006;Freney et al., 2014). Observations suggest that changes in Δorg/ΔCO begin soon after emission. For example, measurements during the MILAGRO campaign showed that Δorg/ΔCO increased from 10-35 $\mu g/m^3$ $ppmv^{-1}$ for fresh emissions to 70-80 $\mu g/m^3$ $ppmv^{-1}$ after approximately one day of photochemical aging (DeCarlo et al., 2010;Kleinman et al., 2008). Changes of similar magnitude over similar aging times have been measure in the urban outflow of: Tokyo (Takegawa et al., 2006), the SE USA (Sullivan et al., 2006), Paris (Freney et al., 2014), and the NE USA (de Gouw et al., 2005).

Measurements have also suggested that organic aerosol production may be enhanced when urban emissions interact with biogenic emissions. Organic aerosol concentrations have shown strong correlation with CO and other tracers of anthropogenic emissions (de Gouw et al., 2005;Volkamer et al., 2006;Weber et al., 2007;Sullivan et al., 2006). Furthermore, satellite observations suggest that the spatial and seasonal patterns of aerosol optical depth coincide with biogenic emissions (Goldstein et al., 2009). At the same time, radiocarbon dating has shown that a large fraction of the carbon in the aerosol phase is modern and that the ~~fraction of~~ modern carbon fraction increased with increasing distance from urban centers (Weber et al., 2007;Schichtel et al., 2008). During the CARES campaign near Sacramento, CA, aircraft observations showed that Δorg/ΔCO measurements were 35-44 $\mu g/m^3$ $ppmv^{-1}$ when anthropogenic emissions evolved in the absence of strong biogenic emissions and 77-157 $\mu g/m^3$ $ppmv^{-1}$ when the urban plume interacted with regions of strong biogenic emissions (Shilling et al., 2013). Measurements from a ground site during CARES report average Δorg/ΔCO values of 36 $\mu g/m^3$ $ppmv^{-1}$ in the Sacramento plume during periods of low biogenic emissions and 97 $\mu g/m^3$ $ppmv^{-1}$ during periods of high biogenic emissions (Setyan et al., 2012). Several additional field studies report enhancements of SOA through interactions of anthropogenic and biogenic emissions~~interactions~~, but may not employ the Δorg/ΔCO metric (Zhou et al., 2016;Xu et al., 2015;Ng et al., 2017;Bean et al., 2016). The potential mechanisms responsible for these enhancements are known in some cases but remain uncertain in others and have been outlined in recent review articles (Shrivastava et al., 2017;Ng et al., 2017;Glasius and Goldstein, 2016;Hoyle et al., 2011).

To date, most studies of the evolution of urban plumes have been conducted in the Northern Hemisphere. Far fewer studies have been performed in the Southern Hemisphere where there is less landmass, lower population, and therefore lower background concentrations of anthropogenic pollutants (Andreae, 2007). The Amazon tropical forest, in particular, is an important ecosystem in which background levels of anthropogenic pollution may sometimes reach levels characteristic of pre-industrial conditions but is becoming increasingly impacted by industrialization and anthropogenic pollution (Martin et al., 2017;Martin et al., 2010b;Andreae et al., 2015). Fuzzi et al. (2007) described chemical analysis of filter samples collected in Rondonia, Brazil (~825 km SW of Manaus, Brazil) from September to November 2002. They found that water-soluble organic species were the main contributors to submicron particles (90%) with the balance consisting of soluble inorganic ions (Fuzzi et al., 2007). ~~The SAAMBA aircraft campaign, based out of Rondonia, Brazil, was focused primarily on biomass burning but~~ Allen et al. (2014) discuss measurements from ~~five~~ flights investigating biogenic processes during the South American Biomass Burning Analysis (SAMBBA) aircraft campaign, based out of Rondonia, Brazil.~~.~~ They report that concentrations of SOA derived from isoprene epoxydiols (IEPOX) were highest in the presence of acidic seed, low NO_x concentrations, and high RH (Allan et al., 2014). The AMAZE-08 campaign was conducted in February and March of 2008 and Chen et al. (2009, 2015) reported on chemical composition measurements made with an AMS ~~from~~ located at a tower site 60 km NNW of Manaus, Brazil (Martin et al., 2010a;Chen et al., 2009;Chen et al., 2015). They found that organics accounted for more than 80% of the non-refractory aerosol mass, with the organic mass often dominated by SOA, and that the aerosol was acidic in composition (Chen et al., 2015). It is important to note that Chen et al. (2009, 2015) excluded data impacted by Manaus emissions from their analysis. de Sá et al. (2017) investigated the production of IEPOX SOA downwind of Manus during GoAmazon2014/5 and found decreased concentrations of IEPOX-SOA in the plume relative to the background which they attribute to suppression of IEPOX formation by elevated NO concentrations in the plume. Kuhn et al. (2010) describe aircraft-based aerosol measurements in the Manaus plume as it was transported downwind. They report increases in $\Delta CCN/\Delta CO$ as the plume aged, which they attribute to condensation of both organic and inorganic mass, but did not measure the aerosol chemical composition (Kuhn et al., 2010). Additional aircraft campaigns conducted in the Amazon often focused on biomass burning and the impact of biomass burning aerosol on cloud properties (Morgan et al., 2013;Yokelson et al., 2007;Andreae et al., 2012).

~~To that end, the~~The Green Ocean Amazon (GoAmazon 2014/5) campaign was conducted in the vicinity of Manaus, Brazil from January 2014 – December 2015. The goal of GoAmazon 2014/5 was to investigate the interaction of Manaus urban emissions with the surrounding pristine Amazon basin and the subsequent impact of these emission on cloud formation and properties (Martin et al., 2017;Martin et al., 2016). Manaus's geography makes it ideal for this mission. Manaus, an industrial city and with a metropolitan population of more than 2 million people, is the largest city in the Amazon basin. The prevailing wind is from the east with the nearest major upwind city, Belem, approximately 1250 km away. The surrounding tropical forest emits vast quantities of biogenic gases and aerosol. Few roads connect Manaus to the rest of Brazil and most freight and traffic from outside the city is via ship or plane. Thus, Manaus acts as a large point source of anthropogenic emissions which are transported to the surrounding ~~and nearly pristine~~ Amazon basin. As part of this campaign, the DOE Gulfstream-1 (G-1)

research aircraft conducted two, six-week-long missions in which it investigated the evolution of the Manaus plume as it was transported into the surrounding Amazon tropical rainforest. ~~-~~ The timing of these flight missions was chosen to provide a contrast between the wet and dry seasons (Martin et al., 2016). In the wet season, back trajectory analysis indicated that the Manaus region was typically under the influence of air originating from the North Atlantic Ocean (Martin et al., 2016). Regular, organized mesoscale convective systems triggered by sea breeze circulation brought widespread, moderate rate precipitation to the region (Giangrande et al., 2017;Machado et al., 2018;Burleyson et al., 2016). The high level of rainfall and moisture in the wet season inhibited biomass burning and a low number of fires were observed (Martin et al., 2016;Machado et al., 2018). Under these conditions, the Amazon basin is one of the cleanest continental regions on Earth onto which the Manaus plume represents a significant perturbation (Martin et al., 2010b;Artaxo et al., 2013). In the dry season, back trajectory analysis indicate air masses originate from the Southern Hemisphere and travel up the Amazon River transporting pollution from the northern coastal cities (Martin et al., 2016). In addition, recirculation events transported air from the southern Amazon basin into the Manaus region (Martin et al., 2016). Intense biomass burning fires in the central and southern portion of the Amazon basin and in central Africa were observed in the dry season and a portion of these emissions were transported to the Manaus region (Martin et al., 2016;Artaxo et al., 2013;Martin et al., 2010b). In the dry season, more intense but less frequent convection produced approximately one quarter of the total rainfall observed in the wet season. As a result of the combination of transport and precipitation frequency, the Manaus region is significantly more polluted in the dry season.

~~Here~~ In this manuscript we report on measurements from instruments deployed on the G-1~~, focusing on measurements of aerosol species and the evolution of organic aerosol particles in the plume~~ focusing primarily on measurements of aerosol species and trace gases that impact the aerosol lifecycle. In the first part of the manuscript, we provide an overview of aerosol and VOC measurements and compare and contrast the wet and dry season data. In the second portion of the manuscript, we examine, in detail, the first 4 – 6.5 hours of photochemical aging of the Manaus plume as it is transported into the surrounding tropical forest and interacts with biogenic emissions.

2 Experimental

2.1 G-1 Flight Strategy

The GoAmazon 2014/5 campaign was conducted in the vicinity of Manaus, Brazil from January 1, 2014 through December 31, 2015 (Martin et al., 2016). During this period, DOE's G~~Gulfstream~~-1 research aircraft, based out of the Manaus International Airport, was deployed for two periods during which time it sampled the Manaus urban plume as it was transported downwind over the Amazon rainforest. The first aircraft deployment period occurred during the wet season from February 15 - March 26, 2014 while the second occurred in the dry season from September 1 - October 10, 2014. Sixteen research flights were conducted in the wet season and 19 were conducted in the dry season. Table 1 lists takeoff and landing times, the altitude of level flight legs, and meteorological parameters measured by the G-1 instrumentation shortly after takeoff on each flight. In general, flight plans were focused on successive perpendicular plume crossings spaced approximately equally at intervals of

24 km downwind of the city. A representative flight path for March 13, 2014, an exemplar ~~golden~~ day in the wet season with few clouds,~~,~~ is shown in Figure 1. The paths for all flights during the two deployments are shown, segregated by altitude, in Martin et al. (2016) and therefore are not reproduced here. ~~The~~ On March 13, the first leg approximately bisected the city along a NW/SE line, the second leg passed near a highly instrumented ground site directly across the Amazon river from Manaus (T2), the fourth leg passed over a second highly instrumented site located NE of Manacaparu (T3), with an additional leg between the T2 and T3 sites, and a final leg downwind of the T3 site. The first pass through the pattern was generally at an altitude of 500-700 m above ground level with a second pass at a higher altitude and often, though not always, focused on sampling clouds. The flight pattern discussed above and shown in Figure 1 was rotated to align with the prevailing wind direction. ~~Most flights departed the airport between 9:30 - 10:30 local time (13:30 - 14:30 UTC) and returned at between 13:00 – 14:30 local (17:30 – 18:30 UTC), lasting 3 – 3.5 hours, with a small number of flights occurring outside this window~~Flights generally departed in the late morning or early afternoon and lasted between 3 and 3.5 hours (Table 1).

2.2 Instrumentation

An Aerodyne High-Resolution Time-of-Flight Aerosol Mass Spectrometer (~~HR-ToF-AMS (~~abbreviated as AMS hereafter) was deployed on the G-1 to measure aerosol chemical composition (Jayne et al., 2000;DeCarlo et al., 2006). The AMS operated only in ~~a higher sensitivity, lower resolution~~the standard "V"- MS mode (the particle sizing mode was not used) with a 13s data ~~sampling~~ averaging interval and equal chopper open and closed periods of 3 seconds. Before, during, and after flights, the AMS-sampled air was periodically diverted through a HEPA filter to remove particulates and these filter periods were used to account for gas-phase interferences with isobaric particulate signals. Based on the standard deviation of these blank measurements (3σ) as described in the literature (DeCarlo et al., 2006), the detection limit of the AMS at the 13s sampling interval were 0.12, 0.01, 0.014, and 0.005 μg/m^3 for organics, sulfate, nitrate, and ammonium respectively. All aerosol instruments, including the AMS, sampled from a common, double-diffuser isokinetic inlet. Flow for the AMS was sub-sampled from the center of the isokinetic inlet and dried to RH < 40% by passage through a 1/2" ID PermaPure Nafion membrane. A constant pressure inlet operating at approximately 620 hPa was used to maintain a constant volumetric flow to the AMS up to altitudes of approximately 3900 m (Bahreini et al., 2008). Because the AMS was powered off between flights, a correction based on the real-time N_2^+ signal was applied to all data to account for drifting sensitivity as the instrument warmed up during flights. The AMS was regularly calibrated in the field using monodisperse ammonium nitrate particles quantified with a TSI condensation particle counter (CPC). Data was analyzed in Igor Pro (v6.37) ~~using both the unit mass resolution analysis (Allan et al., 2003;Jimenez et al., 2003) and the~~ using the high-resolution analysis package (Squirrel v1.55H, PIKA v1.44H) and techniques described in the literature (Canagaratna et al., 2015;Kroll et al., 2011;Aiken et al., 2007;Allan et al., 2003;Jimenez et al., 2003) ~~described in the literature~~. All AMS data in the manuscript have been processed using the high-resolution data analysis routine. The O:C and H:C values reported here use the updated calibrations described in Canagaratna et al. (2015). All AMS data are normalized to the laboratory calibration conditions of 23 °C 1013 hPa. Primary Matrix Factorization (PMF)

Formatted: Font: 10 pt, English (United Kingdom)

Formatted: Font: 10 pt

Formatted: Font: 10 pt

analysis was performed on the wet-season dataset by combining all flight data into a single experiment using the PMF Evaluation Tool (v 2.06) and the PFM2 algorithm (v 4.2) (Ulbrich et al., 2009;Paatero, 1997;Paatero and Tapper, 1994).

An Ionicon quadrupole high-sensitivity Proton Transfer Reaction Mass Spectrometer (PTR-MS) was used to measure selected gas-phase volatile organic carbon (VOC) concentrations (Lindinger et al., 1998). The PTR-MS was ~~used~~ run in the ion monitoring mode in which ~~where it sequentially steps through~~ signals of a limited ~~series~~ number of pre-selected of m/z values ~~with~~ are sequentially measured with one measurement cycle ~~each cycle through the series~~ taking 3.5 s. Averaging time at each m/z in the series varied depending on the sensitivity of the instrument to that species, the expected concentration, and the background, but generally varied between 0.2 and 0.5 s. Isoprene at m/z 69 was sampled multiple times during the cycle to enable flux analysis (Gu et al., 2017). Drift tube temperature, pressure and voltage were held at 60 °C, 2.22 hPa, and 600 V, respectively resulting in an electric field to gas density (E/N) ratio ~~resulting in an E/N value~~ of 134 Td (1 Td = 1×10^{-17} $cm^2V^{-1}s^{-1}$)~~Td~~. The PTR-MS sampled air through a dedicated forward-facing inlet that consisted of approximately 6" of 1/4" OD stainless steel followed by approximately 46" of 1/4" Teflon tubing, and 36" of 1/16" OD PEEK tubing. The flow through the Teflon tubing was 600 ccm with 300 ccm subsampled through the PEEK tubing for introduction into the PTR-MS. To assess the PTR-MS background, air was periodically diverted through a stainless steel tube filled with Shimadzu Pt catalyst heated to 600 °C, which removes VOCs from the airstream without perturbing relative humidity. The catalyst efficiency was tested during the campaign by comparing signal from air containing VOCs passed through the catalyst with signal from VOC-free air. The PTR-MS was calibrated by introducing known concentrations of calibration gases into the instrument with variable dilution by VOC-free air. The calibration tank VOC concentrations were determined gravimetrically and verified using GC analysis by the manufacturer (AiR Environmental, Inc).

Ozone was measured with a Thermo Scientific Model 49i ozone analyzer based on measurement of UV absorption at 254 nm. The instrument was regularly calibrated in-flight by displacement of known quantities of ozone and zeroed in flight using ozone-scrubbed ambient air. CO was measured using a Los Gatos Research $CO/N_2O/H_2O$ analyzer that is based on cavity-enhanced near-IR absorption and was also calibrated regularly in-flight. Additional information on the instrumentation deployed on the G-1 can be found in GoAmazon 2014/5 overview manuscript (Martin et al., 2016).

Formatted: Superscript

Formatted: Superscript

3 Results and Discussion

3.1 Overview of G-1 Aerosol Data and Comparison of Wet and Dry Seasons

As discussed in the introduction, the different precipitation and mesoscale transport patterns in the wet and the dry season are expected to produce considerably different concentrations of pollutants in the Amazon basin and measurements confirmed this expectation. Figure ~~2~~2 and Table ~~1~~ 2 summarize the AMS results for data collected on the G-1 flights in both the wet and the dry season. The top panel of Figure 2 shows box-and-whisker plots summarizing AMS data for organics, sulfate, nitrate, and ammonium particulate concentrations, with one data point representing each flight (note the scale change between the wet and

dry season plot). The middle panel shows the relative distribution of the chemical species on each flight. The bottom panel shows the distribution of the chemical species ~~averaged across the entire wet and dry season~~as a mass weighted average of all data from the respective season. Several trends are readily apparent in the data. First, it is clear that aerosol loadings were significantly higher in the dry season than in the wet season. Median organic loadings for the all wet and dry season data were 0.~~72~~ 85 and 4.~~06~~ 29 μg/m^3, respectively. Median sulfate, nitrate and ammonium loadings increased from 0.~~11~~19, 0.~~04~~02, and 0.~~03~~ 06 μg/m^3 in the wet season to 0.~~67~~77, 0.~~17~~05, and 0.25 μg/m^3 in the dry season. Mean loadings of all species were somewhat higher than the median. Mean organic, sulfate, nitrate, and ammonium loadings were 0.~~85~~91, 0.~~14~~16, 0.~~05~~02, and 0.05 μg/m^3 in the wet season and 4.~~23~~41, 0.~~73~~80, 0.~~23~~1, and 0.~~27~~ 26 μg/m^3 in the dry season. In the wet season, the mass loading of all species are lower than typically observed over continental regions in the Northern Hemisphere (Zhang et al., 2007).

While this manuscript will focus on the particulate data, measurements of the volatile organic compounds provide insights into the precursors that are oxidized to form OA and help to identify the source of an air parcel. Figure 3 and Table 3 summarize the concentrations of several relevant VOCs measured on board the G-1 with the PTR-MS. Similar to the trends seen in the aerosol mass loading data, concentrations of most VOCs measured by the PTR-MS are significantly higher in the dry season than in the wet season. Concentrations of isoprene and its oxidation products, biogenic precursors of OA, are a factor of 2-3 times higher in the dry season than the wet season. The average daily high temperatures in Manaus are 33.5°C in September (dry season) and 30.9°C in March (wet season) and isoprene emissions have been shown to scale with temperature, among other variables (Guenther et al., 2012). Measurements of benzene, which is primarily anthropogenic in origin, were also significantly higher in the dry season. While benzene itself is unlikely to significantly contribute to SOA formation over the timescales we observe on the G-1 flights (4-6.5 hours) due to its ~5 day atmospheric lifetime (Atkinson and Arey, 2003), other unmeasured anthropogenic VOC concentrations which would contribute to more immediate OA formation may have been higher as well. The higher VOC concentrations may contribute to the higher OA concentrations measured in the dry season. However, the PTR-MS data, in addition to satellite and remote sensing measurements (Martin et al., 2016), also show that biomass burning significantly impacted the region. Measurements of acetonitrile, whose major source is biomass burning (Yokelson et al., 2009;Yokelson et al., 2007), are 2-3 times higher in the dry season than the wet season, indicating a significant biomass burning impact in the region. Biomass burning is a known source of OA (Jolleys et al., 2012;Bond et al., 2004;Yokelson et al., 2009;Ferek et al., 1998) and would also contribute to the higher aerosol concentrations observed in the dry season.

The aerosol mass loadings we measure in the dry season are consistent with aircraft-based AMS measurements made during the South American Biomass Burning Analysis (SAMBBA) campaign at the same time of year, though several hundred kilometers to the SW in the state of Rondonia (Allan et al., 2014). Chen et al. reported AMS-measured wet-season campaign (February 7 to March 13, 2008) average organic and sulfate loadings of 0.7 and 0.15 μg/m^3 from a ground site that was within the GoAmazon 2014/5 flight domain, though they excluded data impacted by Manaus emissions from their analysis (Chen et

al., 2009). When comparing aircraft to ground site data, it is important to acknowledge differences in the datasets. First, the aircraft samples a different spatial domain in all three dimensions (latitude, longitude, and altitude) than a ground site. In addition, the G-1 typically sampled the boundary layer in the late morning (~~approximately 10:00 – 11:30 local times~~see Table 1 for flight times), and thus may miss peak concentrations of secondary species. Finally, the goal of the flights was often to sample the Manaus plume for the first half of ~~the~~ each flight and clouds for the second half. The mean aerosol loadings reported here agree well with those reported by Chen et al. (2009), considering the inherent differences in datasets discussed above. We also found good agreement when comparing the G-1 measured aerosol loadings to those measured at the T3 site when the aircraft passed overhead and at ~~an altitude within the boundary layer~~ 500 – 600 m altitude (de Sá et al., 2018). Our loadings are at the low end of the range (1- 2 μg/m^3) reported from a ground site in Rondonia, approximately 825 km to the southwest of Manaus, though those data were more heavily influenced by biomass burning and relied on a combination of offline techniques to speciate the aerosol (Fuzzi et al., 2007). To understand potential bias in the dataset due to altitude, we calculated statistics for data collected below 700 m, which ~~roughly corresponds to data collected within the boundary layer~~captures the lowest altitude portion of each flight. Giagrande et al. (2017) analyzed radiosonde data from the T3 site and report average mixed layer heights of greater than 1000 m above ground level at 10:00 local time in both the wet and dry seasons. Thus, the G-1 was typically sampling in the boundary layer on the lowest flight legs and the 700 m data should represent boundary layer conditions. In the wet season, the low altitude AMS loading statistics are generally either slightly higher or unchanged relative to the full dataset. In the dry season, the low altitude AMS loading statistics are either slightly lower relative or unchanged relative to the full dataset, likely due to transport of biomass burning from the south in elevated layers. Both the median and mean concentrations of most VOCs measured are slightly higher for the data at < 700 m altitude relative to the full dataset (Table 3). This is the expected behavior for most VOCs measured here as they are either directly emitted at the surface (e.g., isoprene, benzene, monoterpenes) or form from oxidation of VOCs emitted at the surface (e.g., isoprene oxidation products). The fractional contribution of each species to the total loading is nearly identical when comparing seasons, despite the large differences in aerosol absolute mass concentrations and ~~sources~~ the larger influence of biomass burning in the dry season (Martin et al., 2016). Organics dominate the chemical composition, comprising ~~78~~ 80 % of the total with sulfate 1~~4~~2%, nitrate ~~5~~2%, and ammonium 4%, regardless of the season. The relative distribution of the products changes only modestly among flights (Figure 2, middle panel). Organics were the largest fraction of the total aerosol mass on each flight, varying between 72 – 83%. Sulfate was the second largest fraction of the total mass (7-20%) and the sum of sulfate and organic were nearly constant. The ~~aircraft product~~fractional contributions of each chemical species described herein ~~distribution is nearly~~are nearly identical to the previous reports from Chen et al. (2009, 2015). The ~~aircraft product distributions~~aircraft-measured chemical composition is~~are~~ also nearly identical to that~~ose~~ measured at the T3 ground site (de Sá et al., 2018) during GoAmazon 2014/5. The agreement between the T3 and G-1 product distributions suggests that the T3 ground site is sampling air that is representative of the regional air and is not unduly biased by local emissions, at least in the aggregate.

The observation that the total concentrations of all aerosol components significantly increases yet remain in the same proportions when comparing the wet and the dry season is unexpected. The more frequent and widespread precipitation events

Formatted: Font: 10 pt, Not Italic

Formatted: Font: 10 pt, Not Italic

Formatted: Font: 10 pt, Not Italic

in the wet season and the lower concentrations of precursor VOCs contribute to the lower aerosol concentrations in the wet season. If the aerosol particles are internally mixed, it would be reasonable to assume that rainfall would remove aerosol in approximately equal proportions. However, as discussed previously, aerosol sources are different between seasons and there was a much larger biomass burning influence in the dry season (Martin et al., 2016), which is a known and significant source of OA (e.g., (Jolleys et al., 2012;Bond et al., 2004;Yokelson et al., 2009;Ferek et al., 1998). Biomass burning was previously shown to emit particulate sulfate and nitrate directly, and NO_x, sulfuric acid, and methane sulfonic acid (MSA), precursors of particulate nitrate and sulfate, but not in the same ratio as OA and its precursors (Yokelson et al., 2009). Thus, given the significant influence of biomass burning in the dry season, it is surprising that the chemical composition of the aerosol does not change. ~~Passage through fresh biomass burning plumes was characterized by increased concentrations of organics and nitrate, with much smaller increases in sulfate, suggesting that sulfate formation occurs on a slower timescale. More aged biomass burning emissions originating from the southern and eastern edges of the Amazon basin also exerts an influence on the Manaus region, increasing the background aerosol concentrations significantly (Martin et al., 2016).~~

Formatted: Subscript

Despite the similarity of the distribution of organic, sulfate and nitrate in the aerosol particles between the wet and dry seasons, the chemical composition of the organic aerosol is quite different between seasons. Figure ~~3~~ 4 shows normalized probability distributions for three metrics of the organic aerosol composition, the hydrogen to carbon ratio (H:C), the oxygen to carbon ratio (O:C), and the mean carbon oxidation state ($\bar{O}S_c$) segregated by season. It is clear that the organic particles are more oxidized in the dry season than the wet season. The median O:C, H:C, and $\bar{O}S_c$ in the dry season were, 0.78, 1.58, and -0.02 respectively, while they were 0.6, 1.65, and -0.45 in the wet season. While the H:C ratios change only slightly between season, the O:C and $\bar{O}S_c$ both show significant increases in the dry season. Thus, the aerosol in the dry season is significantly more aged, consistent with aged biomass burning aerosol dominating the organic aerosol mass in the dry season and relatively fresh, locally generated organic aerosol dominating in the wet season (Martin et al., 2010b). The probability distributions during the wet season are also wider than in the dry season. We postulate that small contributions from a wider range of sources are able to influence the data to a larger degree in the wet season, when the total organic aerosol concentrations were much smaller. In contrast, during the dry season, small sources of organic mass would have a smaller impact on the organic composition due to the significant biomass burning background.

3.2 ~~Case Study, March 13, 2014 Flight~~Evolution of Organic Aerosol in the Manaus Plume

Figure 1 shows the flight path on March 13, 2014, which is an exemplar ~~golden~~ day for observing the evolution of the Manaus plume in the wet season. Flight legs were perpendicular to the prevailing wind direction and spaced approximately 24 km apart at successively increasing distance from Manaus. The length of the legs was chosen such that measurements (e.g., CO concentration) returned to near background levels at the ends of the leg. Due to dispersion of the plume, the length of the legs generally increased downwind of Manaus, ranging from 56 km close to the city to 80 km downwind of the T3 site. The pattern was flown first at an altitude of 500 m with a second pass at 1000 m overlapping the first. This flight was marked by mostly sunny skies with no clouds intercepted by the G-1 at 500 m and only brief passage through spatially small clouds at 1000 m.

There was little local or regional biomass burning during this time period. Thus, this flight represents a case with coherent transport of the Manaus plume downwind into regions of high biogenic emissions with few complicating factors, such as biomass burning or cloud processing.

Figure ~~4~~ 5 shows a time-series of several important gas- and particle-phase species for the March 13, 2014 flight. Passage through the Manaus plume is indicated by clear and significant increases in CO, ozone, and PTR-MS m/z 79 (benzene) above the background levels. While CO may be produced from the oxidation of biogenic VOCs (Slowik et al., 2010), the intense peaks are primarily from urban emissions, given the proximity to Manaus and the correlation of CO with other known anthropogenic species, such as ozone, benzene, and toluene (not shown). Concentrations of CO (80 ppbv) and ozone (10 ppbv) are lowest at the edges of the flight legs and, although we did not sample extensively in regions that were far removed from Manaus, these concentrations are consistent with the background concentrations that have been previously reported in the region (Andreae et al., 2015;Martin et al., 2010b;Harriss et al., 1990). Isoprene concentrations (PTR-MS m/z 69) typically reach their highest levels outside of the plume and are lower inside, though isoprene concentrations of approximately 1 ppbv are still observed in the plume. As seen in Figure 1, much of the land cover outside of Manaus is tropical forest, with some pasture land interspersed. Significant isoprene emissions are expected and indeed measured from the forest (Gu et al., 2017;Guenther et al., 2006). Significant concentrations of methacrolein, methyl vinyl ketone, and isoprene hydroxyhydroperoxides (PTR-MS m/z 71), all first generation oxidation products of isoprene, are also observed and have a more complicated structure (Liu et al., 2016). Concentrations of these products tend to be highest near the edges of the plume and they do not correlate strongly with either isoprene (r^2= 0.24) or with anthropogenic plume markers such as CO (r^2= 0.24). Production of these oxidation products requires OH, the concentration of which depends on NO_x, to oxidize isoprene and thus they are expected to have a more complex relationship with the urban plume and the surrounding biogenic emissions. Taken together, the observations of both isoprene and its oxidation products suggest that photooxidation of BVOCs is enhanced in the plume relative to the background, as would be expected (Martin et al., 2017). Monoterpene concentrations (not shown) on this flight are approximately a factor of ten lower than isoprene concentrations, consistent with previous measurements (Kesselmeier et al., 2000), and are often near or below the instrument limit of detection (~200 pptv). Monoterpene concentrations correlate with isoprene concentrations during the flight, when they are above the instrument detection limit.

Organic aerosol (OA) mass increases from background values of 0.5 μg/m^3 to as high as 3.1 μg/m^3 in the Manaus plume and on this day it is correlated relatively well with both ozone (r^2= 0.65) and CO (r^2=0.76). While OA concentrations do not reach the levels that are typically seen in the outflow of large North American cities, they are significantly larger than background concentrations (up to 6x), indicating a clear impact of the plume on OA concentrations. Sulfate also clearly increases in the plume, though its peak concentrations occur toward the southern edge of the plume, relative to organics, CO, and ozone, suggesting sulfur emissions may not be co-located with other anthropogenic emissions. However, there are also occasional peaks in the sulfate concentration (for example at 10:47) that coincide with minima in other plume indicators, such as CO and ozone. Nitrate concentrations are significantly lower than sulfate concentrations, but tend to correlate more strongly with organic concentrations than sulfate concentrations. There are indications that a significant portion of the nitrate mass exists as

organic nitrates, consistent with measurements at the T3 site and with aircraft measurements (Allan et al., 2014;de Sá et al., 2018;Schulz et al., 2018). The NO^+:NO_2^+ ion ratio is 5-7 in the plume, compared to a NO^+:NO_2^+ ion ratio of 1.2-1.5 measured during the campaign for ammonium nitrate calibration aerosol. NO^+:NO_2^+ ion ratios significantly above that of ammonium nitrate are indicative of the presence of organic nitrates, though quantifying the organic fraction is challenging (Farmer et al., 2010). Ammonium concentrations tend to closely mirror sulfate concentrations. The bottom panel of Figure ~~4~~ 5 shows the fractional composition of the aerosol, which helps to illustrate the relative differences among the aerosol species. Organic species clearly dominate at all points, with sulfate the next most important species.

At 1000 m altitude, the plume can still be observed in the G-1 data, though the concentrations of plume markers such as CO, ozone, and benzene are lower. Increases in organic concentration are less sharp and defined than observed at 500 m, though enhancements are still clear. The organic mass fraction is somewhat smaller at 1000 m and sulfate and ammonium mass fractions are larger. Based on radiosonde measurements, the boundary layer grew from 900 to 1200 m between the beginning and end of the flight on this date. Data from the G-1 suggest that the 1000-m flight path was near the top of the boundary layer. Thus, at 1000-m altitude, the data are influenced by both the local conditions and from air that has been transported over longer distances.

Figure ~~5~~ 6 shows a PMF analysis of the organic species, for the March 13th flight along with independently measured species that might be expected to correlate with the PMF factors. We were able to resolve the organic aerosol into three factors; an OOA factor that is a proxy for SOA, an HOA factor that is a proxy for primary organic particulate emissions, and a IEPOX SOA factor, which forms from the heterogeneous uptake of IEPOX, a product of isoprene oxidation under low-NO_x conditions (Hu et al., 2015;Robinson et al., 2011;Lin et al., 2012;Zhang et al., 2011;Zhang et al., 2005a;de Sá et al., 2017). Details of the PMF analysis, including mass spectra of the factors, can be found in the appendix and supporting information. As expected, both the OOA and HOA factor mass loadings are significantly higher in the plume relative to the background. The HOA factor correlates strongly with CO (r=0.79 for all data at 500 m) while the OOA factor correlates strongly with ozone (r=0.81 for all data at 500 m), though we will show below that the slope of the correlation changes with plume age. The changing slope has the effect of degrading the HOA/CO and OOA/ozone correlations, which are higher for individual plume legs. The HOA factor is a larger fraction of the organic mass on the legs nearest to Manaus and becomes a smaller fraction on the downwind legs. The OOA mass fraction displays the opposite behavior, increasing downwind as the plume ages. The transformation of HOA to SOA/OOA has been observed previously, both in laboratory experiments and in the field (Sage et al., 2008;Robinson et al., 2007;DeCarlo et al., 2008;Zhang et al., 2007;Ng et al., 2010). Taken together, these observations are consistent with the literature assignment of HOA as a marker of primary organic emissions and OOA as a marker of secondary organic aerosol. Outside of the plume, HOA concentrations approach zero. OOA concentrations on the other hand, remain significant and approach the organic aerosol background concentrations. The IEPOX SOA factor does not appear to change with passage through the plume and does not correlate with sulfate aerosol on this day as may be expected based on the chemical mechanism, which requires heterogeneous uptake of gas-phase IEPOX onto inorganic aerosol to generate IEPOX SOA (Hu et al., 2015;Surratt et al., 2010;Gaston et al., 2014;Nguyen et al., 2014). We note that the IEPOX SOA factor is noisy, is near or

below the limit of detection of organic aerosol (0.13 μg/m^3) for much of this flight, and is shown largely for the sake of completeness. Because of the low concentrations, it is difficult to draw definitive conclusions about IEPOX SOA formation on this flight. However, given the focus of this flight was on tracking the Manaus plume which contains significant NO_x, our findings are consistent with de Sa et al. (2017) who report that NO_x from the Manaus plume suppresses IEPOX SOA formation in the plume and that the IEPOX-SOA factor was less than 5% of the total OA at T_3 at the time of G1 overflight.

Figure ~~5~~6-7summarizes several relevant plume quantities at 500 m altitude as a function of the approximate distance downwind from Manaus, which serves as a proxy for the photochemical age of the ~~airmass~~air mass. The ratio of excess organic aerosol to excess CO (Δorg/ΔCO) is a metric that is often used to quantify organic aerosol formation in a source plume as it ages. The utility of the Δorg/ΔCO metric rests mainly the assumptions that CO is conserved on the timescale of the measurements and that urban emissions scale linearly with CO. Using this ratio rather than absolute concentrations of organic aerosol can normalize for dilution due to mixing of the plume with background air. The Δorg/ΔCO values shown in Figure 7 were calculated as the slope of a linear regression line between the AMS-measured organic mass loadings and CO concentrations. All data for each flight leg perpendicular to the wind direction were included. Background values of OA and CO were not subtracted from the data and the regression was not forced through the origin. We acknowledge that calculation of Δorg/ΔCO values can be sensitive to the calculation method and choice of background values for both OA and CO; therefore, we performed calculations using different methods and assuming different background concentrations for both OA and CO ~~(see SI for more details)~~and find general agreement between these methods (see SI for more details).. ~~We did not find significant increases in Δorg/ΔCO in any of these calculations.~~

Two aspects of the Δorg/ΔCO distinguish these measurements from most previous measurements in the literature. First, Δorg/ΔCO is ~31μg/m^3 ppmv^{-1}, a value that is lower than the value of 70 ± 20 μg/m^3 ppmv^{-1} observed in the outflow of cities in North America (e.g., de Gouw and Jimenez (2009) and refs therein). The Δorg/ΔCO values observed here are also significantly smaller than the values of 77 – 157 μg/m^3 ppmv^{-1} we previously observed when fresh urban anthropogenic emissions evolved in the presence of strong biogenic emissions, as is the case in the present data set (Shilling et al., 2013;Setyan et al., 2012). We measure a ΔHOA/ΔCO value of 17.6 μg/m^3 ppmv^{-1} near Manaus (Figure ~~6~~7) which should represent fresh emissions. This value is at the upper end of what is reported in the literature for North American cities, indicating that lower primary particulate emissions from Manaus are not responsible for the lower Δorg/ΔCO values (DeCarlo et al., 2010;de Gouw and Jimenez, 2009).

The second new aspect of these observations is that we do not observe a corresponding increase in Δorg/ΔCO as the plume photochemically ages, contrary to our expectations. We note that, as described above, organic aerosol concentrations are significantly higher in the plume than in the background and the constant Δorg/ΔCO values do not indicate that no OA formation occurs in the plume. Rather, the Δorg/ΔCO analysis that follows focuses on understanding the aging of the Manaus plume. Based on literature observations (de Gouw and Jimenez, 2009;Kleinman et al., 2008;DeCarlo et al., 2010;Takegawa et al., 2006;Sullivan et al., 2006;Freney et al., 2014), we hypothesized that Δorg/ΔCO would rapidly increase in the Manaus plume due to OA formation from sources not associated with urban CO emissions (Setyan et al., 2012;Shilling et al., 2013).

Specifically, we expected that enhanced OH concentrations in the plume would lead to rapid oxidation of BVOCs emitted from the surrounding forest, which would produce OA with little concomitant production of CO. As seen in Figure ~~6~~7, the data did not support this hypothesis. As described in the Supporting Information, we performed the Δorg/ΔCO calculation using several methods and assuming different background CO and OA values and did not find significant increases in Δorg/ΔCO in any of these calculations. ~~We acknowledge that calculation of Δorg/ΔCO values can be sensitive to the calculation method and choice of background values for both OA and CO; therefore, we performed calculations using different methods and assuming different background concentrations for both OA and CO (see SI for more details). We did not find significant increases in Δorg/ΔCO in any of these calculations.~~ Furthermore, though we focus on Δorg values based on the AMS data, we also calculated Δvolume/ΔCO using aerosol size distribution data from two independent instruments, the Ultra-High Sensitivity Aerosol Spectrometer (UHSAS) and the Fast Integrated Mobility Spectrometer (FIMS) that were also ~~onboard~~on board the G-1. Neither of these calculations indicates an increase in Δvolume/ΔCO with plume age. ~~The median Δorg/ΔCO values for the plume as measured at the T2 and T3 sites are also nearly identical to one another in the wet season, suggesting the March 13, 2014 G-1 observations are representative of the Manaus plume behavior across longer timescales in the wet season (Cirino et al.).~~

Previous studies have observed increases in Δorg/ΔCO with plume age, with the largest increases occurring for the first ~1 day of aging and changes in Δorg/ΔCO gradually ~~leveling~~levelling off beyond approximately 1-2 days (DeCarlo et al., 2010;de Gouw and Jimenez, 2009;Kleinman et al., 2008;Freney et al., 2014). Based on the mean wind speeds observed along the flight track (7.3 m s^{-1}) and the transport distance (up to 100 km), we estimate that the plume was 4-5 hours old at the farthest leg and freshly emitted over the city. Unfortunately, photochemical clocks could not be used to more precisely calculate the photochemical age of the plume (de Gouw et al., 2005;Kleinman et al., 2003;Parrish et al., 1992). NO_y measurements were not available on this flight. Benzene and toluene concentrations were low and noisy, particularly at increasingly downwind distances from Manaus~~, so we were unable to use this clock to reliably estimate the plume age, though they do appear to indicate some degree of aging~~. Though our observations are limited to shorter aging timescales (4-5 hours) than many literature studies (1-2 days), the literature studies report measurable changes in Δorg/ΔCO at short aging timescales (Kleinman et al., 2008;DeCarlo et al., 2010). Furthermore, we clearly observe other indicators of photochemical aging in the plume. Ozone concentrations are 30 – 50 ppbv in the plume, compared to background levels of 10-15 ppbv, indicating active photochemistry. Concentrations of isoprene are lower in the plume than the background values observed outside of it. Concentrations of isoprene inside the plume do not show a monotonic dependence on plume age, The concentration of isoprene oxidation products measured in the plume by the PTR-MS at m/z 71 monotonically increases with plume aging, from 0.96 ppbv directly over the city to 1.27 ppbv at the farthest leg. The average toluene:benzene ratio in the plume also monotonically decreases with plume aging as would be expected, though attempts to convert these ratios into a photochemical age resulted in unrealistically high estimates of the plume age, likely due to noise in the data as mentioned above (de Gouw et al., 2005). The mean particle oxidation state ($\bar{O}S_c$) of plume OA increases from -0.6 to -0.44 as it ages. It is expected that photochemical aging would produce progressively more oxygenated species downwind of Manaus that subsequently partition to the aerosol

Formatted: Font: 10 pt, Not Italic

phase, increasing the mean carbon oxidation state. Other studies have observed a similar phenomenon as particles were transported downwind of urban centers (DeCarlo et al., 2010). The particles size distributions measured by both the FIMS and the UHSAS also indicate that particles size increases downwind of Manaus. As discussed in the previous section, we also observe that the mass fraction of HOA decreases and simultaneously the mass fraction of OOA increases as the plume ages. As seen in Figure ~~6~~7, ΔHOA/ΔCO is 17.6 μg/m^3 ppmv^{-1} on the leg nearest to the city and decreases to 10.6 μg/m^3 ppmv^{-1}. At the same time, ΔOOA/ΔCO increases from 9.2 μg/m^3 ppmv^{-1} to 23.1 μg/m^3 ppmv^{-1}. Thus, some fraction of HOA appears to be lost, either through volatilization, ~~or~~ deposition, or a combination of both, with the lost HOA mass balanced by an increase in OOA mass. All of these factors indicate that active photochemistry is occurring and is transforming VOC's into SOA and aging the particles. Thus, we would expect to see significant increases in Δorg/ΔCO for these aging times, if similar observations of outflow from North American cities were representative of the Manaus plume.

The sum of the HOA and OOA factors explains >95% of the total OA mass within the plume, as the IEPOX SOA mass is small. Though calculating the ΔHOA/ΔCO and ΔOOA/ΔCO ratios introduces some noise (particularly ΔOOA/ΔCO close to Manaus), the sum of these ratios is approximately constant with aging and equal to the Δorg/ΔCO values. Thus, the total OA mass is conserved with loss and volatilization of HOA balanced out by formation of OOA. This process appears to explain the lack of an increase in Δorg/ΔCO with aging. It is difficult to determine whether the OOA carbon mass is anthropogenic in origin, biogenic, or (most likely) a combination of both. Volatilized HOA and co-emitted anthropogenic VOCs would undergo oxidation in the plume and the products may condense as OOA (Sage et al., 2008;Robinson et al., 2007). In addition, we see evidence that biogenic VOCs are oxidized in the plume, likely more rapidly than in the background due to enhanced in-plume OH concentrations, and these oxidation products may also condense as OOA. Either mechanism or a combination of both would explain the observed increase in the carbon oxidation state. It is surprising that the volatilized HOA mass is compensated by oxidation and re-condensation of SOA for these relatively fresh particles.

Thus far, we have focused on a detailed analysis of the March 13, 2014 plume because there is a clear contrast between the background and plume data through the portion of the flight in the boundary layer, there is little interference from biomass burning and cloud processing, the flight pattern was extended far enough downwind to investigate a significant aging time, and the data from all key instruments are available and complete. In an effort to understand whether the Δorg/ΔCO observations on March 13 are representative of plume aging in the wet season, we have screened the rest of the wet season flight data and, based on the criteria mentioned above, we have identified two additional flights, March 11 and March 16, 2014, for analysis. The Δorg/ΔCO values for these data as a function of distance from Manaus are shown in Figure 8. On March 11, Δorg/ΔCO values average 29.9 μg/m^3 ppmv^{-1}, show little change with distance from Manaus, and show similar variability as the March 13 flight data. The mean wind speed for the analyzed portion of the flight was 5.3 m/s translating to an approximate maximum plume age of 5-5.5 hours. On March 16, Δorg/ΔCO values average 42.0 μg/m^3 ppmv^{-1}, show little significant increase with distance from Manaus, and exhibit a larger range of values than the other two datasets. The mean wind speed for the analyzed portion of the March 16 flight was 4.6 m/s translating to an approximate maximum plume age of 6-6.5 hours. We estimate that the error in the Δorg/ΔCO measurement is approximately 10 μg/m^3 ppmv^{-1}, thus the difference in average Δorg/ΔCO values

Formatted: Superscript

between the March 16 and the March 11 and 13 datasets are at the edge of what we would consider significant. The average Δorg/ΔCO is 34.3 μg/m^3 ppmv^{-1} for all flights and collectively represent the first 4 – 6.5 hours of aging. In addition to the aircraft data, Cirino et al. (2018) report that the median Δorg/ΔCO values for the plume as measured at the T2 and T3 sites are nearly identical to one another in the wet season and similar to measurements from the G-1(Cirino et al.). Thus, the data from both G-1 and the ground sites suggests that Δorg/ΔCO values of 30-40 μg/m^3 ppmv^{-1} that change little in the first 4-6.5 hours of plume aging are representative of the Manaus plume behaviour in the wet season. As previously discussed, most studies examining outflow of North American cities have shown changes in Δorg/ΔCO that are largest at the shortest aging times and we are unaware of reports of constant Δorg/ΔCO in an aging urban plume. Both the identity and the distribution of Manaus's emissions may very well be distinct from that of a typical North American city. In addition, background concentrations of anthropogenic pollutants are lower and biogenic VOC emissions are higher ~~downwind of~~ in the unperturbed rain forest surrounding Manaus relative to most North American cities. Finally, background OA concentrations near Manaus are lower in the wet season than in most other continental regions and SOA yield is known to increase with OA mass loading (Odum et al., 1996). All of these factors may contribute of the difference in the Δorg/ΔCO observations.

A similar phenomenon, clear chemical aging with little change of Δorg/ΔCO, has been observed in biomass burning plumes by several researchers (Jolleys et al., 2012;Cubison et al., 2011;Hecobian et al., 2011;Akagi et al., 2012;Forrister et al., 2015). Clearly, the mix of organic compounds emitted from a forest fire and from the Manaus urban region will be significantly different and this is not to imply that the detailed chemical mechanisms are the same. However, the similarity of the observations is suggestive that a similar process could occur in both types of plumes.

3.3 Sources of Sulfate in the Manaus Region

Sulfate was the second largest contributor to the non-refractory aerosol mass during the GoAmazon 2014/5 campaign (accounting for 13% of the PM_1 mass in both the wet and dry season), so it is also instructive to examine the source of sulfate in the area. In 2014 Manaus generated much of its power from fuel oil and diesel, which are known to emit SO_2 that eventually oxidizes to form condensable sulfate (Medeiros et al., 2017). However, several observations suggest that the major source of sulfate in the plume may not come from local SO_2 emissions. First, on many flights, particulate ~~SO_4~~ sulfate levels clearly increases in the plume (e.g., Figure 45), including on the legs closest to Manaus and thus very near the source. The lifetime of SO_2 with respect to homogeneous oxidation by OH is expected to be about one week and only small fraction (~5% on the farthest leg) of SO_2 emissions would have time to oxidize to H_2SO_4 in the gas phase. In addition, there is no indication of dramatically enhanced sulfate loading downwind of Manaus on the March 13 flight when $\Delta SO_4/\Delta CO$ ratio averages 2.6 μg/m^3 ppmv^{-1} and does not increase with plume age. On the March 13 flight, there was no precipitation and relatively few clouds along the flight track so heterogeneous oxidation of sulfate in cloud water cannot explain the sulfate enhancement seen in the plume.

We can possibly attribute these observations to two mechanisms. First, it is possible that natural sulfur emissions ~~such as DMS and H_2S~~ originating downwind of Manaus undergo oxidation by enhanced concentrations of OH in the Manaus plume and

subsequently condense (Andreae et al., 1990;Chen et al., 2009). Andrea et al. (1990) estimate that in-basin sulfur emissions are responsible for approximately 0.05 μg/m^3 of the total sulfate loading. Measurements during the AMAZE-08 campaign also suggested natural in-basin emissions and transport of natural out of basin emission were a significant source of particulate sulfate (Chen et al., 2009). A 0.05 μg/m^3 ~~SO_4~~ sulfate loading is roughly consistent with our measured ~~SO_4~~ sulfate concentrations outside of the plume and would account for 15 – 30% of the sulfate in the plume on the March 13 flight. Higher OH concentrations in the plume would speed oxidation of natural sulfur compounds and further increase the fraction of in-plume ~~SO_4~~ sulfate originating from natural emissions. Second, power plant plumes may directly emit sulfuric acid, which then may condenses on pre-existing particles. A previous aircraft study of the Manaus outflow observed high concentrations of particles smaller than 40 nm in power plant plumes, which they attribute to sulfuric acid (Kuhn et al., 2010). Though particles in this size range are unlikely to be detected by the AMS, condensation of sulfuric acid on larger, pre-existing particles would also contribute to the in-plume sulfate observations.

4 Summary and Implications

In summary, we report on measurements of the aerosol chemical composition, sources, and evolution of the urban plume from 35 research flights conducted in both the wet and dry season in the vicinity of Manaus, Brazil. Median mass loading of organics, sulfate, nitrate, and ammonium were 0.85~~72~~, 0.1~~91~~, 0.0~~24~~, and 0.0~~63~~ μg/m^3 in the wet season and 4.29~~06~~, 0.~~76~~7, 0.05~~17~~, and 0.25 μg/m^3 in the dry season. Despite the significant difference in mass loadings, the average fractional composition of the aerosol did not change significantly between seasons. Organics dominate the aerosol chemical composition in both seasons, comprising ~~79~~80% of the total non-refractory aerosol mass. The OA was significantly more oxidized in the dry season with a $\bar{OS}_c$ of -0.02 in the dry season and -0.45 in the wet season.

The flight on March 13, 2014 was a golden day to study the evolution of the Manaus plume as it advected to the surrounding Amazon tropical forest. The organic and sulfate aerosol concentrations were both significantly enhanced in the plume along with CO, ozone, and benzene. The spatial distribution of the sulfate aerosol was shifted toward the southern edge of the plume, relative to organics, CO, and benzene. As the plume is transported downwind of Manaus, we observe a change in the relative fraction of HOA and OOA mass. ΔHOA/ΔCO values decreased from 17.6 μg/m^3 ppmv^{-1} over Manaus to 10.6 μg/m^3 ppmv^{-1} 95 km downwind of Manaus, indicating a substantial loss of HOA mass. This loss of HOA mass was balanced out by OOA formation, with ΔOOA/ΔCO values increasing from 9.2 to 23.1 μg/m^3 ppmv^{-1} during the 4-5 hour aging timescale. Concomitantly, the mean carbon oxidation state of the OA increased from -0.6 to -0.44. Because the loss of HOA mass was balanced out by addition of OOA mass, net changes in Δorg/ΔCO with plume age were not observed and averaged 31 μg/m^3 ppmv^{-1}. Analysis of data from two additional fights during the wet season also found no net changes in Δorg/ΔCO with plume age. The average Δorg/ΔCO for all the anayzed G-1 data was 34 μg/m^3 ppmv^{-1} and collectively represent the first 4- 6.5 hours of plume aging. The observation of constant Δorg/ΔCO with aging was in contrast to our hypothesis that Δorg/ΔCO would increase rapidly due to plume-enhanced oxidation of BVOCs, emitted by the surrounding tropical forest and not associated

with CO emissions, and subsequent conversion to OA mass. Our Δorg/ΔCO observations are also in contrast to literature observations of the outflow of several different North American urban centers, which have shown increases in Δorg/ΔCO for the first 1-2 days of plume aging (Kleinman et al., 2008;de Gouw and Jimenez, 2009;DeCarlo et al., 2010;Freney et al., 2014;Sullivan et al., 2006).

The dataset generated from the G-1 measurements during GoAmazon 2014/5 provide a set of observations for understanding aerosol chemistry in the Amazon region. Our preliminary analysis shows that outflow from the Manaus plume generates less OA in the wet season when compared to outflow of many North American cities. The differences are likely due to a combination of factor including differences in emissions from both Manaus and the surrounding tropical forest, lower levels of background anthropogenic pollution in the Amazon, and lower background OA concentrations into which semi-volatile organics can partition. These results have implications for ~~modeling~~modelling efforts and for understanding how urban pollution impacts the surrounding pristine Amazon.

Appendix

PMF Analysis of AMS data

Positive Matrix Factorization (PMF) analysis was performed on the high-resolution organic aerosol mass spectra and error matrix that were measured using the HR-ToF-AMS on the G-1. The organic aerosol mass spectra ($m/z < 122$) and error matrix were initially prepared using the high resolution AMS analysis package (Squirrel v1.55H, PIKA v1.44H) as described in the literature (Jimenez et al., 2003;Allan et al., 2004;DeCarlo et al., 2006;Aiken et al., 2007;Aiken et al., 2008). As described in the main text, the AMS organic mass loading data were normalized to the laboratory calibration conditions of 23 °C 1013 hPa. Error was estimated from the ion counting statistics (Allan et al., 2003) and a minimum error was assigned to each signal (Ulbrich et al., 2009). Ion with signal below zero (due to noise) were removed from the matrix. In addition, ions with an average signal to noise (S/N) less than 0.75 were removed and ions with average S/N between 0.75 and 2 were downweighted by a factor of two (Ulbrich et al., 2009). Ions whose signals are fixed based on the measured CO_2 signal in the ratios described by Aiken et al., (2008) (CO^+, H_2O^+, HO^+, O^+) are also downweighted by a factor of two (Ulbrich et al., 2009). The PFM2 algorithm version 4.2 (Paatero, 1997;Paatero and Tapper, 1994) was used to analyze the matrix and results were visualized and evaluated using the PMF Evaluation Tool (v 2.06) described by Ulbrich et al. (2009). PMF analysis of this data set was challenging, due the combination of low concentrations of organic aerosol, fast sampling required for aircraft operations, and the often small changes in aerosol concentrations across the flight domain. PMF analysis on a data from a single flight often (though not always) resulted in a failure to resolve factors that are described in the literature (e.g., HOA, IEPOX SOA). Instead, we often observes split factors that are largely dominated by a single high S/N ion (CHO^+, CO_2^+, $C_2H_3O^+$). For example, the IEPOX SOA factor was not resolved when the March 13 flight was analyzed on its own, largely due to the small mass loading

of this factor (Figure 6). Therefore, data from all flights during the wet season was combined into a single matrix and analyzed together, which also forces a common solution for the entire dataset.

We chose a five factor solution to the combined matrix based on number of criteria, including; the residuals and fit quality, the correlation of chosen factors with independently measured species (e.g., CO, ozone), by examining the factor mass spectra for realism (are the spectra representative of a physical compound?), and by comparing the factor spectra to literature data. Table A1 summarizes the residuals as a function of the number of factors and a short summary of the results. First, as seen in Table A1, the residuals continue to significantly decrease in moving from a 2 to 5 factor solution. For example, Q/Q_{exp} decreases from 0.28 to 0.24 and the fraction of the residual aerosol mass decreases from 4% to 0.1% in moving from the two to the five factor solution. Figure S2 shows the residuals and scaled residuals for each time point in the matrix for the 5 factor solution, indicating that all the data are well fit. Solutions with three or fewer factors failed to separate the HOA and the IEPOX SOA factors, which are well described in the literature and were reasonably expected to be present in the data. One of the OOA-like spectra in the three factor solution also appeared to have signs of both the HOA and IEPOX SOA factor in the spectra, as evidenced by significant signal of the key marker ions $C_4H_9^+$ (m/z 57) for HOA and $C_5H_6O^+$ (m/z 82) for IEPOX SOA. In the four factor solution, an HOA factor was resolved along with three OOA-like spectra, though the OOA spectra show evidence of factor splitting (discussed below). The five factor solution was able to resolve an HOA, IEPOX-SOA and three OOA-like factors.

Figure S3 and S4 show the mass spectra and time series for the five factor solution. Examination of the mass spectra (Figure S4) suggests that the OOA factor has split. For example, the mass spectrum of Factor 3 is dominated by the CHO^+ ion with little signal through the rest of the spectra. The spectrum of Factor 1 is dominate by CO_2^+ and other ions that are based on the CO_2^+ signal (CO^+, H_2O^+, HO^+, O^+) in prescribed ratios (Aiken et al., 2008). These factors are unlikely to represent some real aerosol component, as no known OA produces such simple spectra. In addition, the time series of Factors 1 and 2 are highly correlated in time (see Figure S5). In summary, two factors are highly correlated in time (Factors 1 and 2) and a third factor is dominated by a single ion. Thus, we recombine Factors 1, 2, and 3 into a single factor, which we label OOA. The spectra of the resultant three factors (after re-combining) are shown in Figure S6 and the recombined factor is presented in the main text. The mathematical reason for the factor splitting is clear; aerosol loading is low, the AMS is sampling at a relatively fast rate (13 s averaging time), and the AMS spectra are dominated by a relatively small number of high S/N ions. In separate analyzes, we downweighted the CHO^+, $C_2H_3O^+$, and CO_2^+ ion signals by factors of 2-10 in an attempt to minimize the splitting of the OOA factor, but were unsuccessful.

Comparison of the factor mass spectra to literature PMF spectra and correlation of the factor time profiles with independent measurements provides further support for the 5-factor solution. The combined OOA factor compares well with the spectra presented in the literature for OOA (e.g., (Zhang et al., 2007;Zhang et al., 2011;Zhang et al., 2005b;Ng et al., 2010). As shown in Figure 6, the OOA factor correlates well with ozone, a known secondary species that also forms through photochemical reactions. Similarly, the spectrum of Factor 4 compares well with the mass spectrum of HOA widely reported in the literature (e.g., (Zhang et al., 2007;Zhang et al., 2011;Zhang et al., 2005b;Ng et al., 2010). As discussed in the text and shown in Figure

6, the HOA factor correlates well with CO, a known tracer of anthropogenic combustion processes. We label Factor 5 as the IEPOX SOA factor that is widely reported in the literature and believed to represent SOA formed from the heterogeneous uptake of isoprene epoxydiols onto pre-existing aerosol (Hu et al., 2015;Robinson et al., 2011;Lin et al., 2012). Our assignment is based on comparison with the factor mass spectral profile with those in the literature e.g., (Hu et al., 2015).

5 Acknowledgements

The authors thank the G-1 flight and ground crews for supporting the GoAmazon 2014/5 mission. Funding for data collection onboard the G-1 aircraft and at the ground sites was provided by the Atmospheric Radiation Measurement (ARM) Climate Research Facility, a U.S. Department of Energy (DOE) Office of Science user facility sponsored by the Office of Biological and Environmental Research (OBER). Data analysis and research was supported by the U.S. DOE's Atmospheric System Research Program under Contract DE-AC06-76RLO 1830 at PNNL. PNNL is operated for the U.S. DOE by Battelle Memorial Institute. We acknowledge the support from the Central Office of the Large Scale Biosphere Atmosphere Experiment in Amazonia (LBA), the Instituto Nacional de Pesquisas da Amazonia (INPA), and the Instituto Nacional de Pesquisas Espaciais (INPE). P. Artaxo acknowledges Fundação de Amparo à Pesquisa do Estado de São Paulo FAPESP grants 2013/05014-0, and 2017/17047-0. The work was conducted under licenses 001262/2012-2 and 001030/2012-4 of the Brazilian National Council for Scientific and Technological Development (CNPq).

References

Aiken, A. C., DeCarlo, P. F., and Jimenez, J. L.: Elemental analysis of organic species with electron ionization high-resolution mass spectrometry, Anal Chem, 79, 8350-8358, 10.1021/ac071150w, 2007.

Aiken, A. C., DeCarlo, P. F., Kroll, J. H., Worsnop, D. R., Huffman, J. A., Docherty, K., Ulbrich, I. M., Mohr, C., Kimmel, J. R., Sueper, D., Zhang, Q., Sun, Y., Trimborn, A., Northway, M., Ziemann, P. J., Canagaratna, M. R., Alfarra, R., Prevot, A. S. H., Dommen, J., Duplissy, J., Metzger, A., Baltensperger, U., and Jimenez, J. L.: O/C and OM/OC Ratios of Primary, Secondary, and Ambient Organic Aerosols with High Resolution Time-of-Flight Aerosol Mass Spectrometry, Environ. Sci. Technol., 42, 4478-4485, doi:10.1021/es703009q, 2008.

Akagi, S. K., Craven, J. S., Taylor, J. W., McMeeking, G. R., Yokelson, R. J., Burling, I. R., Urbanski, S. P., Wold, C. E., Seinfeld, J. H., Coe, H., Alvarado, M. J., and Weise, D. R.: Evolution of trace gases and particles emitted by a chaparral fire in California, Atmos. Chem. Phys., 12, 1397-1421, 10.5194/acp-12-1397-2012, 2012.

Allan, J. D., Jiminez, J. L., Williams, P. I., Alfarra, M. R., Bower, K. N., Jayne, J. T., Coe, H., and Worsnop, D. R.: Quantitative sampling using an Aerodyne aerosol mass spectrometer - 1. Techniques of data interpretation and error analysis, J. Geophys. Res., 108, 4090, 2003.

Allan, J. D., Delia, A. E., Coe, H., Bower, K. N., Alfarra, M. R., Jimenez, J. L., Middlebrook, A. M., Drewnick, F., Onasch, T. B., Canagaratna, M. R., Jayne, J. T., and Worsnopf, D. R.: A generalised method for the extraction of chemically resolved mass spectra from aerodyne aerosol mass spectrometer data, Journal of Aerosol Science, 35, 909-922, 2004.

Allan, J. D., Morgan, W. T., Darbyshire, E., Flynn, M. J., Williams, P. I., Oram, D. E., Artaxo, P., Brito, J., Lee, J. D., and Coe, H.: Airborne observations of IEPOX-derived isoprene SOA in the Amazon during SAMBBA, Atmos. Chem. Phys., 14, 11393-11407, 10.5194/acp-14-11393-2014, 2014.

Andreae, M. O., Berresheim, H., Bingemer, H., Jacob, D. J., Lewis, B. L., Li, S. M., and Talbot, R. W.: The Atmospheric Sulfur Cycle over the Amazon Basin .2. Wet Season, Journal of Geophysical Research-Atmospheres, 95, 16813-16824, DOI 10.1029/JD095iD10p16813, 1990.

Andreae, M. O.: Atmosphere. Aerosols before pollution, Science, 315, 50-51, 10.1126/science.1136529, 2007.

Andreae, M. O., Artaxo, P., Beck, V., Bela, M., Freitas, S., Gerbig, C., Longo, K., Munger, J. W., Wiedemann, K. T., and Wofsy, S. C.: Carbon monoxide and related trace gases and aerosols over the Amazon Basin during the wet and dry seasons, Atmos. Chem. Phys., 12, 6041-6065, 10.5194/acp-12-6041-2012, 2012.

Andreae, M. O., Acevedo, O. C., Araujo, A., Artaxo, P., Barbosa, C. G. G., Barbosa, H. M. J., Brito, J., Carbone, S., Chi, X., Cintra, B. B. L., da Silva, N. F., Dias, N. L., Dias, C. Q., Ditas, F., Ditz, R., Godoi, A. F. L., Godoi, R. H. M., Heimann, M., Hoffmann, T., Kesselmeier, J., Konemann, T., Kruger, M. L., Lavric, J. V., Manzi, A. O., Lopes, A. P., Martins, D. L., Mikhailov, E. F., Moran-Zuloaga, D., Nelson, B. W., Nolscher, A. C., Nogueira, D. S., Piedade, M. T. F., Pohlker, C., Poschl, U., Quesada, C. A., Rizzo, L. V., Ro, C. U., Ruckteschler, N., Sa, L. D. A., Sa, M. D., Sales, C. B., dos Santos, R. M. N., Saturno, J., Schongart, J., Sorgel, M., de Souza, C. M., de Souza, R. A. F., Su, H., Targhetta, N., Tota, J., Trebs, I., Trumbore, S., van Eijck, A., Walter, D., Wang, Z., Weber, B., Williams, J., Winderlich, J., Wittmann, F., Wolff, S., and Yanez-Serrano, A. M.: The Amazon Tall Tower Observatory (ATTO): overview of pilot measurements on ecosystem ecology, meteorology, trace gases, and aerosols, Atmos. Chem. Phys., 15, 10723-10776, 10.5194/acp-15-10723-2015, 2015.

Artaxo, P., Rizzo, L. V., Brito, J. F., Barbosa, H. M. J., Arana, A., Sena, E. T., Cirino, G. G., Bastos, W., Martin, S. T., and Andreae, M. O.: Atmospheric aerosols in Amazonia and land use change: from natural biogenic to biomass burning conditions, Faraday Discussions, 165, 203-235, 10.1039/C3FD00052D, 2013.

Atkinson, R., and Arey, J.: Atmospheric Degradation of Volatile Organic Compounds, Chemical Reviews, 103, 4605-4638, 10.1021/cr0206420, 2003.

Bahreini, R., Dunlea, E. J., Matthew, B. M., Simons, C., Docherty, K. S., DeCarlo, P. F., Jimenez, J. L., Brock, C. A., and Middlebrook, A. M.: Design and operation of a pressure-controlled inlet for airborne sampling with an aerodynamic aerosol lens, Aerosol Sci. Technol., 42, 465-471, 10.1080/02786820802178514, 2008.

Bean, J. K., Faxon, C. B., Leong, Y. J., Wallace, H. W., Cevik, B. K., Ortiz, S., Canagaratna, M. R., Usenko, S., Sheesley, R. J., Griffin, R. J., and Hildebrandt Ruiz, L.: Composition and Sources of Particulate Matter Measured near Houston, TX: Anthropogenic-Biogenic Interactions, Atmosphere, 7, 23, UNSP 73 10.3390/atmos7050073, 2016.

Bond, T. C., Streets, D. G., Yarber, K. F., Nelson, S. M., Woo, J. H., and Klimont, Z.: A technology-based global inventory of black and organic carbon emissions from combustion, Journal of Geophysical Research-Atmospheres, 109, n/a-n/a, Artn D14203 10.1029/2003jd003697, 2004.

Burleyson, C. D., Feng, Z., Hagos, S. M., Fast, J., Machado, L. A. T., and Martin, S. T.: Spatial Variability of the Background Diurnal Cycle of Deep Convection around the GoAmazon2014/5 Field Campaign Sites, Journal of Applied Meteorology and Climatology, 55, 1579-1598, 10.1175/jamc-d-15-0229.1, 2016.

Canagaratna, M. R., Jimenez, J. L., Kroll, J. H., Chen, Q., Kessler, S. H., Massoli, P., Hildebrandt Ruiz, L., Fortner, E., Williams, L. R., Wilson, K. R., Surratt, J. D., Donahue, N. M., Jayne, J. T., and Worsnop, D. R.: Elemental ratio measurements of organic compounds using aerosol mass spectrometry: characterization, improved calibration, and implications, Atmos. Chem. Phys., 15, 253-272, 10.5194/acp-15-253-2015, 2015.

Chen, Q., Farmer, D. K., Schneider, J., Zorn, S. R., Heald, C. L., Karl, T. G., Guenther, A., Allan, J. D., Robinson, N., Coe, H., Kimmel, J. R., Pauliquevis, T., Borrmann, S., Poschl, U., Andreae, M. O., Artaxo, P., Jimenez, J. L., and Martin, S. T.: Mass spectral characterization of submicron biogenic organic particles in the Amazon Basin, Geophys. Res. Lett., 36, 5, Artn L20806 10.1029/2009gl039880, 2009.

Chen, Q., Farmer, D. K., Rizzo, L. V., Pauliquevis, T., Kuwata, M., Karl, T. G., Guenther, A., Allan, J. D., Coe, H., Andreae, M. O., Poschl, U., Jimenez, J. L., Artaxo, P., and Martin, S. T.: Submicron particle mass concentrations and sources in the Amazonian wet season (AMAZE-08), Atmos. Chem. Phys., 15, 3687-3701, 10.5194/acp-15-3687-2015, 2015.

Cirino, G. G., Brito, J., Barbosa, H. J. M., Rizzo, L. V., Carbone, S., de Sa, S. S., Tunved, P., Jimenez, J. L., Palm, B., Souza, R. A. F., Lavric, J., Tota, J., Oliveira, M., Wolff, S., Martin, S. T., and Artaxo, P.: Ground site observations of Manaus city plume evolution in GoAmazon2014/5, In preparation for Atmsopheric Chemistry and Physics, 2018.

Crosier, J., Allan, J. D., Coe, H., Bower, K. N., Formenti, P., and Williams, P. I.: Chemical composition of summertime aerosol in the Po Valley (Italy), northern Adriatic and Black Sea, Quarterly Journal of the Royal Meteorological Society, 133, 61-75, 10.1002/qj.88, 2007.

Cubison, M. J., Ortega, A. M., Hayes, P. L., Farmer, D. K., Day, D., Lechner, M. J., Brune, W. H., Apel, E., Diskin, G. S., Fisher, J. A., Fuelberg, H. E., Hecobian, A., Knapp, D. J., Mikoviny, T., Riemer, D., Sachse, G. W., Sessions, W., Weber, R. J., Weinheimer, A. J., Wisthaler, A., and Jimenez, J. L.: Effects of aging on organic aerosol from open biomass burning smoke in aircraft and laboratory studies, Atmos. Chem. Phys., 11, 12049-12064, 10.5194/acp-11-12049-2011, 2011.

de Gouw, J., and Jimenez, J. L.: Organic aerosols in the Earth's atmosphere, Environ Sci Technol, 43, 7614-7618, 10.1021/es9006004, 2009.

de Gouw, J. A., Middlebrook, A. M., Warneke, C., Goldan, P. D., Kuster, W. C., Roberts, J. M., Fehsenfeld, F. C., Worsnop, D. R., Canagaratna, M. R., Pszenny, A. A. P., Keene, W. C., Marchewka, M., Bertman, S. B., and Bates, T. S.: Budget of organic carbon in a polluted atmosphere: Results from the New England Air Quality Study in 2002, J. Geophys. Res.-Atmos., 110, 10.1029/2004JD005623, 2005.

de Gouw, J. A., Brock, C. A., Atlas, E. L., Bates, T. S., Fehsenfeld, F. C., Goldan, P. D., Holloway, J. S., Kuster, W. C., Lerner, B. M., Matthew, B. M., Middlebrook, A. M., Onasch, T. B., Peltier, R. E., Quinn, P. K., Senff, C. J., Stohl, A., Sullivan, A. P., Trainer, M., Warneke, C., Weber, R. J., and Williams, E. J.: Sources of particulate matter in the northeastern United States in summer: 1. Direct emissions and secondary formation of organic matter in urban plumes, Journal of Geophysical Research, 113, n/a-n/a, 10.1029/2007jd009243, 2008.

de Sá, S. S., Palm, B. B., Campuzano-Jost, P., Day, D. A., Newburn, M. K., Hu, W., Isaacman-VanWertz, G., Yee, L. D., Thalman, R., Brito, J., Carbone, S., Artaxo, P., Goldstein, A. H., Manzi, A. O., Souza, R. A. F., Mei, F., Shilling, J. E., Springston, S. R., Wang, J., Surratt, J. D., Alexander, M. L., Jimenez, J. L., and Martin, S. T.: Influence of urban pollution on the production of organic particulate matter from isoprene epoxydiols in central Amazonia, Atmos. Chem. Phys., 17, 6611-6629, 10.5194/acp-17-6611-2017, 2017.

de Sá, S. S., Palm, B. B., Campuzano-Jost, P., Day, D. A., Hu, W., Isaacman-VanWertz, G., Yee, L. D., Brito, J., Carbone, S., Ribeiro, I. O., Cirino, G. G., Liu, Y. J., Thalman, R., Sedlacek, A., Funk, A., Schumacher, C., Shilling, J. E., Schneider, J., Artaxo, P., Goldstein, A. H., Souza, R. A. F., Wang, J., McKinney, K. A., Barbosa, H., Alexander, M. L., Jimenez, J. L., and Martin, S. T.: Urban influence on the concentration and composition of submicron particulate matter in central Amazonia, Atmos. Chem. Phys. Discuss., 1-56, 10.5194/acp-2018-172, 2018.

DeCarlo, P. F., Kimmel, J. R., Trimborn, A., Northway, M. J., Jayne, J. T., Aiken, A. C., Gonin, M., Fuhrer, K., Horvath, T., Docherty, K. S., Worsnop, D. R., and Jimenez, J. L.: Field-deployable, high-resolution, time-of-flight aerosol mass spectrometer, Anal Chem, 78, 8281-8289, 10.1021/ac061249n, 2006.

DeCarlo, P. F., Dunlea, E. J., Kimmel, J. R., Aiken, A. C., Sueper, D., Crounse, J., Wennberg, P. O., Emmons, L., Shinozuka, Y., Clarke, A., Zhou, J., Tomlinson, J., Collins, D. R., Knapp, D., Weinheimer, A. J., Montzka, D. D., Campos, T., and Jimenez, J. L.: Fast airborne aerosol size and chemistry measurements above Mexico City and Central Mexico during the MILAGRO campaign, Atmos. Chem. Phys., 8, 4027-4048, DOI 10.5194/acp-8-4027-2008, 2008.

DeCarlo, P. F., Ulbrich, I. M., Crounse, J., de Foy, B., Dunlea, E. J., Aiken, A. C., Knapp, D., Weinheimer, A. J., Campos, T., Wennberg, P. O., and Jimenez, J. L.: Investigation of the sources and processing of organic aerosol over the Central Mexican Plateau from aircraft measurements during MILAGRO, Atmos. Chem. Phys., 10, 5257-5280, 10.5194/acp-10-5257-2010, 2010.

Ehn, M., Thornton, J. A., Kleist, E., Sipila, M., Junninen, H., Pullinen, I., Springer, M., Rubach, F., Tillmann, R., Lee, B., Lopez-Hilfiker, F., Andres, S., Acir, I. H., Rissanen, M., Jokinen, T., Schobesberger, S., Kangasluoma, J., Kontkanen, J., Nieminen, T., Kurten, T., Nielsen, L. B., Jorgensen, S., Kjaergaard, H. G., Canagaratna, M., Maso, M. D., Berndt, T., Petaja, T., Wahner, A., Kerminen, V. M., Kulmala, M., Worsnop, D. R., Wildt, J., and Mentel, T. F.: A large source of low-volatility secondary organic aerosol, Nature, 506, 476-479, 10.1038/nature13032, 2014.

Fan, J., Rosenfeld, D., Zhang, Y., Giangrande, S. E., Li, Z., Machado, L. A. T., Martin, S. T., Yang, Y., Wang, J., Artaxo, P., Barbosa, H. M. J., Braga, R. C., Comstock, J. M., Feng, Z., Gao, W., Gomes, H. B., Mei, F., Pöhlker, C., Pöhlker, M. L., Pöschl, U., and de Souza, R. A. F.: Substantial convection and precipitation enhancements by ultrafine aerosol particles, Science, 359, 411-418, 10.1126/science.aan8461, 2018.

Farmer, D. K., Matsunaga, A., Docherty, K. S., Surratt, J. D., Seinfeld, J. H., Ziemann, P. J., and Jimenez, J. L.: Response of an aerosol mass spectrometer to organonitrates and organosulfates and implications for atmospheric chemistry, Proc Natl Acad Sci U S A, 107, 6670-6675, 10.1073/pnas.0912340107, 2010.

Ferek, R. J., Reid, J. S., Hobbs, P. V., Blake, D. R., and Liousse, C.: Emission factors of hydrocarbons, halocarbons, trace gases and particles from biomass burning in Brazil, Journal of Geophysical Research-Atmospheres, 103, 32107-32118, Doi 10.1029/98jd00692, 1998.

Forrister, H., Liu, J., Scheuer, E., Dibb, J., Ziemba, L., Thornhill, K. L., Anderson, B., Diskin, G., Perring, A. E., Schwarz, J. P., Campuzano-Jost, P., Day, D. A., Palm, B. B., Jimenez, J. L., Nenes, A., and Weber, R. J.: Evolution of brown carbon in wildfire plumes, Geophys. Res. Lett., 42, 4623-4630, 10.1002/2015gl063897, 2015.

Freney, E. J., Sellegri, K., Canonaco, F., Colomb, A., Borbon, A., Michoud, V., Doussin, J. F., Crumeyrolle, S., Amarouche, N., Pichon, J. M., Bourianne, T., Gomes, L., Prevot, A. S. H., Beekmann, M., and Schwarzenboeck, A.: Characterizing the impact of urban emissions on regional aerosol particles: airborne measurements during the MEGAPOLI experiment, Atmos. Chem. Phys., 14, 1397-1412, 10.5194/acp-14-1397-2014, 2014.

Fuzzi, S., Decesari, S., Facchini, M. C., Cavalli, F., Emblico, L., Mircea, M., Andreae, M. O., Trebs, I., Hoffer, A., Guyon, P., Artaxo, P., Rizzo, L. V., Lara, L. L., Pauliquevis, T., Maenhaut, W., Raes, N., Chi, X., Mayol-Bracero, O. L., Soto-García, L. L., Claeys, M., Kourtchev, I., Rissler, J., Swietlicki, E., Tagliavini, E., Schkolnik, G., Falkovich, A. H., Rudich, Y., Fisch, G., and Gatti, L. V.: Overview of the inorganic and organic composition of size-segregated aerosol in Rondônia, Brazil, from the biomass-burning period to the onset of the wet season, Journal of Geophysical Research, 112, n/a-n/a, 10.1029/2005jd006741, 2007.

Gaston, C. J., Riedel, T. P., Zhang, Z., Gold, A., Surratt, J. D., and Thornton, J. A.: Reactive Uptake of an Isoprene-Derived Epoxydiol to Submicron Aerosol Particles, Environ. Sci. Technol., 48, 11178-11186, 10.1021/es5034266, 2014.

Giangrande, S. E., Feng, Z., Jensen, M. P., Comstock, J. M., Johnson, K. L., Toto, T., Wang, M., Burleyson, C., Bharadwaj, N., Mei, F., Machado, L. A. T., Manzi, A. O., Xie, S., Tang, S., Silva Dias, M. A. F., de Souza, R. A. F., Schumacher, C., and Martin, S. T.: Cloud characteristics, thermodynamic controls and radiative impacts during the Observations and Modeling of the Green Ocean Amazon (GoAmazon2014/5) experiment, Atmos. Chem. Phys., 17, 14519-14541, 10.5194/acp-17-14519-2017, 2017.

Glasius, M., and Goldstein, A. H.: Recent Discoveries and Future Challenges in Atmospheric Organic Chemistry, Environ Sci Technol, 50, 2754-2764, 10.1021/acs.est.5b05105, 2016.

Goldstein, A. H., Koven, C. D., Heald, C. L., and Fung, I. Y.: Biogenic carbon and anthropogenic pollutants combine to form a cooling haze over the southeastern United States, Proc Natl Acad Sci U S A, 106, 8835-8840, 10.1073/pnas.0904128106, 2009.

Gu, D., Guenther, A. B., Shilling, J. E., Yu, H., Huang, M., Zhao, C., Yang, Q., Martin, S. T., Artaxo, P., Kim, S., Seco, R., Stavrakou, T., Longo, K. M., Tota, J., de Souza, R. A. F., Vega, O., Liu, Y., Shrivastava, M., Alves, E. G., Santos, F. C., Leng, G., and Hu, Z.: Airborne observations reveal elevational gradient in tropical forest isoprene emissions, Nat Commun, 8, 15541, 10.1038/ncomms15541, 2017.

Guenther, A., Karl, T., Harley, P., Wiedinmyer, C., Palmer, P. I., and Geron, C.: Estimates of global terrestrial isoprene emissions using MEGAN (Model of Emissions of Gases and Aerosols from Nature), Atmos. Chem. Phys., 6, 3181-3210, DOI 10.5194/acp-6-3181-2006, 2006.

Guenther, A. B., Jiang, X., Heald, C. L., Sakulyanontvittaya, T., Duhl, T., Emmons, L. K., and Wang, X.: The Model of Emissions of Gases and Aerosols from Nature version 2.1 (MEGAN2.1): an extended and updated framework for modeling biogenic emissions, Geosci. Model Dev., 5, 1471-1492, 10.5194/gmd-5-1471-2012, 2012.

Harriss, R. C., Sachse, G. W., Hill, G. F., Wade, L. O., and Gregory, G. L.: Carbon-Monoxide over the Amazon Basin during the Wet Season, Journal of Geophysical Research-Atmospheres, 95, 16927-16932, DOI 10.1029/JD095iD10p16927, 1990.

Hecobian, A., Liu, Z., Hennigan, C. J., Huey, L. G., Jimenez, J. L., Cubison, M. J., Vay, S., Diskin, G. S., Sachse, G. W., Wisthaler, A., Mikoviny, T., Weinheimer, A. J., Liao, J., Knapp, D. J., Wennberg, P. O., Kurten, A., Crounse, J. D., St Clair, J., Wang, Y., and Weber, R. J.: Comparison of chemical characteristics of 495 biomass burning plumes intercepted by the NASA DC-8 aircraft during the ARCTAS/CARB-2008 field campaign, Atmos. Chem. Phys., 11, 13325-13337, 10.5194/acp-11-13325-2011, 2011.

Hoyle, C. R., Boy, M., Donahue, N. M., Fry, J. L., Glasius, M., Guenther, A., Hallar, A. G., Hartz, K. H., Petters, M. D., Petaja, T., Rosenoern, T., and Sullivan, A. P.: A review of the anthropogenic influence on biogenic secondary organic aerosol, Atmos. Chem. Phys., 11, 321-343, 10.5194/acp-11-321-2011, 2011.

Hu, W. W., Campuzano-Jost, P., Palm, B. B., Day, D. A., Ortega, A. M., Hayes, P. L., Krechmer, J. E., Chen, Q., Kuwata, M., Liu, Y. J., de Sa, S. S., McKinney, K., Martin, S. T., Hu, M., Budisulistiorini, S. H., Riva, M., Surratt, J. D., St Clair, J. M., Isaacman-Van Wertz, G., Yee, L. D., Goldstein, A. H., Carbone, S., Brito, J., Artaxo, P., de Gouw, J. A., Koss, A., Wisthaler, A., Mikoviny, T., Karl, T., Kaser, L., Jud, W., Hansel, A., Docherty, K. S., Alexander, M. L., Robinson, N. H., Coe, H., Allan, J. D., Canagaratna, M. R., Paulot, F., and Jimenez, J. L.: Characterization of a real-time tracer for isoprene epoxydiols-derived secondary organic aerosol (IEPOX-SOA) from aerosol mass spectrometer measurements, Atmos. Chem. Phys., 15, 11807-11833, 10.5194/acp-15-11807-2015, 2015.

Intergovernmental Panel on Climate, C.: Climate Change 2013 - The Physical Science Basis, Cambridge University Press, Cambridge, United Kingdom and New York, NY, USA, 1535 pp., 2014.

Jayne, J. T., Leard, D. C., Zhang, X. F., Davidovits, P., Smith, K. A., Kolb, C. E., and Worsnop, D. R.: Development of an aerosol mass spectrometer for size and composition analysis of submicron particles, Aerosol Sci. Technol., 33, 49-70, Doi 10.1080/027868200410840, 2000.

Jimenez, J. L., Jayne, J. T., Shi, Q., Kolb, C. E., Worsnop, D. R., Yourshaw, I., Seinfeld, J. H., Flagan, R. C., Zhang, X. F., Smith, K. A., Morris, J. W., and Davidovits, P.: Ambient aerosol sampling using the Aerodyne Aerosol Mass Spectrometer, Journal of Geophysical Research-Atmospheres, 108, 8425, Artn 8425
10.1029/2001jd001213, 2003.

Jimenez, J. L., Canagaratna, M. R., Donahue, N. M., Prevot, A. S., Zhang, Q., Kroll, J. H., DeCarlo, P. F., Allan, J. D., Coe, H., Ng, N. L., Aiken, A. C., Docherty, K. S., Ulbrich, I. M., Grieshop, A. P., Robinson, A. L., Duplissy, J., Smith, J. D., Wilson, K. R., Lanz, V. A., Hueglin, C., Sun, Y. L., Tian, J., Laaksonen, A., Raatikainen, T., Rautiainen, J., Vaattovaara, P., Ehn, M., Kulmala, M., Tomlinson, J. M., Collins, D. R., Cubison, M. J., Dunlea, E. J., Huffman, J. A., Onasch, T. B., Alfarra, M. R., Williams, P. I., Bower, K., Kondo, Y., Schneider, J., Drewnick, F., Borrmann, S., Weimer, S., Demerjian, K., Salcedo, D., Cottrell, L., Griffin, R., Takami, A., Miyoshi, T., Hatakeyama, S., Shimono, A., Sun, J. Y., Zhang, Y. M., Dzepina, K., Kimmel, J. R., Sueper, D., Jayne, J. T., Herndon, S. C., Trimborn, A. M., Williams, L. R., Wood, E. C., Middlebrook, A. M., Kolb, C. E., Baltensperger, U., and Worsnop, D. R.: Evolution of organic aerosols in the atmosphere, Science, 326, 1525-1529, 10.1126/science.1180353, 2009.

Jolleys, M. D., Coe, H., McFiggans, G., Capes, G., Allan, J. D., Crosier, J., Williams, P. I., Allen, G., Bower, K. N., Jimenez, J. L., Russell, L. M., Grutter, M., and Baumgardner, D.: Characterizing the aging of biomass burning organic aerosol by use of mixing ratios: a meta-analysis of four regions, Environ Sci Technol, 46, 13093-13102, 10.1021/es302386v, 2012.

Kesselmeier, J., Kuhn, U., Wolf, A., Andreae, M. O., Ciccioli, P., Brancaleoni, E., Frattoni, M., Guenther, A., Greenberg, J., Vasconcellos, P. D., de Oliva, T., Tavares, T., and Artaxo, P.: Atmospheric volatile organic compounds (VOC) at a remote tropical forest site in central Amazonia, Atmospheric Environment, 34, 4063-4072, Doi 10.1016/S1352-2310(00)00186-2, 2000.

Kleinman, L. I., Daum, P. H., Lee, Y. N., Nunnermacker, L. J., Springston, S. R., Weinstein-Lloyd, J., Hyde, P., Doskey, P., Rudolph, J., Fast, J., and Berkowitz, C.: Photochemical age determinations in the Phoenix metropolitan area, Journal of Geophysical Research-Atmospheres, 108, 14, 10.1029/2002jd002621, 2003.

Kleinman, L. I., Springston, S. R., Daum, P. H., Lee, Y. N., Nunnermacker, L. J., Senum, G. I., Wang, J., Weinstein-Lloyd, J., Alexander, M. L., Hubbe, J., Ortega, J., Canagaratna, M. R., and Jayne, J.: The time evolution of aerosol composition over the Mexico City plateau, Atmos. Chem. Phys., 8, 1559-1575, 10.5194/acp-8-1559-2008, 2008.

Kroll, J. H., Donahue, N. M., Jimenez, J. L., Kessler, S. H., Canagaratna, M. R., Wilson, K. R., Altieri, K. E., Mazzoleni, L. R., Wozniak, A. S., Bluhm, H., Mysak, E. R., Smith, J. D., Kolb, C. E., and Worsnop, D. R.: Carbon oxidation state as a metric for describing the chemistry of atmospheric organic aerosol, Nat Chem, 3, 133-139, 10.1038/nchem.948, 2011.

Kuhn, U., Ganzeveld, L., Thielmann, A., Dindorf, T., Schebeske, G., Welling, M., Sciare, J., Roberts, G., Meixner, F. X., Kesselmeier, J., Lelieveld, J., Kolle, O., Ciccioli, P., Lloyd, J., Trentmann, J., Artaxo, P., and Andreae, M. O.: Impact of Manaus City on the Amazon Green Ocean atmosphere: ozone production, precursor sensitivity and aerosol load, Atmos. Chem. Phys., 10, 9251-9282, 10.5194/acp-10-9251-2010, 2010.

Lin, Y. H., Zhang, Z., Docherty, K. S., Zhang, H., Budisulistiorini, S. H., Rubitschun, C. L., Shaw, S. L., Knipping, E. M., Edgerton, E. S., Kleindienst, T. E., Gold, A., and Surratt, J. D.: Isoprene epoxydiols as precursors to secondary organic aerosol formation: acid-catalyzed reactive uptake studies with authentic compounds, Environ Sci Technol, 46, 250-258, 10.1021/es202554c, 2012.

Lindinger, W., Hansel, A., and Jordan, A.: On-line monitoring of volatile organic compounds at pptv levels by means of proton-transfer-reaction mass spectrometry (PTR-MS) - Medical applications, food control and environmental research, Int. J. Mass Spectrom., 173, 191-241, Doi 10.1016/S0168-1176(97)00281-4, 1998.

Liu, Y., Brito, J., Dorris, M. R., Rivera-Rios, J. C., Seco, R., Bates, K. H., Artaxo, P., Duvoisin, S., Jr., Keutsch, F. N., Kim, S., Goldstein, A. H., Guenther, A. B., Manzi, A. O., Souza, R. A., Springston, S. R., Watson, T. B., McKinney, K. A., and Martin, S. T.: Isoprene photochemistry over the Amazon rainforest, Proc Natl Acad Sci U S A, 113, 6125-6130, 10.1073/pnas.1524136113, 2016.

Machado, L. A. T., Calheiros, A. J. P., Biscaro, T., Giangrande, S., Silva Dias, M. A. F., Cecchini, M. A., Albrecht, R., Andreae, M. O., Araujo, W. F., Artaxo, P., Borrmann, S., Braga, R., Burleyson, C., Eichholz, C. W., Fan, J., Feng, Z., Fisch, G. F., Jensen, M. P., Martin, S. T., Pöschl, U., Pöhlker, C., Pöhlker, M. L., Ribaud, J. F., Rosenfeld, D., Saraiva, J. M. B., Schumacher, C., Thalman, R., Walter, D., and Wendisch, M.: Overview: Precipitation characteristics and sensitivities to environmental conditions during GoAmazon2014/5 and ACRIDICON-CHUVA, Atmos. Chem. Phys., 18, 6461-6482, 10.5194/acp-18-6461-2018, 2018.

Martin, S. T., Andreae, M. O., Althausen, D., Artaxo, P., Baars, H., Borrmann, S., Chen, Q., Farmer, D. K., Guenther, A., Gunthe, S. S., Jimenez, J. L., Karl, T., Longo, K., Manzi, A., Müller, T., Pauliquevis, T., Petters, M. D., Prenni, A. J., Pöschl, U., Rizzo, L. V., Schneider, J., Smith, J. N., Swietlicki, E., Tota, J., Wang, J., Wiedensohler, A., and Zorn, S. R.: An overview of the Amazonian Aerosol Characterization Experiment 2008 (AMAZE-08), Atmos. Chem. Phys., 10, 11415-11438, 10.5194/acp-10-11415-2010, 2010a.

Martin, S. T., Andreae, M. O., Artaxo, P., Baumgardner, D., Chen, Q., Goldstein, A. H., Guenther, A., Heald, C. L., Mayol-Bracero, O. L., McMurry, P. H., Pauliquevis, T., Poschl, U., Prather, K. A., Roberts, G. C., Saleska, S. R., Dias, M. A. S., Spracklen, D. V., Swietlicki, E., and Trebs, I.: Sources and Properties of Amazonian Aerosol Particles, Reviews of Geophysics, 48, n/a-n/a, Artn Rg2002 10.1029/2008rg000280, 2010b.

Martin, S. T., Artaxo, P., Machado, L. A. T., Manzi, A. O., Souza, R. A. F., Schumacher, C., Wang, J., Andreae, M. O., Barbosa, H. M. J., Fan, J., Fisch, G., Goldstein, A. H., Guenther, A., Jimenez, J. L., Poschl, U., Dias, M. A. S., Smith, J. N., and Wendisch, M.: Introduction: Observations and Modeling of the Green Ocean Amazon (GoAmazon2014/5), Atmos. Chem. Phys., 16, 4785-4797, 10.5194/acp-16-4785-2016, 2016.

Martin, S. T., Artaxo, P., Machado, L., Manzi, A. O., Souza, R. A. F., Schumacher, C., Wang, J., Biscaro, T., Brito, J., Calheiros, A., Jardine, K., Medeiros, A., Portela, B., de Sa, S. S., Adachi, K., Aiken, A. C., Albrecht, R., Alexander, L., Andreae, M. O., Barbosa, M. J., Buseck, P., Chand, D., Comstock, J. M., Day, D. A., Dubey, M., Fan, J., Fast, J., Fisch, G., Fortner, E., Giangrande, S., Gilles, M., Goldststein, A. H., Guenther, A., Hubbe, J., Jensen, M., Jimenez, J. L., Keutsch, F. N., Kim, S., Kuang, C., Laskskin, A., McKinney, K., Mei, F., Miller, M., Nascimento, R., Pauliquevis, T., Pekour, M., Peres, J., Petaja, T., Pohlker, C., Poschl, U., Rizzo, L., Schmid, B., Shilling, J. E., Dias, M. A. S., Smith, J. N., Tomlmlinson, J. M., Tota, J., and Wendisch, M.: The Green Ocean Amazon Experiment (Goamazon2014/5) Observes Pollution Affecting Gases, Aerosols, Clouds, and Rainfall over the Rain Forest, Bull. Amer. Meteorol. Soc., 98, 981-997, 10.1175/Bams-D-15-00221.1, 2017.

Medeiros, A. S. S., Calderaro, G., Guimaraes, P. C., Magalhaes, M. R., Morais, M. V. B., Rafee, S. A. A., Ribeiro, I. O., Andreoli, R. V., Martins, J. A., Martins, L. D., Martin, S. T., and Souza, R. A. F.: Power plant fuel switching and air quality in a tropical, forested environment, Atmos. Chem. Phys., 17, 8987-8998, 10.5194/acp-17-8987-2017, 2017.

Morgan, W. T., Allan, J. D., Flynn, M., Darbyshire, E., Hodgson, A., Johnson, T., Haywood, J. M., Freitas, S., Longo, K., Artaxo, P., and Coe, H.: Overview of the South American Biomass Burning Analysis (SAMBBA) Field Experiment, in: Nucleation and Atmospheric Aerosols, edited by: DeMott, P. J., and Odowd, C. D., AIP Conference Proceedings, Amer Inst Physics, Melville, 587-590, 2013.

Ng, N. L., Canagaratna, M. R., Zhang, Q., Jimenez, J. L., Tian, J., Ulbrich, I. M., Kroll, J. H., Docherty, K. S., Chhabra, P. S., Bahreini, R., Murphy, S. M., Seinfeld, J. H., Hildebrandt, L., Donahue, N. M., DeCarlo, P. F., Lanz, V. A., Prevot, A. S. H., Dinar, E., Rudich, Y., and Worsnop, D. R.: Organic aerosol components observed in Northern Hemispheric datasets from Aerosol Mass Spectrometry, Atmos. Chem. Phys., 10, 4625-4641, 10.5194/acp-10-4625-2010, 2010.

Ng, N. L., Brown, S. S., Archibald, A. T., Atlas, E., Cohen, R. C., Crowley, J. N., Day, D. A., Donahue, N. M., Fry, J. L., Fuchs, H., Griffin, R. J., Guzman, M. I., Herrmann, H., Hodzic, A., Iinuma, Y., Jimenez, J. L., Kiendler-Scharr, A., Lee, B. H., Luecken, D. J., Mao, J. Q., McLaren, R., Mutzel, A., Osthoff, H. D., Ouyang, B., Picquet-Varrault, B., Platt, U., Pye, H. O. T., Rudich, Y., Schwantes, R. H., Shiraiwa, M., Stutz, J., Thornton, J. A., Tilgner, A., Williams, B. J., and Zaveri, R. A.: Nitrate radicals and biogenic volatile organic compounds: oxidation, mechanisms, and organic aerosol, Atmos. Chem. Phys., 17, 2103-2162, 10.5194/acp-17-2103-2017, 2017.

Nguyen, T. B., Coggon, M. M., Bates, K. H., Zhang, X., Schwantes, R. H., Schilling, K. A., Loza, C. L., Flagan, R. C., Wennberg, P. O., and Seinfeld, J. H.: Organic aerosol formation from the reactive uptake of isoprene epoxydiols (IEPOX) onto non-acidified inorganic seeds, Atmos. Chem. Phys., 14, 3497-3510, 10.5194/acp-14-3497-2014, 2014.

Odum, J. R., Hoffmann, T., Bowman, F., Collins, D., Flagan, R. C., and Seinfeld, J. H.: Gas/particle partitioning and secondary organic aerosol yields, Environ. Sci. Technol., 30, 2580-2585, DOI 10.1021/es950943+, 1996.

Paatero, P., and Tapper, U.: Positive matrix factorization: A non-negative factor model with optimal utilization of error estimates of data values, Environmetrics, 5, 111-126, 10.1002/env.3170050203, 1994.

Paatero, P.: Least squares formulation of robust non-negative factor analysis, Chemometrics and Intelligent Laboratory Systems, 37, 23-35, Doi 10.1016/S0169-7439(96)00044-5, 1997.

Parrish, D. D., Hahn, C. J., Williams, E. J., Norton, R. B., Fehsenfeld, F. C., Singh, H. B., Shetter, J. D., Gandrud, B. W., and Ridley, B. A.: INDICATIONS OF PHOTOCHEMICAL HISTORIES OF PACIFIC AIR MASSES FROM MEASUREMENTS OF ATMOSPHERIC TRACE SPECIES AT POINT ARENA, CALIFORNIA, Journal of Geophysical Research-Atmospheres, 97, 15883-15901, 10.1029/92jd01242, 1992.

Pierce, J. R., Leaitch, W. R., Liggio, J., Westervelt, D. M., Wainwright, C. D., Abbatt, J. P. D., Ahlm, L., Al-Basheer, W., Cziczo, D. J., Hayden, K. L., Lee, A. K. Y., Li, S. M., Russell, L. M., Sjostedt, S. J., Strawbridge, K. B., Travis, M., Vlasenko, A., Wentzell, J. J. B., Wiebe, H. A., Wong, J. P. S., and Macdonald, A. M.: Nucleation and condensational growth to CCN sizes during a sustained pristine biogenic SOA event in a forested mountain valley, Atmos. Chem. Phys., 12, 3147-3163, 10.5194/acp-12-3147-2012, 2012.

Riipinen, I., Pierce, J. R., Yli-Juuti, T., Nieminen, T., Hakkinen, S., Ehn, M., Junninen, H., Lehtipalo, K., Petaja, T., Slowik, J., Chang, R., Shantz, N. C., Abbatt, J., Leaitch, W. R., Kerminen, V. M., Worsnop, D. R., Pandis, S. N., Donahue, N. M., and Kulmala, M.: Organic condensation: a vital link connecting aerosol formation to cloud condensation nuclei (CCN) concentrations, Atmos. Chem. Phys., 11, 3865-3878, 10.5194/acp-11-3865-2011, 2011.

Riipinen, I., Yli-Juuti, T., Pierce, J. R., Petaja, T., Worsnop, D. R., Kulmala, M., and Donahue, N. M.: The contribution of organics to atmospheric nanoparticle growth, Nature Geoscience, 5, 453-458, 10.1038/ngeo1499, 2012.

Robinson, A. L., Donahue, N. M., Shrivastava, M. K., Weitkamp, E. A., Sage, A. M., Grieshop, A. P., Lane, T. E., Pierce, J. R., and Pandis, S. N.: Rethinking organic aerosols: semivolatile emissions and photochemical aging, Science, 315, 1259-1262, 10.1126/science.1133061, 2007.

Robinson, N. H., Hamilton, J. F., Allan, J. D., Langford, B., Oram, D. E., Chen, Q., Docherty, K., Farmer, D. K., Jimenez, J. L., Ward, M. W., Hewitt, C. N., Barley, M. H., Jenkin, M. E., Rickard, A. R., Martin, S. T., McFiggans, G., and Coe, H.: Evidence for a significant proportion of Secondary Organic Aerosol from isoprene above a maritime tropical forest, Atmos. Chem. Phys., 11, 1039-1050, 10.5194/acp-11-1039-2011, 2011.

Sage, A. M., Weitkamp, E. A., Robinson, A. L., and Donahue, N. M.: Evolving mass spectra of the oxidized component of organic aerosol: results from aerosol mass spectrometer analyses of aged diesel emissions, Atmos. Chem. Phys., 8, 1139-1152, DOI 10.5194/acp-8-1139-2008, 2008.

Schichtel, B. A., Malm, W. C., Bench, G., Fallon, S., McDade, C. E., Chow, J. C., and Watson, J. G.: Fossil and contemporary fine particulate carbon fractions at 12 rural and urban sites in the United States, Journal of Geophysical Research-Atmospheres, 113, D02311, Artn D02311 10.1029/2007jd008605, 2008.

Schulz, C., Schneider, J., Weinzierl, B., Sauer, D., Futterer, D., Ziereis, H., and Borrmann, S.: Aircraft-bases observations of IEPOX-derived isoprene SOA in the tropical upper troposphere over the Amazon Region, In preparation for Atmsopheric Chemistry and Physics, 2018.

Scott, C. E., Spracklen, D. V., Pierce, J. R., Riipinen, I., D'Andrea, S. D., Rap, A., Carslaw, K. S., Forster, P. M., Artaxo, P., Kulmala, M., Rizzo, L. V., Swietlicki, E., Mann, G. W., and Pringle, K. J.: Impact of gas-to-particle partitioning approaches on the simulated radiative effects of biogenic secondary organic aerosol, Atmos. Chem. Phys., 15, 12989-13001, 10.5194/acp-15-12989-2015, 2015.

Setyan, A., Zhang, Q., Merkel, M., Knighton, W. B., Sun, Y., Song, C., Shilling, J. E., Onasch, T. B., Herndon, S. C., Worsnop, D. R., Fast, J. D., Zaveri, R. A., Berg, L. K., Wiedensohler, A., Flowers, B. A., Dubey, M. K., and Subramanian, R.: Characterization of submicron particles influenced by mixed biogenic and anthropogenic emissions using high-resolution aerosol mass spectrometry: results from CARES, Atmos. Chem. Phys., 12, 8131-8156, 10.5194/acp-12-8131-2012, 2012.

Shilling, J. E., Zaveri, R. A., Fast, J. D., Kleinman, L., Alexander, M. L., Canagaratna, M. R., Fortner, E., Hubbe, J. M., Jayne, J. T., Sedlacek, A., Setyan, A., Springston, S., Worsnop, D. R., and Zhang, Q.: Enhanced SOA formation from mixed anthropogenic and biogenic emissions during the CARES campaign, Atmos. Chem. Phys., 13, 2091-2113, 10.5194/acp-13-2091-2013, 2013.

Shrivastava, M., Cappa, C. D., Fan, J. W., Goldstein, A. H., Guenther, A. B., Jimenez, J. L., Kuang, C., Laskin, A., Martin, S. T., Ng, N. L., Petaja, T., Pierce, J. R., Rasch, P. J., Roldin, P., Seinfeld, J. H., Shilling, J., Smith, J. N., Thornton, J. A., Volkamer, R., Wang, J., Worsnop, D. R., Zaveri, R. A., Zelenyuk, A., and Zhang, Q.: Recent advances in understanding secondary organic aerosol: Implications for global climate forcing, Reviews of Geophysics, 55, 509-559, 10.1002/2016rg000540, 2017.

Slowik, J. G., Stroud, C., Bottenheim, J. W., Brickell, P. C., Chang, R. Y. W., Liggio, J., Makar, P. A., Martin, R. V., Moran, M. D., Shantz, N. C., Sjostedt, S. J., van Donkelaar, A., Vlasenko, A., Wiebe, H. A., Xia, A. G., Zhang, J., Leaitch, W. R., and Abbatt, J. P. D.: Characterization of a large biogenic secondary organic aerosol event from eastern Canadian forests, Atmos. Chem. Phys., 10, 2825-2845, 10.5194/acp-10-2825-2010, 2010.

Sullivan, A. P., Peltier, R. E., Brock, C. A., de Gouw, J. A., Holloway, J. S., Warneke, C., Wollny, A. G., and Weber, R. J.: Airborne measurements of carbonaceous aerosol soluble in water over northeastern United States: Method development and an investigation into water-soluble organic carbon sources, Journal of Geophysical Research-Atmospheres, 111, n/a-n/a, Artn D23s46 10.1029/2006jd007072, 2006.

Sullivan, A. P., and Weber, R. J.: Chemical characterization of the ambient organic aerosol soluble in water: 2. Isolation of acid, neutral, and basic fractions by modified size-exclusion chromatography, Journal of Geophysical Research-Atmospheres, 111, Artn D05315 10.1029/2005jd006486, 2006.

Surratt, J. D., Chan, A. W., Eddingsaas, N. C., Chan, M., Loza, C. L., Kwan, A. J., Hersey, S. P., Flagan, R. C., Wennberg, P. O., and Seinfeld, J. H.: Reactive intermediates revealed in secondary organic aerosol formation from isoprene, Proc Natl Acad Sci U S A, 107, 6640-6645, 10.1073/pnas.0911114107, 2010.

Takegawa, N., Miyakawa, T., Kondo, Y., Blake, D. R., Kanaya, Y., Koike, M., Fukuda, M., Komazaki, Y., Miyazaki, Y., Shimono, A., and Takeuchi, T.: Evolution of submicron organic aerosol in polluted air exported from Tokyo, Geophys. Res. Lett., 33, Article L15814, Artn L15814 10.1029/2006gl025815, 2006.

Ulbrich, I. M., Canagaratna, M. R., Zhang, Q., Worsnop, D. R., and Jimenez, J. L.: Interpretation of organic components from Positive Matrix Factorization of aerosol mass spectrometric data, Atmos. Chem. Phys., 9, 2891-2918, 10.5194/acp-9-2891-2009, 2009.

Volkamer, R., Jimenez, J. L., San Martini, F., Dzepina, K., Zhang, Q., Salcedo, D., Molina, L. T., Worsnop, D. R., and Molina, M. J.: Secondary organic aerosol formation from anthropogenic air pollution: Rapid and higher than expected, Geophys. Res. Lett., 33, Article L17811, Artn L17811 10.1029/2006gl026899, 2006.

Weber, R. J., Sullivan, A. P., Peltier, R. E., Russell, A., Yan, B., Zheng, M., de Gouw, J., Warneke, C., Brock, C., Holloway, J. S., Atlas, E. L., and Edgerton, E.: A study of secondary organic aerosol formation in the anthropogenic-influenced southeastern United States, Journal of Geophysical Research-Atmospheres, 112, Artn D13302 10.1029/2007jd008408, 2007.

Xu, L., Guo, H. Y., Boyd, C. M., Klein, M., Bougiatioti, A., Cerully, K. M., Hite, J. R., Isaacman-VanWertz, G., Kreisberg, N. M., Knote, C., Olson, K., Koss, A., Goldstein, A. H., Hering, S. V., de Gouw, J., Baumann, K., Lee, S. H., Nenes, A., Weber, R. J., and Ng, N. L.: Correction to Supporting Information for Xu et al., Effects of anthropogenic emissions on aerosol formation from isoprene and monoterpenes in the southeastern United States, Proc Natl Acad Sci U S A, 112, E4509, 10.1073/pnas.1512279112, 2015.

Yokelson, R. J., Karl, T., Artaxo, P., Blake, D. R., Christian, T. J., Griffith, D. W. T., Guenther, A., and Hao, W. M.: The Tropical Forest and Fire Emissions Experiment: overview and airborne fire emission factor measurements, Atmos. Chem. Phys., 7, 5175-5196, 10.5194/acp-7-5175-2007, 2007.

Yokelson, R. J., Crounse, J. D., DeCarlo, P. F., Karl, T., Urbanski, S., Atlas, E., Campos, T., Shinozuka, Y., Kapustin, V., Clarke, A. D., Weinheimer, A., Knapp, D. J., Montzka, D. D., Holloway, J., Weibring, P., Flocke, F., Zheng, W., Toohey, D., Wennberg, P. O., Wiedinmyer, C., Mauldin, L., Fried, A., Richter, D., Walega, J., Jimenez, J. L., Adachi, K., Buseck, P. R., Hall, S. R., and Shetter, R.: Emissions from biomass burning in the Yucatan, Atmos. Chem. Phys., 9, 5785-5812, DOI 10.5194/acp-9-5785-2009, 2009.

Zaveri, R. A., Easter, R. C., Shilling, J. E., and Seinfeld, J. H.: Modeling kinetic partitioning of secondary organic aerosol and size distribution dynamics: representing effects of volatility, phase state, and particle-phase reaction, Atmos. Chem. Phys., 14, 5153-5181, 10.5194/acp-14-5153-2014, 2014.

Zhang, Q., Alfarra, M. R., Worsnop, D. R., Allan, J. D., Coe, H., Canagaratna, M. R., and Jimenez, J. L.: Deconvolution and quantification of hydrocarbon-like and oxygenated organic aerosols based on aerosol mass spectrometry, Environ Sci Technol, 39, 4938-4952, 2005a.

Zhang, Q., Worsnop, D. R., Canagaratna, M. R., and Jimenez, J. L.: Hydrocarbon-like and oxygenated organic aerosols in Pittsburgh: insights into sources and processes of organic aerosols, Atmos. Chem. Phys., 5, 3289-3311, 2005b.

Zhang, Q., Jimenez, J. L., Canagaratna, M. R., Allan, J. D., Coe, H., Ulbrich, I., Alfarra, M. R., Takami, A., Middlebrook, A. M., Sun, Y. L., Dzepina, K., Dunlea, E., Docherty, K., DeCarlo, P. F., Salcedo, D., Onasch, T., Jayne, J. T., Miyoshi, T., Shimono, A., Hatakeyama, S., Takegawa, N., Kondo, Y., Schneider, J., Drewnick, F., Borrmann, S., Weimer, S., Demerjian, K., Williams, P., Bower, K., Bahreini, R., Cottrell, L., Griffin, R. J., Rautiainen, J., Sun, J. Y., Zhang, Y. M., and Worsnop, D. R.: Ubiquity and dominance of oxygenated species in organic aerosols in anthropogenically-influenced Northern Hemisphere midlatitudes, Geophys. Res. Lett., 34, n/a-n/a, 10.1029/2007gl029979, 2007.

Zhang, Q., Jimenez, J. L., Canagaratna, M. R., Ulbrich, I. M., Ng, N. L., Worsnop, D. R., and Sun, Y.: Understanding atmospheric organic aerosols via factor analysis of aerosol mass spectrometry: a review, Anal Bioanal Chem, 401, 3045-3067, 10.1007/s00216-011-5355-y, 2011.

Zhou, S., Collier, S., Xu, J. Z., Mei, F., Wang, J., Lee, Y. N., Sedlacek, A. J., Springston, S. R., Sun, Y. L., and Zhang, Q.: Influences of upwind emission sources and atmospheric processing on aerosol chemistry and properties at a rural location in the Northeastern US, Journal of Geophysical Research-Atmospheres, 121, 6049-6065, 10.1002/2015jd024568, 2016.

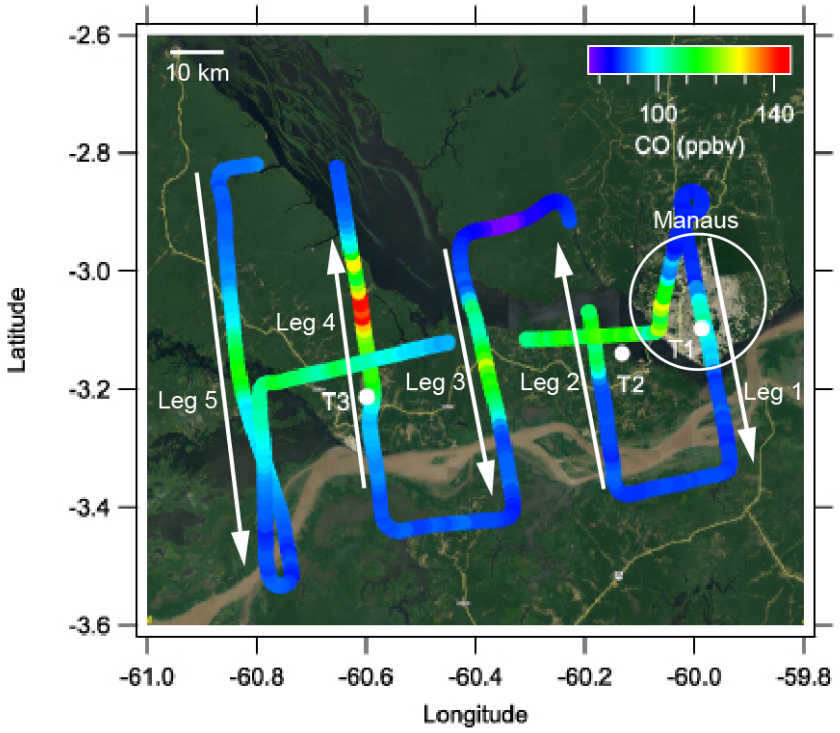

Figure 1. Flight path for the March 13, 2014 flight colored by the CO concentration. Arrows indicate the direction of the flight. The first pass through the pattern was conducted at 500 m then repreated at 1000 m. The G-1 took off at 10:12 (local time) and landed at 13:21 for a total flight duration of three hours and nine minutes. The dots show the location of ground measurement sites. The color scale shows the CO concentration in ppm units. The underlying image is from Google Earth.

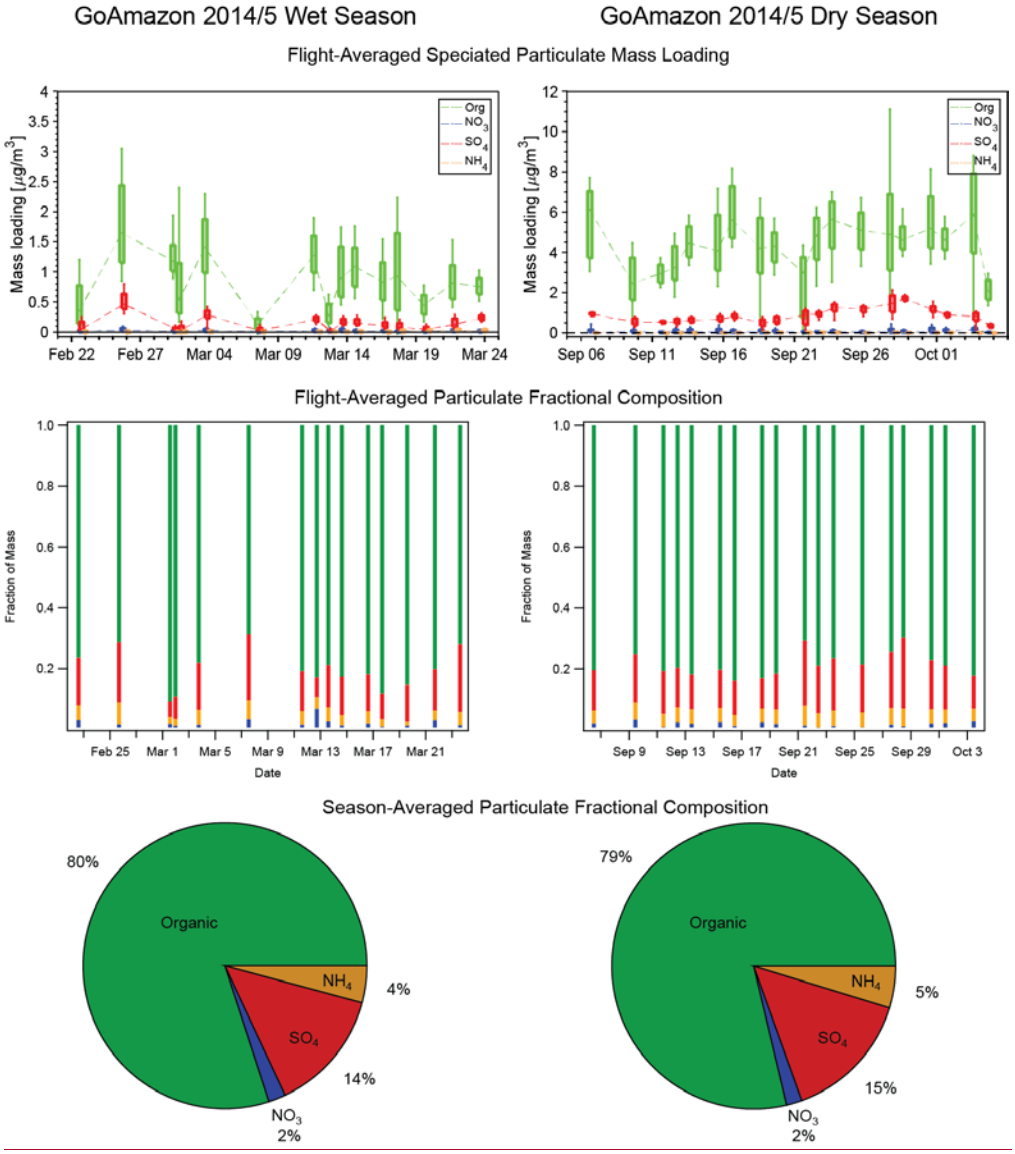
GoAmazon 2014/5 Wet Season
GoAmazon 2014/5 Dry Season
Flight-Averaged Speciated Particulate Mass Loading
Mass loading [μg/m3]
Org
NO3
SO4
NH4
Feb 22
Feb 27
Mar 04
Mar 09
Mar 14
Mar 19
Mar 24
Sep 06
Sep 11
Sep 16
Sep 21
Sep 26
Oct 01
Flight-Averaged Particulate Fractional Composition
Fraction of Mass
Date
Feb 25
Mar 1
Mar 5
Mar 9
Mar 13
Mar 17
Mar 21
Sep 9
Sep 13
Sep 17
Sep 21
Sep 25
Sep 29
Oct 3
Season-Averaged Particulate Fractional Composition
80%
Organic
NH4
4%
SO4
14%
NO3
2%
79%
Organic
NH4
5%
SO4
15%
NO3
2%

Figure 2: Box and whisker representations of the G-1 AMS data for both the wet and dry seasons (top panel), average particle chemical composition for each flight (middle panel), and average aerosol chemical composition for all flights (bottom). Boxes represent the quartiles, with whiskers extending to 10% and 90%. Lines between the boxes connect the ~~mean~~ median and are drawn to guide the eye. Note the scale change between the wet and dry season box and whisker plots. ~~Data presented here use the unit mass resolution analysis routine (e.g., Squirrel).~~ AMS data are normalized to 23 °C and 1013 hPa.

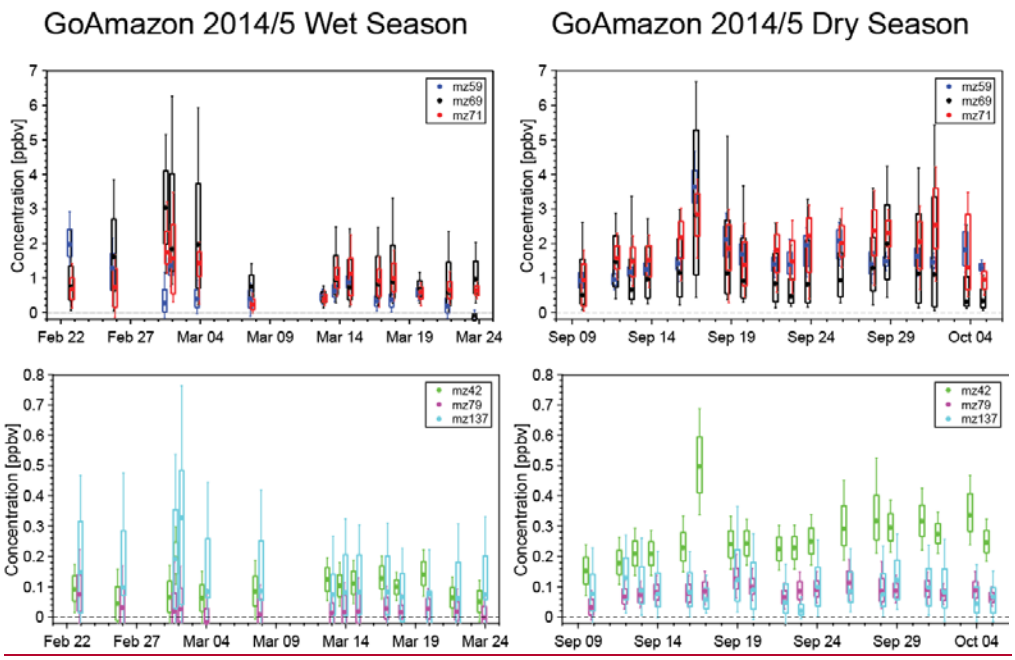

Figure 3. Box and whisker representations of the G-1 PTR-MS data for both the wet and dry seasons. Boxes represent the quartiles, with whiskers extending to 10% and 90%. Note the scale change between the top and bottom panels.

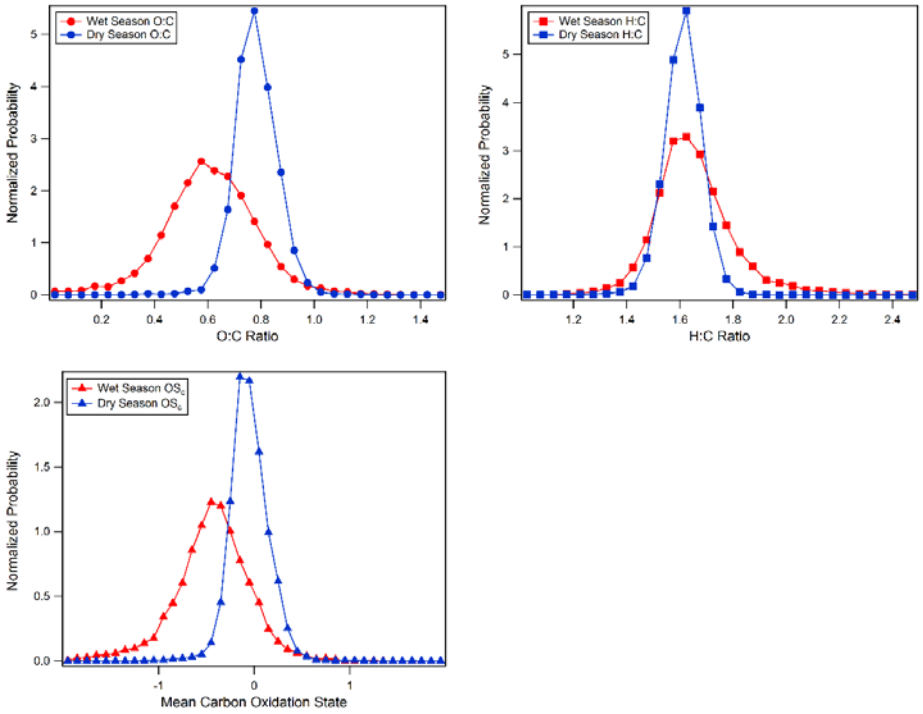

Figure 43. Normalized occurrence probability calculated from G-1 HR-AMS analysis of the organic aerosol during the wet (red) and dry (blue) seasons. O:C and H:C were binned into 0.05 unit wide bins and $\bar{OS}_c$ data were binned in 0.1 unit wide bins. O:C and H:C ratios were calculated using the updated methodology in Canagaratna et al. 2015. Mean carbon oxidation state is calculated according to Kroll et al. 2011. The same data were analyzed for this figure and for Figure 1 and as such cover a range of altitudes and to a lesser extent time of day.

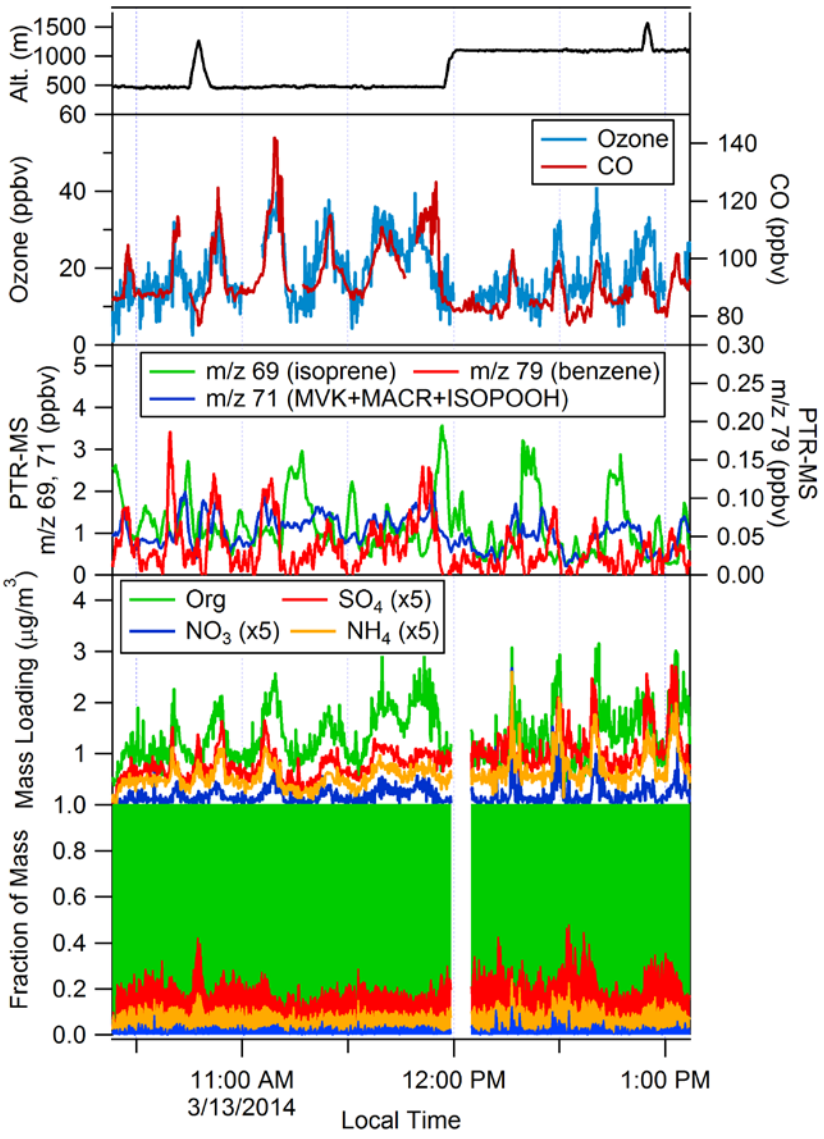
Alt. (m)
1500
1000
500
Ozone (ppbv)
60
40
20
0
Ozone
CO
CO (ppbv)
140
120
100
80
PTR-MS
m/z 69, 71 (ppbv)
5
4
3
2
1
0
m/z 69 (isoprene)
m/z 79 (benzene)
m/z 71 (MVK+MACR+ISOPOOH)
PTR-MS
m/z 79 (ppbv)
0.30
0.25
0.20
0.15
0.10
0.05
0.00
Mass Loading (μg/m3)
4
3
2
1
0
Org
SO4 (x5)
NO3 (x5)
NH4 (x5)
Fraction of Mass
1.0
0.8
0.6
0.4
0.2
0.0
11:00 AM
3/13/2014
12:00 PM
1:00 PM
Local Time

Figure 5. Time traces of relevant quantities on March 13th, 2014 flight. ~~AMS data uses the HR-analysis routine described in the literature to minimize interferences (Aiken et al., 2007).~~ Note the mass of inorganic species (SO_4, NO_3, NH_4) has been multiplied by a factor of five to improve the figure clarity. PTR-MS signal at m/z 69 corresponds to isoprene, m/z 71 corresponds to the sum of methylvinyl ketone (MVK), methacrolein (MACR), and isoprene hydroxyhydroperoxide (ISOPOOH), all oxidation products of isoprene, and m/z 79 corresponds to benzene. AMS data are normalized to 23 °C and 1013 hPa.

Formatted: Subscript

Formatted: Subscript

Formatted: Subscript

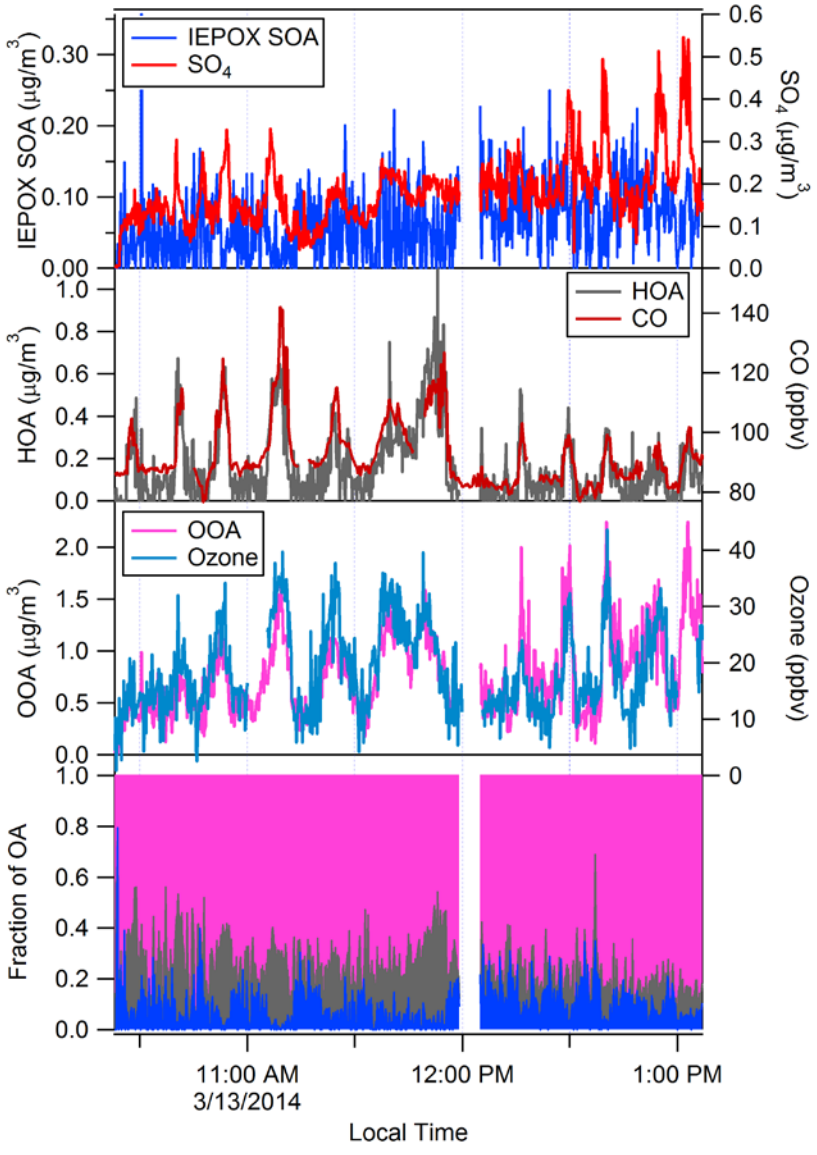
IEPOX SOA
SO4
IEPOX SOA (µg/m3)
SO4 (µg/m3)
HOA
CO
HOA (µg/m3)
CO (ppbv)
OOA
Ozone
OOA (µg/m3)
Ozone (ppbv)
Fraction of OA
11:00 AM
3/13/2014
12:00 PM
1:00 PM
Local Time

Figure 65. PMF analysis of the organic aerosol on the March 13th 2014 flight. ~~The PMF analysis utilized the high resolution dataset. All data from the wet season were included in the analysis.~~AMS data are normalized to 23 °C and 1013 hPa.

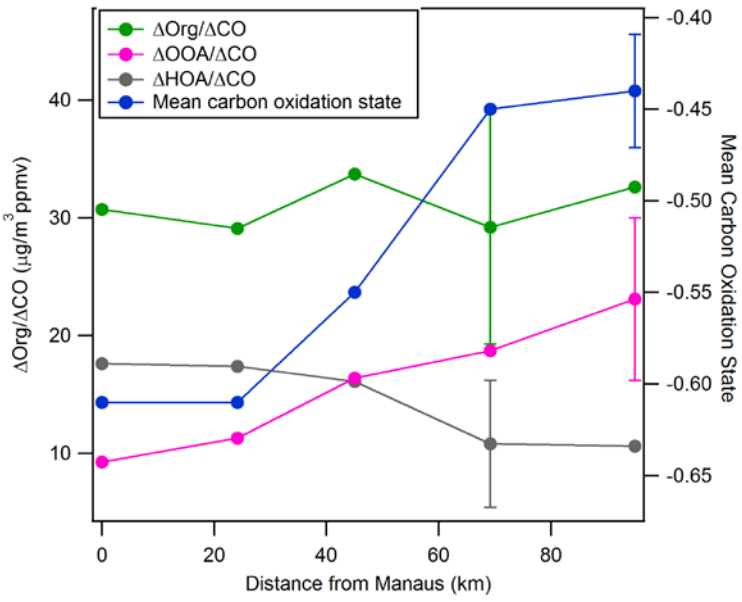

Figure 76. Key metrics describing the evolution of the Manaus urban plume on March 13. Each data point represents the average values for one pass through the plume. A representative error bar is shown for each set of measurements. Mean wind speeds were 7.3 m/s on this flight, thus data capture approximately the first 4-5 hours of the plume aging. Calculations of ΔOrg/ΔCO values use method one with details on the calculations and methods provided in the SI. Spatial locations of each leg are ~~labeled~~labelled in Figure 1.

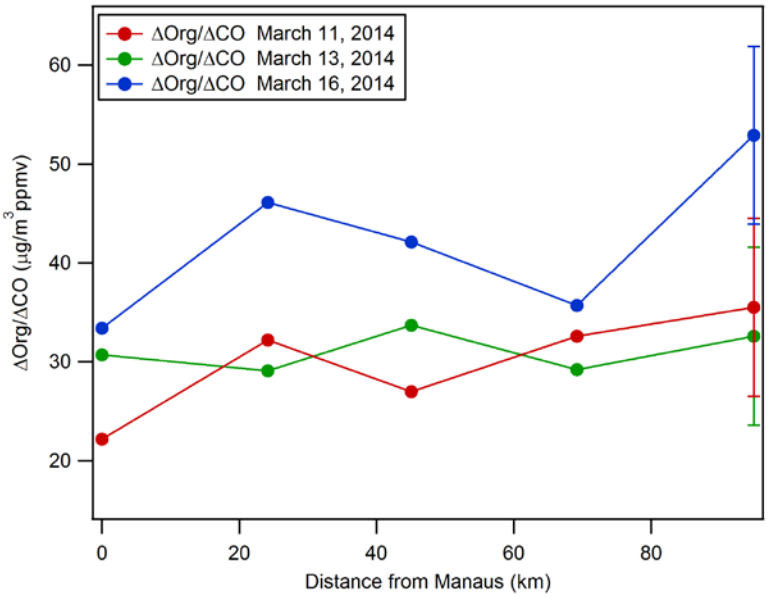

Figure 8 Δorg/ΔCO measurements in the Manaus plume as a function of distance from Manaus for March 11, March 13, and March 16, 2014. A representative error bar is shown for each set of measurements. Mean wind speeds were 5.8 m/s, 7.3 m/s, and 4.6 m/s on March 11, 13, and 16h, respectively. Collectively, the data capture approximately the first 4-6.5 hours of the plume aging.

Formatted: Caption

Flight Date[a]	Takeoff [b]	Landing [b]	Altitude(s) of Level Flight Legs (m)[c]	T (°C)[d]	RH (% water)[d]	Wind Speed (m/s)[d]	Wind Heading[d]
Wet Season							
2/22/2014	10:37:11	13:25:28	600, 1600	25	80	5	ENE
2/25/2014	12:30:31	14:43:04	600, 1300	26	80	8	ENE
3/1/2014 a	9:33:09	11:31:31	600	25	80	6	NE
3/1/2014 b	13:13:59	14:49:34	1100, 4500, 6400	24	80	4	NE
3/3/2014	13:46:34	15:11:57	600	26	90	N/A	N/A
3/7/2014	9:08:11	11:39:18	600, 1300, 1900, 3200, 3800, 4500, 5800	26	65	10	NNE
3/11/2014	10:39:59	13:51:10	600, 1500	25	85	7	ENE
3/12/2014	13:20:25	15:29:44	600	22	80	16	NE
3/13/2014	10:14:14	13:21:29	500, 1100	25	80	7	ENE
3/14/2014	10:17:07	12:48:25	500, 1200, 2200, 3200	25	80	8	E
3/16/2014	10:38:18	13:30:33	500, 1000, 1200, 1600	25	80	5	E
3/17/2014	12:23:11	15:26:38	600, 1200, 1500	26	75	10	ENE
3/19/2014	10:25:33	13:21:48	600, 1600, 3200, 4800, 6500, 7100	22	95	7	ENE
3/21/2014	12:32:34	15:00:22	600, 800, 1300	23	90	6	ENE
3/23/2014	10:56:47	13:46:34	600	23	90	5	NNE
Dry Season							
9/6/2014	11:16:07	13:39:03	500, 1700	29	N/A	4	ESE
9/9/2014	11:01:14	14:11:01	500, 1600, 1900, 5800	25	80	4	NE
9/11/2014	10:32:40	13:37:38	500	27	70	7	ENE
9/12/2014	10:41:26	13:08:04	600, 1600	25	65	6	E
9/13/2014	10:50:05	13:43:21	500, 800, 1600, 2100, 2600	27	70	5	ENE
9/15/2014	10:59:06	14:01:47	500, 1800, 1900, 2600	28	60	5	E
9/16/2014	11:40:15	14:27:54	500, 1900	28	65	3	NE
9/18/2014	10:35:59	13:26:01	500, 1900, 4900	27	70	2	E
9/19/2014	10:30:23	13:46:44	500, 1600	28	70	2	NE
9/21/2014	11:17:32	14:20:51	500, 1300, 1600, 1900, 2500, 4800	26	70	5	ENE
9/22/2014	10:23:40	13:37:40	500, 1800	28	60	3	NE
9/23/2014	11:46:45	14:43:13	500, 1900	28	60	2	E
9/25/2014	13:09:24	15:53:59	500, 1600, 1800	28	70	4	E
9/27/2014	14:29:21	16:21:40	600, 2300	29	55	5	ENE
9/28/2014	11:09:12	14:07:27	600, 1800, 2100	28	65	5	ENE
9/30/2014	10:55:10	13:10:19	500, 2000, 3200	29	55	3	E
10/1/2014	10:39:01	13:09:54	600, 1000, 1300, 1600, 2100, 2500	26	65	6	E

10/3/2014	10:50:51	13:54:57	800, 1000, 1200, 1600, 1900, 2600, 3300, ~~3900~~	26	75	4	ESE
10/4/2014	12:24:46	13:52:31	600	27	55	N/A	N/A

[a]The flight on March 10, 2014 is omitted from this table due to an AMS failure.

[b]local time

[c]altitude above mean sea level from GPS data, only level flight legs on which AMS data were collected listed

[d]immediately after takeoff, altitude < 1000 m, wind speed and heading from Aventech Research AIMMS-20 probe

T from Rosemount 102E probe, RH calculated from T and dewpoint measured by General Eastern 1011-B probe

Table 1. Flight times, altitude of level legs, and meteorological parameters measured by instrumentation onboard the G-1 research aircraft for research flights described in this manuscript. Temperature, RH, wind speed, and wind heading correspond to values measured shortly after takeoff at altitudes less than 1000 m. Note that meteorological parameters are not homogeneous in space or time.

Formatted: Font: Times New Roman, 9 pt

Formatted: Font: Times New Roman, 9 pt

Formatted: Font: Times New Roman, 9 pt

Formatted: Font: Times New Roman, 9 pt

Formatted: Font: Times New Roman, 9 pt

Formatted: Font: Times New Roman, 9 pt

Formatted: Font: Times New Roman, 9 pt

Formatted: Font: Times New Roman, 9 pt

	Wet Season	Dry Season
Median Loading (All Data)		
Org	0.85	4.29
SO_4	0.19	0.77
NO_3	0.02	0.05
NH_4	0.06	0.25
Median Loading (Altitude < 700 m)		
Org	0.89	4.22
SO_4	0.15	0.7
NO_3	0.02	0.03
NH_4	0.04	0.21
Mean Loading (All data)		
Org	0.91	4.41
SO_4	0.16	0.83
NO_3	0.02	0.1
NH_4	0.05	0.26
Mean Loading (Altitude < 700 m)		
Org	1.02	4.45
SO_4	0.18	0.85
NO_3	0.03	0.05
NH_4	0.06	0.23

Table ~~1~~2. Chemically resolved mass loading measured by the AMS onboard the G-1. Mass loadings are normalized to 23 °C and 1013 hPa. Units are µg/m^3. The statistics for altitudes below 700 m approximate the boundary layer conditions at the time of the flights.

	Wet Season	Dry Season
Median Concentration (all data)		
m/z 42 (acetonitrile)	0.1	0.25
m/z 59 (acetone)	0.47	1.46
m/z 69 (isoprene)	0.43	1.09
m/z 71 (isoprene oxidation products)	0.66	1.84
m/z 79 (benzene)	0.03	0.08
m/z 137 (monoterpenes)	0.1	0.08
Median Concentration (<700 m)		
m/z 42 (acetonitrile)	0.09	0.26
m/z 59 (acetone)	0.43	1.65
m/z 69 (isoprene)	0.52	1.86
m/z 71 (isoprene oxidation products)	0.76	2.16
m/z 79 (benzene)	0.02	0.09
m/z 137 (monoterpenes)	0.12	0.11
Mean Concentration (all data)		
m/z 42 (acetonitrile)	0.12	0.36
m/z 59 (acetone)	0.59	1.91
m/z 69 (isoprene)	0.67	1.82
m/z 71 (isoprene oxidation products)	0.87	1.99
m/z 79 (benzene)	0.04	0.1
m/z 137 (monoterpenes)	0.12	0.11
Mean Concentration (<700 m)		
m/z 42 (acetonitrile)	0.11	0.4
m/z 59 (acetone)	0.7	2.31
m/z 69 (isoprene)	0.82	2.37
m/z 71 (isoprene oxidation products)	1.07	2.4
m/z 79 (benzene)	0.04	0.11
m/z 137 (monoterpenes)	0.15	0.14

Table 3. Measurements of VOC species made by the PTR-MS onboard the G-1. Units are ppbv. The statistics for altitudes less than 700 m capture the lowest altitude data during the campaign (Table 1).

Number of Factors	Q/Q_{exp}	Notes
2	0.28	4% of mass unresolved, OOA-like factors resolved but look mixed
3	0.26	2% of mass still unresolved, OOA factors looks split and unrealistic, no HOA or IEPOX SOA factor
4	0.25	Most of mass resolved (0.1 % residual) , HOA factor now resolved, OOA factor split, unrealistic
5	0.24	IEPOX factor resolved, OOA factor split, unrealistic

Table A1. Summary of scaled residuals and reasoning used in the choice of a 5 factor solution in the PMF analysis of the wet season HR-AMS data.

Formatted: Normal